

Panda: AdaPtive Noisy Data Augmentation for Regularization of Undirected Graphical Models

Yinan Li¹, Xiao Liu, and Fang Liu^{1*}

¹ Department of Applied and Computational Mathematics and Statistics

² Department of Psychology

University of Notre Dame, Notre Dame, IN 46556, U.S.A.

Abstract

We propose PANDA, an AdaPtive Noise Augmentation technique to regularize estimating and constructing undirected graphical models (UGMs). PANDA iteratively solves MLEs given noise augmented data in the regression-based framework until convergence to achieve the designed regularization effects. The augmented noises can be designed to achieve various regularization effects on graph estimation, including the bridge, elastic net, adaptive lasso, and SCAD penalization; it can also offer group lasso and fused ridge when some nodes belong to the same group. We establish theoretically that the noise-augmented loss functions and its minimizer converge almost surely to the expected penalized loss function and its minimizer, respectively. We derive the asymptotic distributions for the regularized regression coefficients through PANDA in GLMs, based on which, the inferences for the parameters can be obtained simultaneously with variable selection. Our empirical results suggest the inferences achieve nominal or near-nominal coverage and are far more efficient compared to some existing post-selection procedures. On the algorithm level, PANDA can be easily programmed in any standard software without resorting to complicated optimization techniques. We show the non-inferior performance of PANDA in constructing graphs of different types in simulation studies and also apply PANDA to the autism spectrum disorder data to construct a mixed-node graph.

keywords: generalized linear models (GLMs), adjacency matrix, empirical Bayes and MAP, confidence interval, augmented Fisher information; noise injection

*Corresponding author email: fang.liu.131@nd.edu

1 Introduction

1.1 Noise Injection

Noise injection (NI) is a simple and effective statistical technique to improving the generalization ability of statistical and machine learning methods. There are two types of NI techniques. In the first type, additive or multiplicative noises are injected into the observed and latent variables without changing the dimension of original data ($n \times p$). In the second approach, NI can realized through expanding the dimensionality of the original data (either n or p increases). In both cases, the learned signals from the noise-augmented data are less prone to overfitting and associated with smaller generalization errors as compared to that learned from the original data.

NI has wide applications in regularizing and learning neural networks (NNs). [Matsuoka \(1992\)](#) proved that training NNs with noise injected to the input layers decreases the learned NN’s sensitivity to small input perturbation. [Holmstrom and Koistinen \(1992\)](#) viewed NI in input nodes in NNs as kernel smoothing of the observed data for classification and mapping problems. [Grandvalet and Boucheron \(1997\)](#) and [Wager et al. \(2013\)](#) showed that NI in NNs are equivalent to the Tikhonov regularization in expectation with regard to the distribution of injected noises with the second order approximation. ([Grandvalet, 1998](#)) proposed the adaptive ridge regression realized through an iterative algorithm that converges to the Lasso. [this paper doesn’t belong to the NN settings](#). The best known NI technique in NN training is the multiplicative Bernoulli noise. The Bernoulli NI is shown to achieve the l_2 regularization effect (for dropout) ([Srivastava et al., 2014](#)) or the l_2 plus some sparsity regularization on model parameters in the setting of generalized linear models (GLMs) ([Kang et al., 2018](#)). [Gal and Ghahramani \(2016\)](#) developed a theoretical framework that connects dropout in deep NNs with approximate Bayesian inference in deep Gaussian processes. [Noh et al. \(2017\)](#) suggested that NI regularization optimizes the lower bound of the objective function marginalized over the distribution of hidden nodes. Whiteout ([Li and Liu, 2017](#)) injects additive and multiplicative Gaussian noises in NNs, where the variance of the Gaussian noise is a function of NN parameters and contains three tuning parameters that leads to a variety of regularization effects, including the bridge, ridge, lasso, adaptive lasso, elastic net, and group lasso. The above NI techniques directly perturb the existing input and hidden nodes in the NNs without altering the dimensionality of the original data. [Brown et al. \(2003\)](#) augmented the original data with noisy observations drawn from a fixed distribution (e.g., Normal or Uniform) before learning NNs to deal with insufficient data in mineral exploration. Their experiments showed good generalization of the learned NNs but provided no theoretical considerations.

Given the success of NI in regularizing NNs, one would expect that NI, conditional on that noises are designed properly, can be potentially useful in regularizing other types of large and complex models. We were able to locate two relatively simple applications of NI in other analysis settings than NNs. In the first case, NI is applied to the linear discriminant analysis [Skurichina and Duin \(1999\)](#), where adding redundant features to the data (p increases while n remains the same) yields similar effects as other regularization techniques. In the second case, the ridge (l_2) regularization effect can be realized by appending a $p \times p$ diagonal matrix $\sqrt{\lambda}\mathbf{I}$ (where λ is the tuning parametric) to the design matrix and p rows of 0 to the outcome variable in a linear regression model ([Allen, 1974](#); [Hastie et al., 2009a](#)).

In this discussion, we explore the utility of NI in regularizing undirected graphical models (UGMs) including the Gaussian graphical models (GGMs), where the injected noises are adaptive to the learned parameters during the computational iterations rather than being drawn from a fixed distribution, so to achieve various regularization effects on the graph parameters.

1.2 undirected graphical models (UGMs)

A graphical model is a probabilistic model that expresses the conditional dependence structure among random variables. The random variables are often referred to as the nodes. If two nodes are dependent conditional on all the other nodes in the graph, then the relationship is represented by an edge between the two nodes in the graph; otherwise, there is no edge. The edges in an UGM have no orientation. We denote a UGM by $G(\mathbf{X}, \mathbf{A})$, where \mathbf{X} refer to the data observed in the p nodes in a graph and \mathbf{A} is the $p \times p$ a symmetric adjacency matrix (weighted or unweighted) to be estimated. A non-zero entry A_{ij} represents conditional dependence between nodes i and j .

Many real-life networks are believed to be sparse, such as biological networks (Leclerc, 2008). In addition, data collected for estimating edges often have $n < p$. Given both the practical and technical needs, regularization techniques that promotes sparsity are often employed when constructing a UGM. A popular approach is the neighborhood selection (NS) method which estimates \mathbf{A} by columns via modeling the conditional distribution of each node (the outcome node) given all the other nodes (the covariates nodes). In each of the p regression models, regularization techniques that promote sparsity in the relationships between the outcome node and the covariate nodes can be applied, such as the lasso (Meinshausen and Bühlmann, 2006), the graphical Dantzig selector (Yuan, 2010; Cai et al., 2011), the graphical scaled lasso (Sun and Zhang, 2012) and the SQRT-Lasso (Liu and Wang, 2012; Belloni et al., 2012). When the conditional distributions belong to the exponential family, the generalized linear models (GLMs) can be used in each of the p regression models, including the well-know Gaussian graphical models (GGMs), the logistic regression models and Ising models for Bernoulli nodes (Ravikumar et al., 2010; Hofing and Tibshirani, 2009; Kuang et al., 2017; Jalali et al., 2011), the Poisson regression for count nodes (Allen and Liu, 2012). In addition to modeling nodes of the same type in a UGM, there also exist works for mixed graph models (MGMs) where the nodes are of mixed types in a UGM (Fellinghauer et al., 2013; Yang et al., 2012a, 2014).

For GGMs, there exist other approaches for edge estimation besides the NS approach. Huang et al. (2006) applied the l_1 penalty on the elements of the Cholesky decomposition (CD) of the precision matrix Ω , leading to the Lasso-type shrinkage of the coefficients with zeros in the triangular matrix L . Levina et al. (2008) applied the adaptive banding method with a novel nested Lasso penalty on the coefficients of linear regressions after the CD, motivated by the banding method (Bickel and Levina, 2008). Inspired by the matrix logarithm of a covariance matrix (Chiu et al., 1996) and the unconstrained parameterizations using covariates (Pourahmadi, 1999, 2000), Liu and Xi (2015) reformulated the NS as a regularized quadratic optimization problem without directly employing the Gaussian likelihood. Another line of research focuses on estimating Ω as a whole while ensuring its positive-definiteness and sparsity. Yuan and Lin (2007) proposed a l_1 penalized likelihood approach that accomplishes model selection and estimation simultaneously and also ensures the positive-definiteness of the estimated Ω . J. Friedman and Tibshirani (2008); O. Banerjee and d’Aspremont (2008); Rothman et al. (2008) proposed efficient computational algorithms to implement the l_1 penalized likelihood approach. Theoretical properties of the penalized likelihood methods were developed in (Ravikumar et al., 2008), (Rothman et al., 2008) and (Lam and Fan, 2009).

1.3 our contributions

We propose AdaPtive Noisy Data Augmentation (PANDA) - a general, novel, and effective NI technique to regularize the estimation and constructions of a single UGM and joint estimation of multiple UGMs. PANDA augments the original data of size n with properly designed noisy observations of size n_e to achieve the desired regularization effects on the graph parameters.

Since the augmented data set has $n^* = n + n_e > p$, the regular ordinary least squares (OLS) or maximum likelihood estimation (MLE) approaches can be employed to estimate the model parameters without complicated optimization algorithms.

To the best of our knowledge, this is the first paper that explores NI, more specifically, the data augmentation technique for regularizing UGMs. The overarching goal is to show PANDA delivers non-inferior performance to the existing UGM construction approaches and on top of that, offers additional learning, inferential and computational advantages, as listed below.

1. By properly designing the variance terms of the augmented observations, PANDA can achieve various regularization effects on UGM estimation, including lasso (l_1), ridge (l_2), bridge (l_{2-p} for $0 < p \leq 2$), elastic nets ($l_1 + l_2$), SCAD, group lasso, and graphical ridge in single graph estimation.
2. The PANDA algorithm can be used to construct mixed graph models, where the nodes are of different type in a graph, just as easy as estimating a graph with the same types of nodes, given its GLM regression-based framework.
3. The computation in PANDA is straightforward and only employs the regular OLS in linear regression and MLE approaches in GLMs to iteratively estimate the model parameters as it can given that the size of the augmented data ($n + n_e$) surpasses the dimensionality p of the regression model. The variances of the augmented noises are adaptive to the most up-to-date parameter estimates throughout iterations in PANDA until convergence.
4. We establish the almost sure (a.s) convergence of the noise-augmented loss function to its expectation and the the a.s convergence of the minimizer of the former to the minimizer of the latter as $n_e \rightarrow \infty$ with $(n_e \sigma_e^2) = O(1)$, supporting the practical trainability of the PANDA in estimating graphs.
5. We offer a Bayesian interpretation for PANDA in constructing UGMs from two perspectives and connect PANDA with the empirical Bayes and *maximum a posteriori probability* (MAP) estimate in each iteration of PANDA.
6. We provide the asymptotic distributions for the regularized regression coefficients in GLMs in general through PANDA, based on which, the inferences for the parameters, whether null-valued or not, can be obtained. This is an improvement over some of existing inferential approaches in the framework in variable selection that are either are computationally intensive (e.g. the boot-strap based procedures), or don't provide inferences for null-valued parameters, or are only amenable to certain regression models. In addition, our empirical results suggest the inferences are valid with nominal or near-nominal coverage, and more efficient compared to some existing post-selection procedures.

The rest of the paper is organized as follows. Section 2 presents the PANDA methodology, its expected regularization effects, and the associated computational algorithms. Section 3 presents the Bayes interpretation for PANDA in GGM and UGM construction. Section 4 establishes the consistency on the noise-augmented loss function and the regularized parameter estimates, and provides the asymptotic distributions for the parameter estimates via PANDA in the GLM setting. Section 5 compares PANDA to the constrained optimization approach in edge detection for several types of UGMs, and to a post selection inferential approach in obtaining valid statistical inferences in the GLM settings. Section 6 applies PANDA to understand the dependency structure among the attributes of various types in the autism spectrum disorder data. Section 7 provides some concluding remarks and discusses future development on PANDA.

2 PANDA (AdaPtive Noisy Data Augmentation) for Graph Construction with Regularization

In this section, we present PANDA to regularize the construction of GGMs and UGMs via NS (Sec 2.1, 2.1.1, 2.1.3). In the case of GGM construction, in addition to NS, PANDA can also be implemented in the context of other types of regularization than the NS framework, which will be detailed in Sec 2.2.2, 2.2.3, and 2.2.4.

2.1 NA via PANDA in UGM

For NS via PANDA, we assume the conditional distributions of the nodes in a UGM come from the exponential family

$$p(X_j|\mathbf{X}_{-j}) = \exp(X_j\eta_j - B_j(\eta_j) + h_j(X_j)), \quad (1)$$

where $j = 1, \dots, p$ is the index for the p nodes, $\mathbf{X}_{-j} = (X_1, \dots, X_{j-1}, X_{j+1}, \dots, X_p)^T$, and η_j is the natural parameter (we assume the dispersion/scale parameter is known). In the GLM framework, $\eta_j = \sum_{k \neq j} \theta_{jk} X_k$. If the canonical link function g_j is used (e.g., g_j is the identity link for Gaussian X_j and is the logit link for Bernoulli X_j). If the regression coefficient $\theta_{jk} = 0$, then $A[j, k] = 0$ and there is no edge between nodes j and k ; otherwise, the two nodes are connected and the edge weight is quantified by θ_{jk} . Yang et al. (2012b, 2015) proved that asymptotically with probability 1 that the neighborhood structure of conditionally exponential family graphical models can be recovered exactly.

The PANDA technique estimates $\boldsymbol{\theta} = \{\theta_{jk}\}$ by first augmenting the observed data \mathbf{x} with a noisy data matrix. Figure 1 depicts a schematic of the data augmentation step in PANDA for a single graph. Specifically, the ‘‘outcome’’ node X_j is augmented with values that depend on

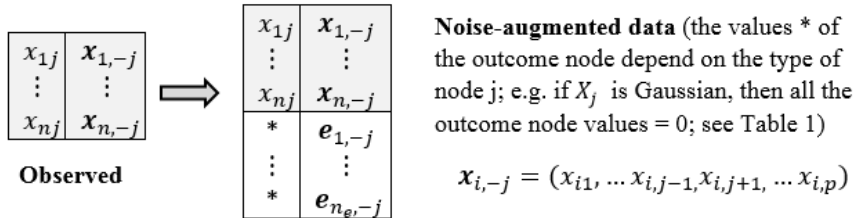


Figure 1: A schematic of the data augmentation for a single graph in PANDA

the type of the outcome variables (refer to Table 1; e.g., 0’s if X_j is a Gaussian), while the augmented observations for the ‘‘covariate’’ node X_k ($k \neq j$) are drawn independently from a Gaussian distribution with mean 0 and variance term that depends on θ_{jk} and tuning parameters, which are referred to as the *Noise Generating Distributions* (NGDs) (Eqns (2) to (7)).

$$e_{jk} \sim N(0, \lambda|\theta_{jk}|^{-\gamma}) \quad (2)$$

$$e_{jk} \sim N(0, \lambda|\theta_{jk}|^{-1} + \sigma^2) \quad (3)$$

$$e_{jk} \sim N\left(0, \lambda|\theta_{jk}|^{-1}|\hat{\theta}_{jk}|^{-\gamma}\right), \text{ where } \hat{\theta}_{jk} \text{ is a consistent estimate for } \theta_{jk}, \quad (4)$$

$$e_{jk} \sim N\left(0, \frac{\lambda}{|\theta_{jk}|} 1_{(0, \lambda n_e)}(|\theta_{jk}|) + \frac{1}{(a-1)} \left(\frac{a\lambda}{|\theta_{jk}|} - \frac{\lambda^2 n_e}{2\theta_{jk}^2} - \frac{1}{2} \right) 1_{[\lambda n_e, a\lambda n_e]}(|\theta_{jk}|) + \frac{(a+1)\lambda^2 n_e}{2\theta_{jk}^2} 1_{(a\lambda n_e, \infty)}(|\theta_{jk}|) \right), \text{ where } 1_{(l,u)}(|\theta_{jk}|) = 1 \text{ if } l < |\theta_{jk}| < u, 0 \text{ otherwise.} \quad (5)$$

$\sigma^2 \geq 0, \lambda > 0, \gamma < 2, a > 2$ are tuning parameters, either user-specified or chosen by a model selection criterion such as cross validation (CV), AIC, or BIC in the practical implementation. Different formulation of the variance term in leads to different regularization effects θ_{jk} . Specifically, Eqn (2) leads to the bridge-type regularization, Eqn (3) for elastic net, Eqn (4) for adaptive lass, and Eqn (5) for SCAD, respectively. Eqns (2) to (5) suggest that the dispersion of the noise terms varies by node: nodes associated with small-valued $|\theta_{jk}|$ will be augmented with more spread out noises, where those with large-valued $|\theta_{jk}|$ will be augmented with noises around zero.

In addition to the regularization effects realized by the NGDs listed in Eqns (2) to (5), PANDA can also implement other types of regularization. For example, if regularization is desired for a group of q covariate nodes simultaneously that share connection patterns with the same node (e.g., genes on the same pathway, binary dummy variables created from the same categorical variable), the augmented noises to these q nodes, denoted by $\mathbf{e} = (e_1, \dots, e_q)^T$, can be generated from Eqn (6) to yield a group lasso-like penalty on a group of θ 's, or from Eqn (7) to yield a fused-ridge type penalty on θ 's.

$$\mathbf{e} \sim N_{(q)} \left(\mathbf{0}, \text{diag} \left\{ \lambda \left(\sum_{k=1}^q \theta_k^2 \right)^{-1/2} \right\} \right), \quad (6)$$

$$\mathbf{e} \sim N_{(q)} \left(\mathbf{0}, \lambda (\mathbf{T}\mathbf{T}^T) \right), \quad (7)$$

where the entries $T_{kk} = 1, T_{k+1-k,1(k=q),k} = -1$ for $k = 1, \dots, q$; and 0 otherwise.

The group-lasso regularization in Eqn (6) sets all θ_{jk} 's in the same group either at zero or nonzero simultaneously, whereas the fused ridge regularization in Eqn (7) promotes numerical similarity among θ_k 's in the same group and does not necessarily lead to edge sparsity. A fused lasso type of regularization can be obtained by using $|\theta_k - \theta_{k'}|^{-1}$ ($k \neq k'$) in the covariance matrix of \mathbf{e} ; however, it does not outperform the fused ridge in terms of promoting similarity on parameter estimation (or similarity on edge patterns when jointly estimating multiple graphs). Therefore we focus our discussion on the fused ridge through the rest of the paper.

In the practical implementation of PANDA, θ_{jk} , on which the variance of the NGD depends, is unknown. The augmented noises at iteration t are drawn from the NGD the variance of which uses the estimate of θ_{jk} from iteration $t - 1$. In that sense, PANDA is an adaptive procedure given that the dispersion of the augmented noise depends on the latest estimate of θ_{jk} and varies with iteration. The iterative procedure continues until the convergence criterion is met.

2.1.1 PANDA-NS for GGM

When $\mathbf{X} \sim N_p(\boldsymbol{\mu}, \Sigma)$, where Σ is the covariance matrix, the conditional distribution X_j given \mathbf{X}_{-j} is $N(\mu_j + \Sigma_{j,-j} \Sigma_{-j,-j}^{-1} (\mathbf{X}_{-j} - \boldsymbol{\mu}_{-j}), \Sigma_{j,j} - \Sigma_{j,-j} \Sigma_{-j,-j}^{-1} \Sigma_{-j,j})$ for $j = 1, \dots, p$, where $\Sigma_{j,j}$ is the j -th diagonal element of Σ , $\Sigma_{-j,-j}$ is the submatrix of Σ with the j -th row and the j -th column removed, and $\Sigma_{j,-j}$ is the j -th row of Σ with the j -th element removed, and $\Sigma_{-j,j} = \Sigma_{j,-j}^T$. The conditional distribution suggests the following linear model

$$\begin{aligned} X_j &= \alpha_j + \mathbf{X}_{-j}^T \boldsymbol{\theta}_j + \epsilon_j, \text{ where } \epsilon_j \sim N(0, \sigma_j^2), \\ \alpha_j &= \mu_j - \Sigma_{j,-j} \Sigma_{-j,-j}^{-1} \boldsymbol{\mu}_{-j}, \boldsymbol{\theta}_j = \Sigma_{-j,-j}^{-1} \Sigma_{-j,j}, \text{ and } \sigma_j^2 = \Sigma_{j,j} - \Sigma_{j,-j} \Sigma_{-j,-j}^{-1} \Sigma_{-j,j} \end{aligned} \quad (8)$$

The intercepts α_j ($j = 1, \dots, p$) can be set at 0 with centered \mathbf{X} . Let $\Omega = \Sigma^{-1}$ and ω_{jk} denote the elements in Ω ; then $\omega_{jj} = \hat{\sigma}_j^{-2}$ and $\theta_{kj} = -\omega_{jj}^{-1} \omega_{kj}$ for $k \neq j$ (Hastie et al., 2009b), implying that $\theta_{kj} = 0$ ($k \neq j$) is equivalent to $\omega_{kj} = 0$ and no edge between nodes j and k .

Running p regressions separately in Eqn (8) on a data set does not lead to a symmetric Ω estimate nor does it guarantee its positive definiteness. The situation is similar when an explicit penalty

term is imposed on θ_j in Eqn (8) to achieve a certain type of regularization (e.g., sparsity). If the main goal is to determine the existence of an edge between nodes j and k , there are two common practices leading to null-edge between nodes j and k (Meinshausen and Bühlmann, 2006): the intersection rule $\{\hat{\theta}_{jk} = 0\} \cap \{\hat{\theta}_{kj} = 0\}$ and the union rule $\{\hat{\theta}_{jk} = 0\} \cup \{\hat{\theta}_{kj} = 0\}$, with the latter resulting in less edges.

PANDA regularizes the estimation of θ_{jk} with iterative injection of Gaussian noises drawn from the NGDs. During an iteration, in the j -th regression with outcome node X_j , PANDA combines the observed data in node j with 0's, i.e., $\mathbf{e}_{jj} = (e_{1,jj}, \dots, e_{n_e,jj})^T = (0, \dots, 0)$, and those in node k ($k \neq j$) with noise $\mathbf{e}_{jk} = (e_{1,jk}, \dots, e_{n_e,jk})^T$ drawn from a NGD in Eqns (2) to (5). n_e , the size of augmented noisy data, should be large enough so that $n + n_e > p$ and θ_j can be estimated with the OLS estimation from the regression model in Eqn (8) with the augmented data.

Proposition 1 establishes that PANDA, in expectation with regard to the distribution of the injected noise, is equivalent to minimizing the overall penalized SSE in the p linear regression models with a penalty term on $\Theta = \{\theta_j\}$ for $j = 1, \dots, p$. In other words, PANDA achieves the same global optimum as in Yuan (2010) by iteratively solving the OLS of Θ until convergence. The proof of Proposition 1 is given in Appendix A.

Proposition 1 (Regularization effects of PANDA-NS in a single GGM). *Define the loss function as the overall SSE $l(\Theta|\mathbf{x}) = \sum_{j=1}^p \sum_{i=1}^n (x_{ij} - \sum_{k \neq j} x_{ik} \theta_{jk})^2$. The loss function based on the augmented data is $l_p(\Theta|\mathbf{x}, \mathbf{e}) = \sum_{i=1}^{n+n_e} \sum_{j=1}^p (\tilde{x}_{ij} - \sum_{k \neq j} \tilde{x}_{ik} \theta_{jk})^2$ and its expectation over the distribution of noise \mathbf{e} is*

$$E_{\mathbf{e}}(l_p(\Theta|\mathbf{x}, \mathbf{e})) = l(\Theta|\mathbf{x}) + P(\Theta; \lambda, \gamma, \sigma^2, a). \quad (9)$$

The penalty term $P(\Theta; \lambda, \gamma, \sigma^2, a)$ takes different forms for different NGDs, as listed below:

- $(\lambda n_e) \sum_{j=1}^p \sum_{j \neq k} |\theta_{jk}|^{2-\gamma}$ when $e_{jk} \sim N(0, \lambda |\theta_{jk}|^{-\gamma})$, resulting a bridge-type penalty (the lasso and ridge-type penalties are special case when $\gamma = 1$ and $\gamma = 0$, respectively).
- $(\lambda n_e) \sum_{j=1}^p \sum_{j \neq k} |\theta_{jk}| + (\sigma^2 n_e) \sum_{j=1}^p \sum_{j \neq k} \theta_{jk}^2$ when $e_{jk} \sim N(0, \lambda |\theta_{jk}|^{-1} + \sigma^2)$, resulting a elastic net-type penalty.
- $(\lambda n_e) \sum_{j=1}^p \sum_{j \neq k} |\theta_{jk}| |\hat{\theta}_{jk}|^{-\gamma}$ when $e_{jk} \sim N(0, \lambda |\theta_{jk}|^{-1} |\hat{\theta}_{jk}|^{-\gamma})$, where $\hat{\theta}_{jk}$ is a \sqrt{n} -consistent estimator of θ_{jk} , resulting in an adaptive lasso type of penalty.
- $\sum_{j=1}^p \sum_{j \neq k} \left(n_e \lambda |\theta_{jk}| 1_{(0, \lambda n_e)}(|\theta_{jk}|) + \frac{1}{2(a-1)} \left(2a \lambda n_e |\theta_{jk}| - (\lambda n_e)^2 - \theta_{jk}^2 \right) 1_{[\lambda n_e, a \lambda n_e]}(|\theta_{jk}|) + \frac{a+1}{2} (\lambda n_e)^2 1_{(a \lambda n_e, \infty)}(|\theta_{jk}|) \right)$ when $e_{jk} \sim N\left(0, \frac{\lambda}{|\theta_{jk}|} 1_{(0, \lambda n_e)}(|\theta_{jk}|) + \frac{(a+1)\lambda^2 n_e}{2\theta_{jk}^2} 1_{(a \lambda n_e, \infty)}(|\theta_{jk}|) + \frac{1}{(a-1)} \left(\frac{a\lambda}{|\theta_{jk}|} - \frac{\lambda^2 n_e}{2\theta_{jk}^2} - \frac{1}{2} \right) 1_{[\lambda n_e, a \lambda n_e]}(|\theta_{jk}|) \right)$ for $a > 2$, resulting in a SCAD type of penalty.
- $(\lambda n_e) \sum_{l=1}^g \sqrt{p_l} \|\boldsymbol{\theta}_l\|_2$ when $e_{lk} \sim N\left(0, \frac{\lambda \sqrt{p_l}}{\|\boldsymbol{\theta}_l\|_2}\right)$, where $\boldsymbol{\theta}_l = \{\theta_{l1}, \dots, \theta_{lp_l}\}$, $l = 1, \dots, g$ in the index for the g groups.

The expected regularization $P(\Theta; \lambda, \gamma, \sigma^2, a)$ can be realized in at least two ways empirically, by letting $m \rightarrow \infty$ as in $\sum_{j=1}^p \lim_{m \rightarrow \infty} m^{-1} \sum_{t=1}^m \sum_{i=1}^{n_e} \left(e_{ijj}^{(t)} - \sum_{k \neq j} e_{ijk}^{(t)} \theta_{jk} \right)^2$, or letting $n_e \rightarrow \infty$ as in $n_e \sum_{j=1}^p \lim_{n_e \rightarrow \infty} n_e^{-1} \sum_{i=1}^{n_e} \left(e_{ijj}^{(t)} - \sum_{k \neq j} e_{ijk}^{(t)} \theta_{jk} \right)^2$ unde the constraint $n_e V(e_{ijk}) = O(1)$

With the constraint $n_e V(e_{jk}) = O(1)$, $n_e \rightarrow \infty$ does not imply the injected noise \mathbf{e} would trump the information about Θ in the observed data \mathbf{x} , but $n_e V(e_{jk})$ together is chosen properly to provide the right amount of regularization. For example, the augmented information about Θ through injecting the lass-type \mathbf{e} to regularize a graph estimation is proportional to $n + n_e \lambda$ rather than $n + n_e$ (see Sec 4.2).

Algorithm 1 lists the computational steps of the PANDA to estimate the structure of a GGM, along with some remarks on the choosing some of the algorithmic parameters (Remarks 1,3,4).

Algorithm 1 NS for Single GGM via PANDA

- 1: **Pre-processing:** standardize the observed data \mathbf{x}
 - 2: **Input**
 - initial parameter estimates $\bar{\theta}_j^{(0)}$ for $j = 1, \dots, p$.
 - A NGD in Eqns (2) to (5) and the associated tuning parameters, the maximum iteration T (Remark 1), noisy data size n_e (Remark 4), width of moving average (MA) window m (Remark 4), thresholds τ_0 (Remark 3), banked parameter estimates after convergence r (Remark 3)
 - 3: $t \leftarrow 0$; convergence $\leftarrow 0$
 - 4: **WHILE** $t < T$ **AND** convergence = 0
 - 5: $t \leftarrow t + 1$
 - 6: **FOR** $j = 1 : p$
 - a) Generate noisy data $\mathbf{e}_{.j}$ from $\bar{\theta}_j^{(t-1)}$ plugged in the variance term of the NGD.
 - b) Obtain augmented data $\tilde{\mathbf{x}}_j$ by row-combining $(\mathbf{x}_j, \mathbf{x}_{-j})$ and $(\mathbf{0}, \mathbf{e}_{.j})$
 - c) Obtain OLS estimate $\hat{\theta}_j^{(t)}$ by regressing $\tilde{\mathbf{x}}_j$ on $\tilde{\mathbf{x}}_{-j}$
 - d) If $t > m$, calculate $\bar{\theta}_j^{(t)} = m^{-1} \sum_{l=t-m+1}^t \hat{\theta}_j^{(l)}$; otherwise $\bar{\theta}_j^{(t)} = \hat{\theta}_j^{(t)}$. Calculate the sum of squared error $\text{SSE}_j^{(t)}$ with $\bar{\theta}_j^{(t)}$ plugged in.
 - 7: **END FOR**
 - 8: Calculate loss function $\bar{l}^{(t)} = m^{-1} \sum_{l=t-m+1}^t \sum_{j=1}^p \text{SSE}_j^{(l)}$ and apply one of the convergence criteria listed in Remark 2 to $\bar{l}^{(t)}$. Let convergence $\leftarrow 1$ if the convergence is reached.
 - 9: **END WHILE**
 - 10: Continue to execute the command lines 5 to 7 for another r iterations, and record $\bar{\theta}_j^{(l)}$ for $l = t + 1, \dots, t + r$, calculate the degrees of freedom $\nu_j^{(t)} = \text{trace}(\mathbf{x}_j(\tilde{\mathbf{x}}_j' \tilde{\mathbf{x}}_j)^{-1} \mathbf{x}_j')$ and $\hat{\sigma}_j^{2(l)} = \text{SSE}_j^{(l)} / (n - \nu_j^{(l)})$. Let $\bar{\theta}_{jk} = (\bar{\theta}_{jk}^{(t+1)}, \dots, \bar{\theta}_{jk}^{(t+r)})$.
 - 11: Set $\hat{\theta}_{jk} = \hat{\theta}_{kj} = 0$ if $(|\max\{\bar{\theta}_{jk}\} \cdot \min\{\bar{\theta}_{jk}\}| < \tau_0) \cap (\max\{\bar{\theta}_{jk}\} \cdot \min\{\bar{\theta}_{jk}\} < 0)$ or $(|\max\{\bar{\theta}_{kj}\} \cdot \min\{\bar{\theta}_{kj}\}| < \tau_0) \cap (\max\{\bar{\theta}_{kj}\} \cdot \min\{\bar{\theta}_{kj}\} < 0)$; $\hat{\theta}_{jk} = \hat{\theta}_{kj} = \min\{\bar{\theta}_{jk}^{(t+r)}, \bar{\theta}_{kj}^{(t+r)}\}$ otherwise.
 - 12: To estimate Ω , set $\hat{\omega}_{jj} = \hat{\sigma}_j^{-2(t+r)}$ and $\hat{\Omega}_{-j,j} = -\hat{\theta}_j \hat{\omega}_{jj}$
 - 13: **Output:** $\hat{\theta}$ and $\hat{\Omega}$
-

Remark 1 (maximum iteration T). T should be set at a number large enough so to allow the algorithm to reach per the convergence criterion given in Remark 2 in a reasonable time period. In the simulation and case studies in Sections 5 and 6, and convergence was reached within $T = 50 \sim 150$.

Remark 2 (Convergence criterion). Due to the randomness of the augmented noises from iteration to iteration, there is always some level of fluctuation around the loss function $\bar{l}^{(t)}$ for finite m and n_e . To evaluate the convergence of the PANDA algorithm, we list 3 choices. First, eyeball the trace plots of \bar{l}^t , which is the most straightforward and often sufficient and effective. Second, use a cutoff value, say τ on the absolute percentage change on $\bar{l}^{(t)}$ from two consecutive iterations. That is, if $|\bar{l}^{(t+1)} - \bar{l}^{(t)}| / \bar{l}^{(t)} < \tau$, then we may declare convergence for the PANDA algorithm. τ should be close to 0 when $\bar{\theta}_j^{(t)}$ stabilizes. In the simulation and case studies in Sections 5 and 6, τ was about 1% or less upon convergence. Third, apply a formal statistical test on \bar{l}^t , the details of which is provided in Section 4.4.

Remark 3 (Hard thresholding τ_0 and choice of r). *The hard thresholding τ_0 is necessary and as well as justified. It is needed for setting nonsignificant edges at 0 because, though $\hat{\theta}_{jk}$ can get arbitrarily close to 0, exact 0 estimate for θ_{jk} cannot be achieved computationally in PANDA due to the numerical errors from calculating $(\tilde{\mathbf{x}}'_{j,-j}\tilde{\mathbf{x}}_{j,-j})^{-1}$ and $|\hat{\theta}_{jk}^{(t)}|^{-\gamma}$ in the variance term of the NGD. In addition, even after the convergence of the PANDA algorithm, there might still be mild fluctuation around the parameter estimates, especially for not so large n_e and m . We thus need a sequence of regularized estimates after convergence to apply the hard thresholding to. The sequence length is referred to as r . The hard thresholding is justified because of the estimation and selection consistency property of the PANDA estimator established in Section 4.1.*

Remark 4 (Choice of n_e and m). *As stated in Proposition 1, the expected regularization can be realized empirically by letting $m \rightarrow \infty$ or $n_e \rightarrow \infty \cap [n_e V(e_j k)] = O(1)$. Our empirical results suggest the convergence of Algorithm 1 is faster in the latter case. When n_e is set at a large number, convergence can be reached with $O(10)$ iterations and m as small as 1 or 2 – at least in our simulation setting. Regarding the choice of n_e specifically, the first requirement is $n + n_e > p$ so that a unique OLS can be obtained in each iteration. Second, Proposition 1 suggests n_e , bundled with the tuning parameters from an NGD, such as $n_e \lambda$ in the bridge-type penalty, has some tuning capacity. Regarding the choice of m , it more or less depends on n_e ; if a large enough n_e still results in noticeable fluctuation around $\hat{\Theta}$, then a large m will help to speed up the stabilization $\hat{\Theta}$.*

2.1.2 Connection between PANDA-NS for GGM and weighted ridge regression

Algorithm 1 shows the OLS estimator is obtained from the noise-augmented data in each iteration of the PANDA algorithm. Corollary 1 states that the OLS estimator obtained this way can be regarded as a weighted ridge estimator. Compared to the regular ridge estimator, where the same constant λ is added onto all the diagonal elements of $\mathbf{x}'_{j,-j}\mathbf{x}_{j,-j}$, λ varies by the diagonal elements in the weighted ridge estimator.

Corollary 1 (PANDA and weighted ridge regression). *The OLS estimator with outcome node X_j in each iteration of PANDA on the noise augmented data is equivalent to the weighted ridge estimator $\hat{\theta}_j = (\mathbf{x}'_{j,-j}\mathbf{x}_{j,-j} + \mathbf{e}_{j,-j}^T \mathbf{e}_{j,-j})^{-1} \mathbf{x}_{j,-j} \mathbf{x}_j$.*

The proof is straightforward. Let $\tilde{\mathbf{x}} = (\mathbf{x}, \mathbf{e})^T$. In each iteration of PANDA, the OLS estimator $\hat{\theta}_j = (\tilde{\mathbf{x}}^T_{j,-j}\tilde{\mathbf{x}}_{j,-j})^{-1} \tilde{\mathbf{x}}^T_{j,-j}(\mathbf{x}_j, \mathbf{0}) = (\mathbf{x}'_{j,-j}\mathbf{x}_{j,-j} + \mathbf{e}_{j,-j}^T \mathbf{e}_{j,-j})^{-1} \mathbf{x}_{j,-j} \mathbf{x}_j$, leading to Corollary 1. If $n_e \rightarrow \infty$, then $\mathbf{e}_{j,-j}^T \mathbf{e}_{j,-j} \rightarrow n_e V(\mathbf{e}_{j,-j})$. For example, if the NGD is $N(0, \lambda |\theta_{jk}^{-\gamma}|)$, then $n_e V(\mathbf{e}_{j,-j}) = \text{diag}((n_e \lambda) |\theta_{jk}^{-\gamma}|)$ for $k \neq j$; and (λn_e) can be tuned as one single tuning parameter.

2.1.3 PANDA for UGMS with non-Gaussian nodes

When the conditional distribution of a node given the others comes from the Exponential family, then regardless whether the nodes are of the same type or mixed types, PANDA-NS can regularize its construction via running GLMs with the canonical link functions on noise-augmented data. Proposition 2 states the expected regularization effects of PANDA in UGMs. The proof is given in Appendix B.

Proposition 2 (Regularization effects of PANDA in UGMs). *Let the loss function given \mathbf{x} be the summation of the negative log-likelihood over p GLMs $l(\Theta|\mathbf{x}) = -\sum_{j=1}^p \sum_{i=1}^n (h_j(x_{ij}) + (\sum_{k \neq j} \theta_{jk} x_{ik})) x_{ij} - B_j(\sum_{k \neq j} \theta_{jk} x_{ik})$, and the loss function given with the noise augmented data*

$\tilde{\mathbf{x}} = (\mathbf{x}, \mathbf{e})$ is

$$l_p(\Theta|\mathbf{x}, \mathbf{e}) = - \sum_{j=1}^p \left\{ \sum_{i=1}^{n+n_e} \left(h_j(\tilde{x}_{ij}) + \left(\sum_{k \neq j} \theta_{jk} \tilde{x}_{ik} \right) \tilde{x}_{ij} \right) - B_j \left(\sum_{k \neq j} \theta_{jk} x_{ik} \right) \right\}. \quad (10)$$

Denote by Θ the collection of $\theta_j = \{\beta_{jk}\}$ ($j \neq k$). Apply the second-order expansion of l_p around $\sum_{k \neq j} \theta_{jk} x_{ik} = 0$, the expectation of which over the distribution of \mathbf{e} is

$$E_{\mathbf{e}}(l_p(\Theta|\mathbf{x}, \mathbf{e})) = l(\Theta|\mathbf{x}) + P(\Theta; V(e_{jk}), n_e), \text{ where} \\ P(\Theta; V(e_{jk}), n_e) = n_e \sum_{j=1}^p \left(C_{j2} \sum_{k \neq j} \theta_{jk}^2 V(e_{jk}) \right) + C_1 + O\left(n_e \sum_{j=1}^p \sum_{k \neq j} \left(\theta_{jk}^4 V^2(e_{jk}) \right) \right), \quad (11)$$

where $C_1 = \sum_{j=1}^p \sum_{i=1}^{n_e} h_j(e_{ijj}) + B_j(0)$ and $C_{j2} = B_j''(0)$, constants independent of Θ .

The actual form $P(\Theta; V(e_{jk}), n_e)$ depends on the type of X_j and the NGD from which \mathbf{e} is drawn. Table 1 lists $P(\Theta; V(e_{jk}), n_e)$ if the lasso-type NSG in Eqn (2) ($\gamma = 1$) is use for several types of graphs. The graphs are named after the outcome node X_j . For examples, if all the nodes follow a Bernoulli distribution given all other nodes, then the graph is called Bernoulli graph model (BGM); similarly for EGM (Exponential), PGM (Poisson), and NBGM (Negative Binomial). For different type of outcome node X_j , different values of e_{jj} are augmented, the reasons for which involves consistency considerations (see Sec 4.1 and the associated proofs).

Graph	e_{jj}	$P(\Theta; V(e_{jk}), n_e)$
GGM	0	$\frac{\lambda n_e}{2} \sum_{j=1}^p \sum_{k \neq j} \theta_{jk} $
BGM	1	$\frac{\lambda n_e}{2} \sum_{j=1}^p \sum_{k \neq j} \theta_{jk} + p n_e \log 2 + O(\lambda^2 n_e \ \Theta\ _2^2)$
EGM	1	$\frac{\lambda n_e}{2} \sum_{j=1}^p \sum_{k \neq j} \theta_{jk} + p n_e + O(\lambda^2 n_e \ \Theta\ _2^2)$
PGM	1	$\frac{\lambda n_e}{2} \sum_{j=1}^p \sum_{k \neq j} \theta_{jk} + 2 p n_e + O(\lambda^2 n_e \ \Theta\ _2^2)$
NBGM [†]	1	$\frac{\lambda n_e r}{2(r+1)} \sum_{j=1}^p \sum_{k \neq j} \theta_{jk} + p n_e (r+1) \log(r) + O(\lambda^2 n_e \ \Theta\ _2^2)$

[†] r is the number of failures.

Table 1: Expected penalty term in PANDA with lass-type noise augmentation for various graphs

Similar to Proposition 1, there are at least 2 ways to realize the expectation of $l_p(\Theta|\mathbf{x}, \mathbf{e})$ empirically. The straightforward way is let $l_p(\Theta|\mathbf{e})$ be approximated by

$$\lim_{m \rightarrow \infty} m^{-1} \sum_{t=1}^m \sum_{j=1}^p \sum_{i=1}^{n_e} l(\theta_j | \mathbf{e}_{i,-j}^{(t)}). \quad (12)$$

The second approach, suggested by Eqn (11), under the constraint $n_e V(e_{jk}) = O(1)$, is to let $n_e \rightarrow \infty$, and the second term in Eqn (11)

$$n_e \sum_{j=1}^p C_{j2} \sum_{k \neq j} \theta_{jk}^2 V(e_{ijk}) = n_e \sum_{j=1}^p C_{j2} \sum_{k \neq j} \left(\theta_{jk}^2 \lim_{n_e \rightarrow \infty} n_e^{-1} \sum_{i=1}^{n_e} \mathbf{e}_{ijk}^2 n_e V(e_{ijk}) \right). \quad (13)$$

Between Eqns (12) and (13), the latter is better in that $O\left(\sum_{j=1}^p \sum_{k \neq j} \left(\theta_{jk}^4 n_e V^2(e_{jk})\right)\right) \rightarrow 0$ in Eqn (11). In other words, the second order Taylor approximation of $E_{\mathbf{e}}(l_p(\Theta|\mathbf{x}, \mathbf{e}))$ is arbitrarily close to $E_{\mathbf{e}}(l_p(\Theta|\mathbf{x}, \mathbf{e}))$, which does not hold when $m \rightarrow \infty$. The O residual term, which is a function of Θ , might bring additional regularization effect Θ in addition to $\theta_{jk}^2 (n_e V(e_{jk}))$ when it is non-ignorable.

To illustrate the regularization effects on PANDA in GLMs and how they vary by using large n_e vs large m , we display in Figure 2 $P(\Theta; V(e_{jk}), n_e)$ vs θ in different graph types, along with its empirical version when the augmented noises are drawn from the NGD in Eqn (2) with λn_e set at 1 and γ at 1 (thus $V(e_{jk}) = \lambda |\theta_{jk}|^{-1}$ and the lasso penalty). The regularization effect in EGM looks very similar to the PGM and is not provided. The penalty imposed PANDA on θ is linear in

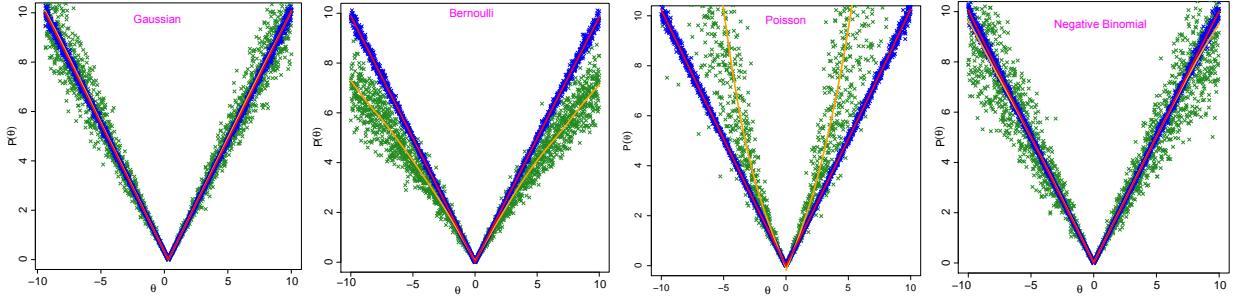


Figure 2: Penalty $P(\theta; \lambda, n_e)$ for θ . Red and orange lines are the expected penalty when $(n_e \rightarrow \infty) \cap (\lambda n_e = 1)$ and $m \rightarrow \infty$, respectively; blue and green dots are their respective empirical penalty by setting $(n_e = 100, m = 50)$ and $(n_e = 5, m = 50)$.

$|\theta|$ all four GLMs by $n_e \rightarrow \infty$ (with $\lambda n_e = 1$ fixed at 1), which are the red lines; and its empirical version (the blue dots) at $n_e = 100$ is already close to the analytic forms in all four GLM cases. On the other hand, the penalty on θ by $m \rightarrow \infty$ while n_e is small (5 in this case) varies by the GLM and is not necessarily linear, demonstrating the penalty introduced by the O residual term in addition to the second term in Eqn (11) when $|\theta|$ is large, except for the linear regression where the O residual term is exactly 0. For example, the additional regularization from the residual term makes the penalty sub-linear in logistic regression and NB regression (though it is not obvious in the latter), and super-linear in Poisson regression (and Exponential regression; results not shown), and only gets stronger as $|\theta|$ increase. When $|\theta|$ is small, the distinction between $n_e \rightarrow \infty$ and $m \rightarrow \infty$ is barely there in four cases.

Due to space limitation, we list the computational steps in PANDA for constructing UGMs in Algorithm S1 in the Supplementary Materials. Most of the steps are similar to Algorithm 1 for GGMs, with a few differences. First, there is no need to standardize data as a pre-processing step. Second, each iteration t obtains the MLE $\hat{\theta}_j^{(t)}$ from regressing \tilde{x}_j on all other columns \tilde{x}_{-j} with a proper GLM for $j = 1, \dots, p$. Third, the loss function used in evaluating the convergence of the algorithm is the sum of the negative log-likelihood in Eqn (10). The guidelines for choosing of the algorithmic parameters, such as T, τ_0, n_e and m , and evaluating the convergence as laid out in Remarks 1 to 4 also apply to the UGM algorithm as well. When choosing n_e , besides the guidance listed in Remark 4, that is, $n + n_e > p$, n_e also needs to be set at a large value so to get the nominal regularization effects. If n_e is not large enough, there will be extra regularization not per design, as demonstrated with the non-ignorable residual term (see Eqn (11) and Figure 2).

2.2 Other regularization in GGMs via PANDA

In GGMs, leveraging the connection between the graph structure and the precision matrix of the multivariate Gaussian distribution, additional approaches have been proposed to construct GGMs. We list three of these approaches and show PANDA can realize them through noise augmentation.

2.2.1 PANDA-SPACE for hub nodes detection in GGM

In GGM, the elements in the precision matrix Ω are related to partial correlation coefficient ρ_{jk} 's in the regression with outcome node X_j and covariate nodes X_k for $k \neq j = 1, \dots, p$ as in $\rho_{jk} = -\omega_{jk} / \sqrt{\omega_{jj}\omega_{kk}}$. SPACE (Sparse Partial Correlation Estimation) is an approach to select nonzero partial correlations when $n < p$ (Peng et al., 2009). Corollary 2 shows that PANDA can

be used to construct GGM by imposing a bridge-type penalty on ρ_{jk} . The biggest advantage of PANDA-SPACE, compared to NS through estimating regression coefficients θ_{jk} , is that it identifies not only nonzero partial correlations, but also is efficient for identifying hub nodes.

Corollary 2 (PANDA-SPACE). *Let $e_{jk} \stackrel{ind}{\sim} N(0, \lambda |\rho_{jk}|^{-\gamma} \omega_{jj} \omega_{kk}^{-1})$, $e_{jj} \equiv 0$, $\Theta = \{\rho_{jk}, \omega_{jj}\}$, and $l(\Theta|\mathbf{x}) = \sum_{i=1}^n \sum_{j=1}^p \left(x_{ijj} - \sum_{k \neq j} x_{ijk} \rho_{jk} \sqrt{\omega_{kk}/\omega_{jj}}\right)^2$. Then*

$$\begin{aligned} l_p(\Theta|\mathbf{x}, \mathbf{e}) &= l(\Theta|\mathbf{x}) + \sum_{i=1}^{n_e} \sum_{j=1}^p \left(\sum_{k \neq j} e_{ijk} \rho_{jk} \sqrt{\omega_{kk}/\omega_{jj}}\right)^2, \\ E(l_p(\Theta|\mathbf{x}, \mathbf{e})) &= l(\Theta|\mathbf{x}) + \lambda n_e \sum_{j=1}^p \sum_{j \neq k} |\rho_{jk}|^{2-\gamma}. \end{aligned}$$

2.2.2 PANDA-CD in GGMs

The Cholesky decomposition (CD) approach refers to estimating the precision matrix through the LDL decomposition, a variant of the CD. Compared to the NS approach in Section 2.1.1, the CD approach guarantees symmetry and positive definiteness of the estimated $\hat{\Omega}$. WLOG, let $\mathbf{x}_{n \times p} \sim N_p(\mathbf{0}, \Omega)$. The corresponding negative log-likelihood is $l(\Omega|\mathbf{x}) = -n \log(|\Omega|) + \frac{1}{2} \sum_{i=1}^n \mathbf{x}_i^T \Omega \mathbf{x}_i$. There exists a unique CD (more specifically, the LDL decomposition) of $\Omega = L^T D^{-1} L$, such that $|\Omega| = |D|^{-1} = \prod_{j=1}^p \sigma_j^{-2}$, where $D = \text{diag}(\sigma_1^2, \dots, \sigma_p^2)$, and L is a lower uni-triangular matrix with elements $-\theta_{jk}$ for $j > k$, 0 for $k < j$, and 1 for $j = k$. Therefore,

$$l(\Omega|\mathbf{x}) = l(L, D|\mathbf{x}) = n \log |D| + \sum_{i=1}^n \mathbf{x}_i^T L^T D^{-1} L \mathbf{x}_i = n \log |D| + \sum_{i=1}^n (L \mathbf{x}_i)^T D^{-1} L \mathbf{x}_i \quad (14)$$

$$= n \sum_{j=1}^p \log \sigma_j^2 + \sum_{i=1}^n \sum_{j=1}^p \sigma_j^{-2} \left(x_{ij} - \sum_{k=1}^{j-1} x_{ik} \theta_{jk}\right)^2. \quad (15)$$

Huang et al. (2006) apply the l_γ ($\gamma > 0$) regularization on θ_{jk} to the negative log-likelihood (15) and minimize it by solving Eqns (17) and (16) alternatively in an iterative manner.

$$\hat{\theta}_j = \arg \min_{\theta_j} \hat{\sigma}_j^{-2} \sum_{i=1}^n \left(\mathbf{x}_{ij} - \sum_{k=1}^{j-1} \mathbf{x}_{ik} \theta_{jk}\right)^2 + \xi \sum_{k=1}^{j-1} |\theta_{jk}|^\gamma. \quad (16)$$

$$\hat{\sigma}_j^2 = n^{-1} \sum_{i=1}^n \left(\mathbf{x}_{ij} - \sum_{k=1}^{j-1} \mathbf{x}_{ik} \hat{\theta}_{jk}\right)^2, \quad (17)$$

Optimization and regularization occurs only on θ_j in Eqn (16), whereas Eqn (16) is fully determined once θ_j is estimated. We show below the above framework can also be realized via PANDA. Instead of solving the optimization problem in Eqn (16), PANDA calculates the OLS of θ_j based on noise-augmented data. Eqn (14) implies $L\mathbf{X} = \boldsymbol{\epsilon}$, where $\boldsymbol{\epsilon} \sim N(\mathbf{0}, D)$. Then

$$X_1 = \epsilon_1 \text{ and } X_j = \sum_{k=1}^{j-1} X_k \theta_{jk} + \epsilon_j \text{ for } j = 2, \dots, p, \quad (18)$$

suggesting the following sequence of regression models: X_2 regressed on X_1 , X_3 regressed on (X_1, X_2) , and so on. PANDA first augments the observed data in the outcome node X_j with 0 and those in each of the predictor nodes in Eqn (18) with n_e noise terms sampled from a NGD (Eqns 2) to 5). Figure 3 depicts a schematic of the data augmentation step in PANDA-CD. Note though the earlier regression has less predictors and thus does not suffer the $n < p$ problem, n_e and the tuning parameters in the NGD should be the same in every regression, so to achieve the nominal regularization effect.

The steps of the PANDA-CD algorithm are listed in Algorithm S2 in the Supplementary Materials. Proposition 3 establishes that the expected noised-augmented likelihood function over the distribution of the bridge-type noise \mathbf{e} is equivalent to the penalized likelihood function in Eqn (16), with λn_e as a turning parameter (similar to ξ in Eqn (16)). The proof of Proposition

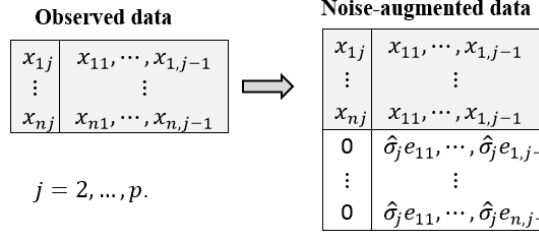


Figure 3: A schematic of the data augmentation in PANDA-CD for a single GGM estimation

3 is given in Appendix C. It is very straightforward to extend Proposition 3 to other types of noises by replacing the NGDs with one given in Eqns (3) to (5), which will lead to other types of regularization effects on θ_j .

Proposition 3 (Regularization effects of PANDA for CD in a single GGM). *Let $l(L|\mathbf{x}) = \sum_{j=1}^p \hat{\sigma}_j^{-2} \sum_{i=1}^n \left(x_{ij} - \sum_{k=1}^{j-1} x_{ik} \theta_{jk} \right)^2$. The noise-augmented loss function $l_p(L|\mathbf{x}, \mathbf{e}) = \sum_{j=1}^p \hat{\sigma}_j^{-2} \sum_{i=1}^n \left(x_{ij} - \sum_{k=1}^{j-1} x_{ik} \theta_{jk} \right)^2 + \sum_{j=1}^p \hat{\sigma}_j^{-2} \sum_{i=1}^{n_e} \left(e_{ijj} - \sum_{k=1}^{j-1} e_{ijk} \theta_{jk} \right)^2$; and its expectation over the distribution of \mathbf{e} drawn from the NGD in Eqn (2) is*

$$E_{\mathbf{e}}(l_p(L|\mathbf{x}, \mathbf{e})) = l(L|\mathbf{x}) + \lambda n_e \sum_{j=1}^p \sum_{k=1}^{j-1} |\theta_{jk}|^{2-\gamma} \quad (19)$$

2.2.3 PANDA-SCIO in GGMs

The Sparse Columnwise Inverse Operator (SCIO) estimator (Liu and Xi, 2015) of the precision matrix Ω of a GGM is realized by solving p l_1 -regularized quadratic optimization problems:

$$\hat{\theta}_j = \arg \min_{\theta_j \in \mathbb{R}^p} \left\{ l_j + \lambda \sum_{k \neq j} |\theta_{jk}| \right\}, \text{ where the objective function } l_j = \frac{1}{2} \theta_j^t \hat{\Sigma} \theta_j - \mathbf{1}_j \theta_j \quad (20)$$

for $j = 1, \dots, p$. θ_j is the j -th column of Ω , $\hat{\Sigma} = n^{-1} x'x$, $\mathbf{1}_j$ is a row binary vector of dimension p with 1 at the j^{th} element and 0 otherwise, and $\lambda > 0$ is a tuning parameter. Once θ_j is estimated for $j = 1, \dots, p$, ω_{jk} in Ω is estimated by $\hat{\omega}_{kj} = \min\{\hat{\theta}_{jk}, \hat{\theta}_{kj}\}$.

We show that the PANDA technique can be used to obtain the SCIO estimator that only needs to take the inverses of a positive definitive matrices, without resorting to complicated optimization algorithms with constraints. Since the SCIO estimator in (Liu and Xi, 2015) only used the l_1 regularization in Eqn (20), we demonstrate PANDA using the lasso-type augmented noise. However other types of noises from NGDs in Eqns (2) to (6) can be similarly applied. In brief, PANDA draws e_{jk} drawn from $N(0, \lambda |\theta_{jk}|^{-1})$, scales the observed data \mathbf{x} with $\sqrt{(n + n_e)n^{-1}}$ to get $\mathbf{z} = \sqrt{(n + n_e)n^{-1}} \mathbf{x}$, and \mathbf{e} to obtain $\mathbf{d} = \sqrt{2(n + n_e)n_e^{-1}} \mathbf{e}$. Calculate $\tilde{\Sigma} = (n + n_e)^{-1} \tilde{\mathbf{x}}^T \tilde{\mathbf{x}}$ on the scaled augmented data $\tilde{\mathbf{x}} = (\mathbf{z}, \mathbf{d})$. Plugging in $\tilde{\Sigma}$ in the objective function, we have

$$l_j = \frac{1}{2} \theta_j^t \tilde{\Sigma} \theta_j - \mathbf{1}_j \theta_j. \quad (21)$$

Taking the first derivative of Eqn (21) with regard to θ_j and setting it at 0 leads to $\tilde{\Sigma} \theta_j - \mathbf{1}_j = 0$. With data augmentation, the inverse of $\tilde{\Sigma}$ always exists, leading to a direct closed-form SCIO estimator $\hat{\theta}_j$, which is $\tilde{\Sigma}^{-1} \mathbf{1}_j$.

It is easy to show that the expectation of the loss function in Eqn (21) over the distribution of \mathbf{e} delivers the same type of penalty for SCIO in Eqn (20). Specifically,

$$l_j = \frac{1}{2} \theta_j^T \left(\sum_{i=1}^n \mathbf{z}_i \mathbf{z}_i^T + \sum_{i=1}^{n_e} \mathbf{d}_i \mathbf{d}_i^T \right) \theta_j - \mathbf{1}_j \theta_j = \frac{1}{2} \theta_j^T \left(\frac{1}{n} \sum_{i=1}^n \mathbf{x}_i \mathbf{x}_i^T + \frac{2}{n_e} \sum_{i=1}^{n_e} \mathbf{e}_{ij} \mathbf{e}_{ij}^T \right) \theta_j - \mathbf{1}_j \theta_j,$$

and $E(l_j) = \frac{1}{2}\boldsymbol{\theta}_j^t \hat{\Sigma} \boldsymbol{\theta}_j - \mathbf{1}_j \boldsymbol{\theta}_j + \lambda \sum_{k=1}^p |\theta_{jk}|$.

The computational steps of the PANDA-SCIO algorithm are given in Algorithm S3 in the Supplementary Materials.

2.2.4 PANDA- graphical ridge in GGMs

The PANDA technique can also be employed to regularize the off-diagonal elements in Ω simultaneously in GGMs. Existing work on regularization of ω_{jk} ($k \neq j$) simultaneously includes graphical lasso (J. Friedman and Tibshirani, 2008) and graphical ridge (Kuismin et al., 2017). The graphical lasso imposes the l_1 penalty $\sum_{k \neq j} |\omega_{jk}|$ while the graphical ridge imposes the l_2 penalty $\sum_{k \neq j} \omega_{jk}^2$. The l_2 penalty is used when sparsity is not critical such as in principal component analysis or in prediction problems. The graphical regularization via PANDA is similar to the graphical ridge.

Specifically, the augmented noise is generated from a multivariate Gaussian (MVN) distribution $\mathbf{e}_i \sim \text{MVN}_{(p)}(0, \lambda\Omega)$, $i = 1, \dots, n$. PANDA starts with supplying an initial value for Ω and draw \mathbf{e} .

It then combines $\sqrt{n^{-1}(n+n_e)}\mathbf{x}$ with $\sqrt{n_e^{-1}(n+n_e)}\mathbf{e}$ and obtains the MLE of Ω , which is just the inverse of the sample covariance matrix, based on the noise augmented data. The Ω estimates is updated at every iteration. As $(n_e \rightarrow \infty) \cap (n_e\lambda = O(1))$, or $m \rightarrow \infty$, PANDA achieves the same global optimum on Ω as the graphical ridge, the expected regularization effect, as listed in Proposition 4. The proof is straightforward, given that $E_{\mathbf{e}}(e_{ij}e_{ik}) = \lambda\omega_{jk}$.

Proposition 4. *Let $\mathbf{z}_i = \sqrt{n^{-1}(n+n_e)}\mathbf{x}_i$ for $i = 1, \dots, n$ and $\mathbf{d}_i = \sqrt{n_e^{-1}(n+n_e)}\mathbf{e}_i$ for $i = 1, \dots, n_e$, where $\mathbf{e}_i \sim \text{MVN}(0, \lambda\Omega)$. The negative log-likelihood of Ω based on the augmented data (\mathbf{z}, \mathbf{d}) is $l_p(\Omega|\mathbf{x}, \mathbf{e}) = (n+n_e)n^{-1}l(\Omega|\mathbf{x}) + (n+n_e)n_e^{-1} \sum_{i=1}^{n_e} \sum_{j,k=1}^p (e_{ij}e_{ik})\omega_{jk}$, the expectation of which with regard to the distribution of \mathbf{e} is*

$$E_{\mathbf{e}}(l_p(\Omega|\mathbf{x}, \mathbf{e})) = (n+n_e) \left(n^{-1}l(\Omega|\mathbf{x}) + \lambda \sum_{j=1}^p \sum_{k=1}^p \omega_{jk}^2 \right). \quad (22)$$

2.3 noise augmentation vs additive noise injection

As mentioned in Section 1, PANDA is the first adaptive noise augmentation approach to regularize GGMs and UGMs in general, inspired by the adaptive NI approach used in whiteout which is a regularization technique for neural networks (Li and Liu, 2017). The additive NI approach does not change the observed data dimension but directly perturbs the observed data with additive noise drawn from a NGD. Proposition 5 shows there exists an additive NI counterpart to PANDA, which achieves the same regularization effect on the parameters from a UGM in expectation with regard to the distribution of injected noise.

Proposition 5 (Additive NI counterpart to PANDA). *The expected loss functions in PANDA-NS for GGMs and UGMs (with second-order approximation for UGMs), PANDA-CD, PANDA-SCIO and PANDA-graphical ridge for GGMs are equivalent to the expected loss function constructed with using the additive NI $\tilde{\mathbf{x}}_{ij} = \mathbf{x}_{ij} + \mathbf{e}_{ij}$ ($i = 1, \dots, n; j = 1, \dots, p$) in the regression on outcome node X_i , where $\mathbf{e}_{ij} = (e_{ijj}, \mathbf{e}_{ij,-j})$ is designed in the same way as its counterpart PANDA procedure.*

The proof of Proposition 5 is given in Appendix D. Though using NI to construct a UGM would achieve approximately the same regularization effects as PANDA per Proposition 5, NI, unlike

PANDA, does not enjoy the computational convenience in parameter estimation as PANDA as $n < p$ as is in NI. IN addition, PANDA can provide the exact expected regularization effects asymptotically when $n_e \rightarrow \infty$ whereas the expected regularization effects are only second-order approximate for the NI methods.

3 Bayesian Interpretation of PANDA

Both the data augmentation technique employed by PANDA and Bayesian modeling introduce endogenous information into the observed data as a way to regularize large models. we can draw connection between PANDA and the Bayesian frameworks in two aspects.

The first connection is obvious: almost each regularization type can be realized by imposing some types of priors on the model parameters through Bayesian hierarchical modeling, such as Bayesian lasso (Park and Casella, 2008), Bayesian bridge (Polson et al., 2012), Bayesian elastic net (Li and Lin, 2010), Bayesian group lasso (Xu and Ghosh, 2015), and Bayesian graphical lasso (Wang, 2012). However, the “formats” of the endogenous information brought into the regularization process are different between PANDA the Bayesian hierarchical modeling. In the Bayesian framework, the additional information is formulated as the prior knowledge (distribution) on the model parameters; while in PANDA, the additional information enters as additional “noisy data”, the generative distribution of which depends on the model parameters, in parallel to the observed data. In addition, the computational approaches are different – PANDA solves an optimization problem in an iterative manner while the Bayesian hierarchical modeling relies on sampling from the posterior distribution of the parameters.

The second connection between PANDA and Bayesian modeling is less obvious as it occurs during the computational steps in PANDA. Specifically, estimating $\boldsymbol{\theta}$ in each iteration can be regarded as calculating the maximum a posterior (MAP) estimator, where the prior of $\boldsymbol{\theta}$ is estimated from data – resembling the empirical Bayesian (EB) framework. We illustrate the resemblance between PANDA and EB-MAP using two examples.

We first consider imposing a bridge-type prior on $\boldsymbol{\theta}_j = \{\theta_{jk}\} (k \neq j)$, which contains the regression coefficients in the regression with outcome node X_j in a GGM or a UGM in the $(t+1)$ -th iteration. Rather than using a hierarchical model, we formulate the prior as

$$\text{GGM: } \pi(\theta_{jk}|\sigma_j^2) = N\left(0, \lambda^{-1} \left|\theta_{jk}^{(t)}\right|^\gamma \sigma_j^2\right) \text{ for } k \neq j; \text{ and } \pi(\sigma_j^2) \propto \sigma_j^{-2}, \quad (23)$$

$$\text{UGM: } \pi(\theta_{jk}) = N\left(0, (2\lambda)^{-1} |\theta_{jk}|^\gamma\right) \quad (24)$$

in the GGM and UGM frameworks, respectively. Note $\theta_{jk}^{(t)}$ is the MAP estimate from the t -th iteration given data \mathbf{x} and $\mathbf{e}^{(t)}$, so the information about θ_{jk} contained in \mathbf{x} is used to formulate the the prior distribution for θ_{jk} – this is the EB part. We then calculate update the MAP from the posterior distribution of θ_{jk} given the EB prior in Eqn (23) or (23), and the data $(\mathbf{x}, \mathbf{e}^{(t+1)})$ and move onto the next iteration. Upon the convergence of the MAP estimates, the negative logarithm of the joint posterior distribution of $\boldsymbol{\theta}$ and $\boldsymbol{\sigma}^2 = \{\sigma_j^2\}_{j=1,\dots,p}$ is

$$2\sum_{j=1}^p \log(\sigma_j^2) + \sum_{j=1}^p \frac{1}{2\sigma_j^2} \left(\sum_{i=1}^n \left(x_{ij} - \sum_{k \neq j} x_{ik} \theta_{jk} \right)^2 + \lambda \sum_{k \neq j} |\theta_{jk}|^{2-\gamma} \right)$$

in the GGM framework and the negative logarithm of the posterior distribution of $\boldsymbol{\theta}$ in the UGM

framework is

$$-\sum_{j=1}^p \left(\sum_{i=1}^n \left(h_j(x_{ij}) + \sum_{k \neq j} \theta_{jk} x_{ij} x_{ik} - B_j \left(\sum_{k \neq j} \theta_{jk} x_{ik} \right) - \lambda \sum_{k \neq j} |\theta_{jk}|^{2-\gamma} \right) \right),$$

which are the same as the expected loss functions in Eqns (9) and (11), respectively. In other words, obtaining the minimizer of $l_p(\Theta|\mathbf{x}, \mathbf{e})$ in PANDA is equivalent to calculating the MAP estimation in the EB framework.

As a second example, we consider the graphical ridge regularization. The EB prior on the precision matrix Ω in iteration $(t+1)$ is

$$\Omega \sim \text{Wishart}_p \left(\left(\lambda \Omega^{(t)} \right)^{-1}, \nu = p + 1 \right),$$

where $\Omega^{(t)}$ is estimated from data \mathbf{x} and augmented noise $\mathbf{e}^{(t)}$ at iteration t . Given the EB prior and the \mathbf{x} and augmented noise $\mathbf{e}^{(t+1)}$, we obtain the new MAP estimate Ω from its posterior distribution. Upon the convergence of the MAP estimate, the negative logarithm of the posterior distribution Ω is

$$\frac{n}{2} \log(|\Omega|) + \frac{n}{2} \sum_{i=1}^n \mathbf{x}_i^T \Omega \mathbf{x}_i + \lambda \|\Omega\|_2,$$

which is equivalent to the penalized loss function with the graphical ridge penalty in Eqn (22).

4 Theoretical Properties of PANDA and Inferences

Section 2 examines the expected noise-augmented loss function $l_p(\Theta|\mathbf{x}, \mathbf{e})$ with regard to the distribution of \mathbf{e} that establishes PANDA as a regularization techniques in UGMs and GGMs. In this section, we establish the almost sure (a.s.) convergence of $l_p(\Theta|\mathbf{x}, \mathbf{e})$ to its expectation and the a.s. convergence and consistency of its minimizer to the minimizer of the expected loss function as $n_e \rightarrow \infty$ or $m \rightarrow \infty$ in the framework of PANDA-NS for GGMs and UGMs (Sec 4.1). The asymptotic properties of PANDA-CD for GGMs can be established in a similar fashion as it also utilizes the regression-based framework as PANDA-NS, only differing in how the precision matrix is re-parameterized. In addition, we examine the Fisher information matrix about the model parameters in the noise-augmented data (Sec 4.2), and the inferences of the parameters estimated via PANDA in the GLM setting (Section 4.3). We also provide a formal test on convergence for the PANDA algorithms (Section 4.4).

4.1 Consistency of noise-augmented loss function and its minimizer

Let Θ denote the collection of all parameters from the p linear regression models in NS for GGMs and UGMs. In a single UGM, where the conditional distribution of each node given others is modelled by the Exponential family, the distribution function and the link functions would be different by the node type. We use GGMs, PGMs and the NBGMs as examples to establish the consistency of parameters estimated by PANDA. The process is similar for other graph types.

The averaged loss function over $m \geq 1$ iterations of the PANDA algorithm $\bar{l}_p(\Theta|\mathbf{x}, \mathbf{e})$ is

$$l(\Theta|\mathbf{x}) + m^{-1} \sum_{t=1}^m \sum_{i=1}^{n_e} \sum_{j=1}^p \left(\sum_{k \neq j} e_{ijk}^{(t)} \theta_{jk} \right)^2$$

$$l(\Theta|\mathbf{x}) - m^{-1} \sum_{t=1}^m \sum_{i=1}^{n_e} \sum_{j=1}^p \left(e_{ij} \sum_{k \neq j} e_{ijk} \theta_{jk} - \log(e_{ijj}^{(t)}) - \exp \left(\sum_{k \neq j} e_{ijk}^{(t)} \theta_{jk} \right) \right) \text{ and}$$

$$l(\Theta|\mathbf{x}) - m^{-1} \sum_{t=1}^m \sum_{i=1}^{n_e} \sum_{j=1}^p \left\{ \log \left(\frac{\Gamma(e_{ijj} + r_j) r_j^{r_j}}{\Gamma(e_{ijj} + 1) \Gamma(r_j)} \right) + e_{ijj} \sum_{k \neq j} e_{ijk} \theta_{jk} - (r_j + e_{ijj}) \log \left(r_j + \exp \left(\sum_{k \neq j} e_{ijk} \theta_{jk} \right) \right) \right\}$$

for GGMs, PGMs and NBGMs, respectively, where $l(\Theta|\mathbf{x}) = \sum_{i=1}^n \sum_{j=1}^p \left(x_{ij} - \sum_{k \neq j} x_{ik} \theta_{jk} \right)^2$ for GGMs, and is the respective negative log-likelihood for PGMs and NBGMs, respectively. Theorem 1 presents the asymptotic properties of $\bar{l}_p(\Theta|\mathbf{x}, \mathbf{e})$ in two asymptotic cases: 1) $n_e \rightarrow \infty$ while $n_e V(e_{jk}) = O(1)$ and m (≥ 1) is fixed at a finite constant; 2) $m \rightarrow \infty$ while n_e ($n_e > p - n$) is fixed at a finite constant. We show $\bar{l}_p(\Theta|\mathbf{x}, \mathbf{e})$ converges in distribution to a Gaussian distribution with mean $l_p(\Theta|\mathbf{x}) = E_{\mathbf{e}}(l_p(\Theta|\mathbf{x}, \mathbf{e}))$ at the rate of $n_e^{1/2}$ and $m^{1/2}$ in the two cases, respectively. In addition, $\bar{l}_p(\Theta|\mathbf{x}, \mathbf{e})$ converges almost surely to a penalized loss function given \mathbf{x} with a different penalty term on Θ between the two cases. The proof of Theorem 1 is given in Appendix E.

Theorem 1. (Asymptotic properties of the noise-augmented loss function and its minimizer in PANDA) Assume Θ belongs to a compact set. Let $l_p(\Theta|\mathbf{x}) = E_{\mathbf{e}}(l_p(\Theta|\mathbf{x}, \mathbf{e}))$.

1) If $n_e \rightarrow \infty$ while λn_e and m (≥ 1) are held at constants, then

$$n_e^{1/2} C^{-1} (\bar{l}_p(\Theta|\mathbf{x}, \mathbf{e}) - l_p(\Theta|\mathbf{x})) \xrightarrow{d} N(0, 1) \quad (25)$$

$$\bar{l}_p(\Theta|\mathbf{x}, \mathbf{e}) \xrightarrow{a.s.} l_p(\Theta|\mathbf{x}) = l(\Theta|\mathbf{x}) + \frac{n_e}{2} \sum_{j=1}^p \sum_{j \neq k} \theta_{jk}^2 V(\mathbf{e}_{jk}) \quad (26)$$

$$\arg \inf_{\Theta} \bar{l}_p(\Theta|\mathbf{x}, \mathbf{e}) \xrightarrow{a.s.} \arg \inf_{\Theta} l_p(\Theta|\mathbf{x}). \quad (27)$$

2) If $m \rightarrow \infty$ while n_e is fixed, then

$$m^{1/2} C^{-1} (\bar{l}_p(\Theta|\mathbf{x}, \mathbf{e}) - l_p(\Theta|\mathbf{x})) \xrightarrow{d} N(0, 1) \quad (28)$$

$$\bar{l}_p(\Theta|\mathbf{x}, \mathbf{e}) \xrightarrow{a.s.} l_p(\Theta|\mathbf{x}) + P(\Theta; \lambda, \gamma, \sigma^2, a) \quad (29)$$

$$\arg \inf_{\Theta} \bar{l}_p(\Theta|\mathbf{x}, \mathbf{e}) \xrightarrow{a.s.} \arg \inf_{\Theta} l_p(\Theta|\mathbf{x}). \quad (30)$$

C in Eqns (25) and (28) is a function of Θ and the tuning parameters from a given NGD.

The regularization term $P(\Theta; \lambda, \gamma, \sigma^2, a)$ in Eqn (29) takes different forms for different graph types. For example, it has the same penalty term as Eqn (26) for GGMs, and is equal to $n_e \sum_{j=1}^p \exp \left(\lambda \sum_{j \neq k} |\theta_{jk}|^{1-\gamma/2} \right)^2$ for PGMs and EGMs if the bridge-type noise is employed, and does not have a closed analytical form for BGMs and NBGMs (See Eqn (E.15)).

We also examine the asymptotic properties of PANDA-graphical ridge. The average loss is $\bar{l}_p(\Omega|\mathbf{x}, \mathbf{e}) = n^{-1} (n + n_e) l(\Omega|\mathbf{x}) + m^{-1} n_e^{-1} (n + n_e) \sum_{t=1}^m \sum_{i=1}^{n_e} \sum_{j,k=1}^p (e_{ijj} e_{ijk}) \omega_{jk}$. It can be shown the conclusions in Theorem 1 still hold (the proof is also available in Appendix E).

When there exist multicollinearity issues and the imposed sparsity regularization effect is not strong enough, the loss function has a global optimum region, rather than a single point. To examine the asymptotic properties in this case, we first define the *optimum parameter set* that leads to the global minimum (Definition 1), then we show that the parameters learned from minimizing the $l_p(\Theta|\mathbf{x}, \mathbf{e})$ by PANDA fall into the optimum parameter set asymptotically (Proposition 6). The proof is given in Appendix F.

Definition 1. (Optimum parameter set) Let the expected loss function be a continuous function in θ . The optimum parameter set is defined as $\hat{\Theta}^0 = \{ \theta^0 \in \Theta \mid l_p(\theta^0|\mathbf{x}) \leq l_p(\theta|\mathbf{x}), \forall \theta \in \Theta \}$, and the distance from $\theta \in \Theta$ to $\hat{\Theta}^0$ is defined as $d(\theta, \hat{\Theta}^0) = \min_{\theta^0 \in \hat{\Theta}^0} \|\theta - \theta^0\|_2$.

The presence of multicollinearity does not affect the convergence of the loss functions in the GLM

setting. Therefore, according to the proof of Theorem 1, Eqn (31) holds

$$\sup_{\Theta} |\bar{l}_p(\Theta|\mathbf{x}, \mathbf{e}) - \bar{l}_p(\Theta|\mathbf{x})| \rightarrow 0 \text{ as } n_e \rightarrow \infty \text{ or } m \rightarrow \infty. \quad (31)$$

Proposition 6. (Consistency of PANDA Estimation in the Presence of multicollinearity) Denote the minimizer of the averaged loss function by $\hat{\boldsymbol{\theta}}_p^0 = \arg \min_{\Theta} l_p(\Theta|\mathbf{x}, \mathbf{e})$. Given Eqn (31) and assuming that Θ is compact,

$$\Pr \left(\limsup_{m \rightarrow \infty} d \left(\hat{\boldsymbol{\theta}}_p^0, \hat{\Theta}^0 \right) \leq \epsilon \right) = 1 \quad \forall \delta > 0.$$

4.2 Fisher information in noise augmented data

The augmented noisy data in PANDA bring additional information to observed data \mathbf{x} to regularize the estimation of parameter $\boldsymbol{\theta}_j$; and the expected regularization is realized by either letting $(n_e \rightarrow \infty) \cap (n_e V(e_{jk}) = O(1))$, or $m \rightarrow \infty$. At first sight, letting $(n_e \rightarrow \infty)$ seems counter-intuitive as the noisy data would take over the estimation rather than serving merely to regulate. There are several justifications for $(n_e \rightarrow \infty)$ under the $n_e V(e_{jk}) = O(1)$ constraint. First, as shown in Sec 2, $n_e \rightarrow \infty$ achieves the nominal designed regularization while $m \rightarrow \infty$ with small n_e does not except for in the linear regression. Second, The regression line with the canonical link function in the GLM setting in PANDA is through origin, while . Last but not the least, we show in Proposition 7 that as long as $n_e V(e_{jk}) = O(1)$, the amount of information about θ_{jk} remains at constant even as $n_e \rightarrow \infty$. Proposition 7 uses the bridge-type noise as a special case, the Proof of which is provided in Appendix H. The conclusion can be easily generalized to other types of noises.

Proposition 7. In the GLM framework, the additional information about regression coefficient θ_k introduced by the augmented noisy data drawn from the bridge-type NGD is proportional to $n_e \lambda |\theta_k|^{-\gamma}$.

$$I_p(\boldsymbol{\theta}_j) = I_{\mathbf{x}}(\boldsymbol{\theta}_j) + (\lambda n_e) B_j''(0) \text{Diag}\{|\theta_{j1}|^{-\gamma}, \dots, |\theta_{jp}|^{-\gamma}\} + O(\lambda^2 n_e). \quad (32)$$

Eqn (32) suggests that the information about θ_{jk} does not increase with n_e as long as $\lambda n_e |\theta_{jk}|^{-\gamma}$ is kept at constant. In addition, the closer $|\theta_k|$ is to 0, the more regularization effect the augmented information will bring to $\boldsymbol{\theta}_k$.

4.3 Asymptotic distribution of regularized parameters via PANDA in GLMs

In this section, we derive the asymptotic distribution for the regularized $\hat{\boldsymbol{\theta}}_j$ in GLMs (linear regression included as a special case), based on which we could construct confidence intervals (CIs) for $\boldsymbol{\theta}_j$, whether some of the estimated $\hat{\boldsymbol{\theta}}_j$ are 0 or not. This is contrast to as well as an improvement over some existing post-selection inferential approaches in the context of variable selection in that that PANDA achieves selection, estimation and inferences simultaneously rather than using a two-step procedure (selection followed by inferences). We are note interested in constructing interval estimation for the whole UGM per se as it is difficult to comprehend what that mean for a graph.

Proposition 8 (Asymptotic distribution of parameter estimates via PANDA in GLMs). Consider the GLM with outcome node X_j . Denote the model parameter by $\boldsymbol{\theta}_j$, and its estimate via PANDA by $\bar{\boldsymbol{\theta}}_j = m^{-1} \sum_{t=1}^m \hat{\boldsymbol{\theta}}_{j,\mathbf{e}}^{(t)}$ for $m \geq 1$ after convergence. Let $I_{\mathbf{x}}(\boldsymbol{\theta}_j)$ denote the Fisher

information contained in original data \mathbf{x} , and $I(\boldsymbol{\theta}_j|\mathbf{x}, \mathbf{e})$ the Fisher information in noise-augmented data (\mathbf{x}, \mathbf{e}) . Let $V(e_{jk})n_e = o(\sqrt{n})$ for any fixed θ_{jk} . Upon the convergence of the PANDA-NS algorithms (Algorithms 1 and S1),

$$\sqrt{n}(\hat{\boldsymbol{\theta}}_{j,\mathbf{e}}^{(t)} - \boldsymbol{\theta}_j) \xrightarrow{d} N(\mathbf{0}, \Sigma_{j,\mathbf{e}}^{(t)}), \text{ as } n \rightarrow \infty, \quad (33)$$

$$\sqrt{n}(\bar{\boldsymbol{\theta}}_j - \boldsymbol{\theta}_j) \xrightarrow{d} N(\mathbf{0}, \bar{\Sigma}_j + \Lambda_j) \text{ as } n, m \rightarrow \infty, \quad (34)$$

where $\Sigma_{j,\mathbf{e}}^{(t)} = I(\boldsymbol{\theta}_j|\mathbf{x}, \mathbf{e})^{-1}I(\boldsymbol{\theta}_j)I(\boldsymbol{\theta}_j|\mathbf{x}, \mathbf{e})^{-1}$ in iteration t upon convergence, $\bar{\Sigma}_j = m^{-1} \sum_{t=1}^m \Sigma_{j,\mathbf{e}}^{(t)}$, and $\Lambda_j = (m-1)^{-1} \sum_{t=1}^m \left(\hat{\boldsymbol{\theta}}_{j,\mathbf{e}}^{(t)} - \bar{\boldsymbol{\theta}}_j \right) \left(\hat{\boldsymbol{\theta}}_{j,\mathbf{e}}^{(t)} - \bar{\boldsymbol{\theta}}_j \right)^T$.

The regularity condition $V(e_{jk})n_e = o(\sqrt{n})$ would have different specific form for different NGDs. The proof of Proposition 8 is given in Appendix G. For example, for the lasso-type noise, the condition becomes $\lambda n_e = o(\sqrt{n})$. Based on the asymptotic distributions given in the proposition, we could construct CIs for $\boldsymbol{\theta}_j$. $I(\boldsymbol{\theta}_j|\mathbf{x}, \mathbf{e})$, which contains the unknown $\boldsymbol{\theta}_j$, can be estimated by plugging in $\hat{\boldsymbol{\theta}}_{j,\mathbf{e}}^{(t)}$ in the CI calculation, with the caveat that the uncertainty around of $\hat{\boldsymbol{\theta}}_{j,\mathbf{e}}$ and thus $\bar{\boldsymbol{\theta}}_j$ is not accounted for. The asymptotic variances of $\hat{\boldsymbol{\theta}}_{j,\mathbf{e}}$ and $\bar{\boldsymbol{\theta}}_j$ involves the inverse of $I(\boldsymbol{\theta}_j|\mathbf{x}, \mathbf{e})$, the existence of which would be guaranteed with the data augmentation in PANDA.

A special case of Proposition 8 is for linear regression, where the asymptotic distribution of $\hat{\boldsymbol{\theta}}_{j,\mathbf{e}}^{(t)}$ becomes

$$\sqrt{n}(\hat{\boldsymbol{\theta}}_{j,\mathbf{e}}^{(t)} - \boldsymbol{\theta}_j) \xrightarrow{d} N\left(\mathbf{0}, \sigma_j^2 (M_j^{(t)})^{-1} (\mathbf{x}'_{-j} \mathbf{x}_{-j}) (M_j^{(t)})^{-1}\right), \quad (35)$$

where $M_j^{(t)} = (\mathbf{x}'_{-j} \mathbf{x}_{-j} + \mathbf{diag}(n_e V(\mathbf{e}_j)))$. For example, if the lasso-type noise is used, then $V(\mathbf{e}_j) = \lambda |\boldsymbol{\theta}_j|^{-1}$. When constructing CIs for $\boldsymbol{\theta}_j$, the unknown σ_j^2 in Eqn (35) can be estimated by $\text{SSE}_j / (n - \nu_j) = \sum_{i=1}^n (\mathbf{x}_j - \mathbf{x}_{-j} \hat{\boldsymbol{\theta}}_{j,\mathbf{e}}^{(t)})^2 / (n - \nu_j)$, which converges to $\sigma_j^2 \chi_{n-\nu_j}^2$ in distribution; and $\nu_j = \text{tr}(\mathbf{x}_{-j} (M_j^{(t)})^{-1} \mathbf{x}'_{-j})$. The asymptotic difference between $\hat{\boldsymbol{\theta}}_{j,\mathbf{e}}^{(t)}$ and $\boldsymbol{\theta}_j$ in the linear regression case is actually $\text{sign}(\boldsymbol{\theta}_j) \sqrt{n} \lambda n_e M^{-1}$, the limit of which is 0 as $n \rightarrow \infty$, given $n_e V(e_{jk}) = o(\sqrt{n})$ for any fixed θ_{jk} .

Based on a constructed CI on θ_{jk} based on Propositions 8, we could claim $\theta_{jk} = 0$ if the CI contains 0 in place of the hard-thresholding rule used in the PANDA algorithms. However, we would not be as confident to conclude that a CI that does not contain 0 implies $\theta_{jk} \neq 0$ due to multiplicity considerations.

4.4 Test of convergence of PANDA algorithm

In all the PANDA algorithms presented in Section 2, the threshold τ is pre-specified by users. We present here a formal statistical test on the convergence of the PANDA algorithms in the framework of NS for constructing GGMs and UGMs. This test is asymptotic in the sense it is based on $n_e \rightarrow \infty$ or $m \rightarrow \infty$, but should work well either n_e or m is relatively large in practice, which is often the case when the PANDA algorithm is implemented. The test also applies to PANDA-CD, PANDA-SCIO, and PANDA-graphical ridge in GGM construction.

WLOG, we establish the test by letting $n_e \rightarrow \infty$. The procedure is similar in the case of $m \rightarrow \infty$ by replacing n_e below with m or $(m \times n_e)$. Consider iteration t of the PANDA algorithm. When $n_e \rightarrow \infty$, per the CLT, the loss function in iteration t given data \mathbf{x} is

$$l^{(t)} = l_p(\Theta^{(t)}|\mathbf{x}) + (n_e)^{-\frac{1}{2}} C^{(t)} z + O((n_e)^{-1}), \quad (36)$$

where $z \sim N(0, 1)$ and $C^{(t)} = \frac{\lambda n_e}{2} \left(\sum_{j=1}^p c \left\| \left(\boldsymbol{\theta}_{j,-j}^{(t)} |\boldsymbol{\theta}_{j,-j}^{(t)}|^{-\gamma/2} \right) \left(\boldsymbol{\theta}_{j,-j}^{(t)} |\boldsymbol{\theta}_{j,-j}^{(t)}|^{-\gamma/2} \right)^T \right\|_2^2 \right)^{1/2}$; c is a constant that depends on the graph type ($c = 8$ for GGM, 2 for PGM and EGM, and $r_j^2/(r_j + 1)^2$ for NBGM where r_j is the failure numbers in regression on X_j ; also see Eqns (E.2), (E.7) and (E.14). Eqn (36) suggests that $l^{(t)}$ still fluctuates due to the randomness of z from iteration to iteration as long as n_e is finite, even after $l_p(\Theta^{(t)}|\mathbf{x})$ would stabilize. But the fluctuation is just white noise rather than carrying any true signal after the algorithm converges. Specifically, Let $d^{(t)} = l^{(t)} - l^{(t-1)}$. As $n_e \rightarrow \infty$, $d^{(t)} = (n_e)^{-1/2} C^{(t)} z$. In other words, under the null hypothesis of convergence, the difference between the noise-augmented loss functions from two consecutive iterations of the PANDA algorithm follow a Gaussian distribution with mean 0 and standard deviation $(n_e^{-1} (C^{(t)2} + C^{(t+1)2}))^{1/2}$. The test of convergence can thus be formulated as $z^{(t)} = d^{(t)} / \sqrt{n_e^{-1} (C^{(t)2} + C^{(t+1)2})}$. If $|z^{(t)}| > z_{1-\alpha/2}$, then we claim the PANDA algorithm has not converged at iteration t (at the significance level of α).

4.5 Minimizer of averaged noise-augmented loss functions vs averaged minimizers of noise-augmented loss functions

Theoretically, as $n_e \rightarrow \infty$, PANDA provides the exact regularization on parameter estimations. In practice, when n_e is large, setting $m = 1$ in a PANDA algorithm is sufficient to achieve the expected regularization effect. On the other hand, a very large n_e will slow down the computation in each iteration. In practice, when n_e is relatively large to give us the expected regularization effect but too large for computation, we could let $m > 1$ to help average out the fluctuation around the estimated parameters due to the not-too-large n_e . Per Propositions 1 and 2, one would take the Monte Carlo average over m noise-augmented loss function $l(\Theta|\mathbf{x}, \mathbf{e})$ to yield a single minimizer $\hat{\boldsymbol{\theta}}$. However, this approach would lose the computational convenience of PANDA. To maintain the PANDA's computational advantage, one could instead calculate the average of m minimizers of $l(\Theta|\mathbf{x}, \mathbf{e})$ from the latest m iterations, $\bar{\boldsymbol{\theta}}$. We establish in Corollary 3 that $\bar{\boldsymbol{\theta}}$ and $\hat{\boldsymbol{\theta}}$ are first-order equivalent with finite n_e , given that all noises are drawn from the same distribution in PANDA-NS for GGMs. The proof is given in Appendix I. We also present a simulation study in Section 5.3 to illustrate the similarity between $\bar{\boldsymbol{\theta}}$ and $\hat{\boldsymbol{\theta}}$.

Corollary 3 (First-order equivalence between minimizer of averaged noise-augmented loss functions vs averaged minimizers of single noise-augmented loss functions). *The averaged minimizer $\bar{\boldsymbol{\theta}}$ of m perturbed loss function in PANDA-NS for GGMs upon convergence is first-order equivalence to the minimizer $\hat{\boldsymbol{\theta}}$ of the average of the m noise-augmented loss functions which is the Monte Carlo version of $E_{\mathbf{e}}(l_p(\boldsymbol{\theta}|\mathbf{x}, \mathbf{e}))$ as $m \rightarrow \infty$. The difference between $\bar{\boldsymbol{\theta}}$ and $\hat{\boldsymbol{\theta}}$ in the higher-order terms approaches 0 as $n_e \rightarrow \infty$.*

5 Simulation

5.1 Graph construction

We implemented PANDA with the lasso-type penalty for constructing three graphs (GGM, PGM, and BGM) and benchmarked its performance against the NS approach with the constrained optimization. In the estimation of GGM, besides the NS approach, we also constructed graphs using the CD and SCIO approaches. To simulate the graphs, we first generated the adjacency matrix \mathbf{A} , conditional on which nodes \mathbf{X} were generated, using via R function `XMRF.sim` in package

XMRF (Wan et al., 2015). Table 2 summarizes the simulation schemes, the tuning parameters in PANDA, and the algorithmic parameter specification for the PANDA algorithms.

simulation schemes				tuning and algorithmic parameters							
graph	n	p	$\neq 0$ /total edges	γ	σ^2	T	n_e	m	τ_0	other parameters	
GGM	100	50	322/1225	NS	1	0	70	2000	1	10^{-6}	-
				CD	1	0	70	2000	1	10^{-6}	$k = 5$
				SCIO	1	0	150	2500	1	10^{-5}	$\text{red}\tau_1 = 10^{-6}$
BGM	100	50	322/1225	1	0	100	2000	20	10^{-5}	-	
PGM	100	50	322/1225	1	0	70	2000	1	10^{-5}	-	

Table 2: Simulation schemes, and tuning and algorithmic parameter specifications in PANDA

We run 100 repetitions in each graph case, and calculated the false positive (FP) and true positive (TP) rates at different λ values, where “positive” is defined as the identification of a non-zero edge. The ROC curves are depicted in Figure 4. Overall, PANDA delivered either similar or superior ROC performance compared to the constrained optimization in all three graph types. The largest margin of superiority of PANDA is observed in the PGM, where PANDA implemented through both the Poisson regression and the NB regression showed noticeably higher TP rates over the constrained optimization when the FP ranged 15% to 80%. The ROC curves in GGM suggest the SCIO method (the green curves) seems to performs lightly better in constructing the GGM than the CD and NS approaches, likely because the regularizations are directly imposed on the entries of the precision matrix in SCIO where both NS and CD regularizes regression coefficients from some linear models, from which the precision matrix is calculated.

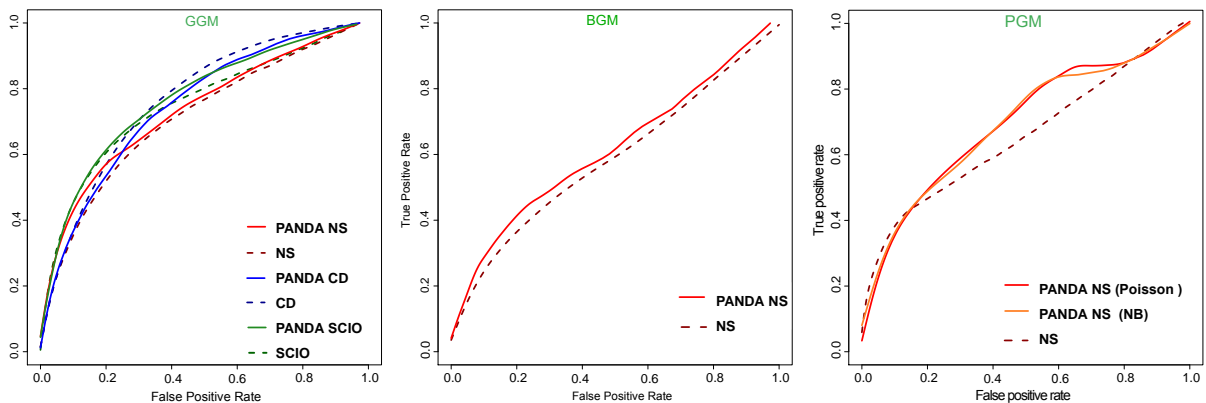


Figure 4: ROC curves for non-zero edge identifications in GGMs, BGM and PGMs. The dash lines represent the results from constrained optimization with the lasso penalty, and the solid lines represent the results from PANDA.

5.2 Inference on regression coefficient in GLMs via PANDA

In the NS framework, PANDA constructs UGMs via running GLMs on noise-augmented data. In this simulation, we investigate the inferential validity for the regression coefficients β from the GLMs based the asymptotic distributions presented in Proposition 8.

We examined the cases when the outcome Y followed the Gaussian ($\sigma^2 = 1$), Poisson, Bernoulli, Exponential (Exp) and Negative Binomial (NB) distributions (number of failure was fixed at $r = 5$)

with $p = 30$ in each case. For Gaussian and NB Y , \mathbf{X} were simulated from $N(0, 1)$; for Bernoulli, Exp, and Poisson Y , X were simulated from $\text{Unif}(-3, 3)$, $\text{Unif}(-1, 2)$ and $\text{Unif}(-0.3, 0.5)$, respectively. We examined three sample size scenarios at $n = 100, 200, 300$ with 200 repetitions in each distribution case. In each repeat, we constructed the 95% CIs for the 30 regression coefficients β (among which 21 were non-zero and 9 were zero) and examined the empirical coverage probability (CP) and the CI width. Tables 3 and 4 present the range of the CP and the corresponding CI width for the 30 β . We used the lasso-type NGD for noise augment with $n_e = 1000$, $\lambda \in (1.5, 7) \times 10^{-3}$ varying by n . We bench marked the results against the post-selection inferential procedure in the lasso regression (Lee et al., 2016; Taylor and Tibshirani, 2017), implemented using the R package `selectiveInference`.

In summary, the empirical CPs for $\beta = 0$ were around the nominal level 95% (Table 3). When $\beta \neq 0$, there was slight under-coverage for small sample sizes (e.g., $n = 100$), especially in the case of Exponential or NB Y . The CPs from the post-selection procedure were around the nominal levels for both $\beta = 0$ and $\beta \neq 0$ for Gaussian Y , and for $\beta = 0$ for Bernoulli outcome, but suffered from moderate under-coverage when $\beta \neq 0$. In addition, the post-selection procedure does not provide CIs for Exp, Poisson or NB outcomes where as PANDA does. In terms of the efficiency of the inferences, PANDA was the obvious winner as its CI widths were generally much narrower than those from the post-selection procedure, especially for $\beta = 0$ (Table 4). The difference in the CI width ranged 2 to 7-folds. For instance, when Y was Gaussian and $n = 100$, the CI width for $\beta = 0$ was 2.021 from the post-selection procedure, which was approximately 9 times that from PANDA (0.254).

Table 3: Empirical CPs of 95% and 99% CIs from PANDA in GLMs

outcome	true β	range of CP of 95% CI			post-selection inference approach		
		n=100	n=200	n=300	n=100	n=200	n=300
Gaussian	$\neq 0$	(88.5, 96.0)	(90.5, 97.5)	(90.5, 96.5)	(95.5, 97.5)	(95.0, 97.0)	(94.0, 97.0)
	0	(92.0, 96.0)	(93.0, 97.5)	(93.0, 97.0)	(97.5, 99.0)	(97.5, 98.5)	(96.5, 99.0)
Bernoulli	$\neq 0$	(89.0, 98.0)	(91.5, 97.5)	(92.5, 98.5)	(78.5, 91.0)	(86.5, 90.5)	(86.5, 89.5)
	0	(96.5, 99.0)	(95.0, 99.0)	(95.5, 98.5)	(96.0, 98.0)	(94.5, 96.5)	(94.5, 96.0)
Exp	$\neq 0$	(84.5, 93.5)	(89.0, 94.5)	(88.5, 94.5)	-	-	-
	0	(85.0, 91.0)	(86.5, 90.5)	(87.5, 92.5)	-	-	-
Poisson	$\neq 0$	(87.0, 95.0)	(90.0, 95.5)	(91.0, 96.5)	-	-	-
	0	(93.5, 98.0)	(94.0, 99.5)	(95.5, 98.5)	-	-	-
NB	$\neq 0$	(83.5, 91.5)	(92.5, 99.0)	(98.0, 100.0)	-	-	-
	0	(86.0, 94.0)	(96.5, 99.0)	(96.0, 100.0)	-	-	-

-Package `selectiveInference` only produces CIs for linear and logistic regression with the l_1 regularization.

Table 4: CI widths from PANDA in GLMs

outcome	true β	range 95% CI width			post-selection inference		
		n=100	n=200	n=300	n=100	n=200	n=300
Gaussian	$\neq 0$	(0.417, 0.433)	(0.285, 0.291)	(0.232, 0.235)	(1.175, 1.333)	(0.634, 0.708)	(0.437, 0.482)
	0	(0.254, 0.283)	(0.180, 0.193)	(0.159, 0.169)	(1.883, 2.021)	(1.136, 1.178)	(0.847, 0.932)
Bernoulli	$\neq 0$	(1.360, 1.577)	(0.863, 1.017)	(0.669, 0.789)	(4.380, 4.964)	(1.625, 1.773)	(1.082, 1.242)
	0	(1.170, 1.217)	(0.715, 0.727)	(0.553, 0.565)	(3.833, 4.392)	(2.011, 2.229)	(1.443, 1.702)
Exp	$\neq 0$	(0.515, 0.553)	(0.356, 0.369)	(0.288, 0.295)	-	-	-
	0	(0.321, 0.347)	(0.214, 0.232)	(0.162, 0.180)	-	-	-
Poisson	$\neq 0$	(0.757, 0.807)	(0.488, 0.504)	(0.390, 0.398)	-	-	-
	0	(0.639, 0.653)	(0.379, 0.391)	(0.295, 0.299)	-	-	-
NB	$\neq 0$	(0.368, 0.386)	(0.327, 0.342)	(0.295, 0.304)	-	-	-
	0	(0.197, 0.232)	(0.143, 0.164)	(0.127, 0.137)	-	-	-

-Package `selectiveInference` only produces CIs for linear and logistic regression with the l_1 regularization.

5.3 Similarity between minimizer of averaged noise-augmented loss functions vs averaged minimizers of single noise-augmented loss functions

To first illustrate the similarity between $\bar{\theta}$ and $\hat{\theta}$, as outlined in Section 4.5, we simulated data from a linear regression and a Poisson regression, with linear predictor $\mathbf{X}^T\theta = X_1 + 0.75X_2 + 0.5X_3 + 0X_4$. \mathbf{X} and the error term in the linear regression were simulated from $N(0, 1)$ independently ($n = 30$). The PANDA augmented noises \mathbf{e} in both cases was draw from $N(0, \lambda^2)$ ($n_e = 200$). We examined $m = 30, 60, 90, 120$ and $\lambda^2 = 0.25, 0.5, 1, 2$, calculated $\hat{\theta}$ and $\bar{\theta}$, and plotted their differences in Figure 5. The results suggest there is minimal difference between $\hat{\theta}$ and $\bar{\theta}$.

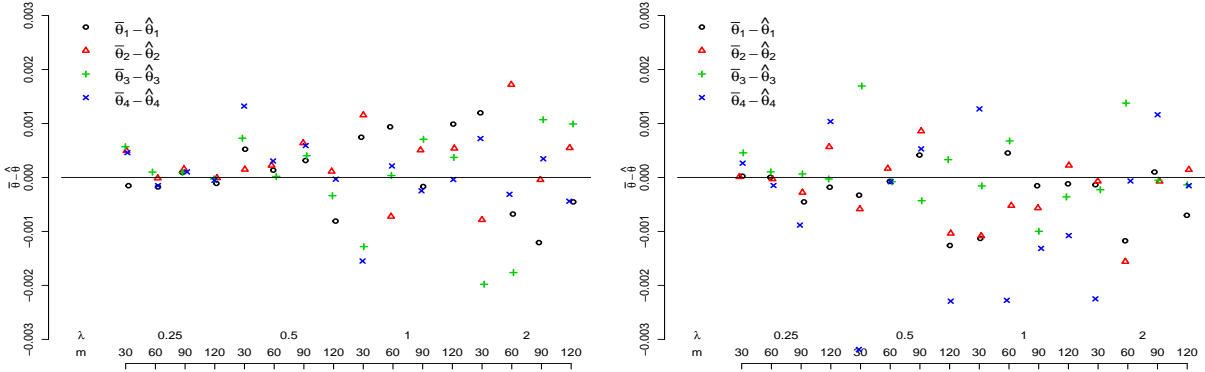


Figure 5: Differences between $\bar{\theta}$ and $\hat{\theta}$ in linear regression (left) and in Poisson regression (right)

6 Case study: the autism spectrum disorder data

We apply PANDA to an autism spectrum disorder (ASD) data collected by the Dutch Association for Autism (Nederlandse Vereniging voor Autisme, NVA) and the VU University Amsterdam (VU) (Begeer et al., 2013). The dataset contains 28 variables of various types (10 continuous, 7 categorical, and 11 count variables) from 3521 participants; and is available in the R package `mgm` (Haslbeck and Waldorp, 2016).

In estimating the relationship among the variable, the continuous variables (nodes) were assumed to follow Gaussian distributions conditional on other nodes and were standardized before implementing PANDA. The count variables were assumed to follow Poisson distributions given other nodes. Each of the 7 categorical variables was dummy-coded. For each of the 7 categorical variables, $k - 1$ Bernoulli nodes were generated. All taken together, there were $p = 35$ nodes in the graph. Algorithm 1 was used to construct the UGM. We set the tuning parameters $\gamma = 1$ and $\sigma = 0$ to obtain a lasso-type penalty, leaving $\lambda = 0.667$ chosen by the EBIC criterion (Chen and Chen, 2008; Foygel and Drton, 2010; Haslbeck and Waldorp, 2015). We used $n_e = 1000$ and threshold $\tau_0 = 10^{-5}$, and iteration $T = 500$. The computation took approximately 16 minutes in R (version 3.4.0 (R Core Team, 2017)) on the Linux x86_64 operating system.

Figure 6 presents a visualization of the estimated UGM via PANDA. The force-directed algorithm of Fruchterman and Reingold (1991) is used to generate the graph layout. Figure 6 suggests that node ‘GCdtA’ (Good Characteristics due to Autism) is connected with multiple nodes of different domains including ‘NoSC’ (Number of Social Contacts), ‘NoI’ (Number of Interests) and ‘IQ’ (Intelligence Quotient), indicating that the uniquely positive traits of people with autism connects with various aspects of their lives (social environment, well-being, diagnostic measurements). PANDA is also able to detect expected relationship among the nodes, such as the strong positive relationship between the present age of a participant (‘Age’) and the age when the participant

was diagnosed with autism (“Agd”).

In addition to the relationships among the variables, we can obtain some insights on the relative importance of those variables in the structure of the estimated graph. Figure 7 displays the standardized centrality measures (strength, closeness and betweenness) (Opsahl et al., 2010) for each node. The results suggest that some variables, such as “Good Characteristics due to Autism”, “Satisfaction: Work” and “No of Social Contacts” were identified as having relatively high centrality level while some other variables, such as “Openness about Diagnosis”, “Type of Work”, “Type of Housing” and “Gender”, had low values in the centrality measures, implying that those variables were not as important in the constitution of the network structure (Figure 6 also shows that these three nodes are not connected to the rest of the nodes).

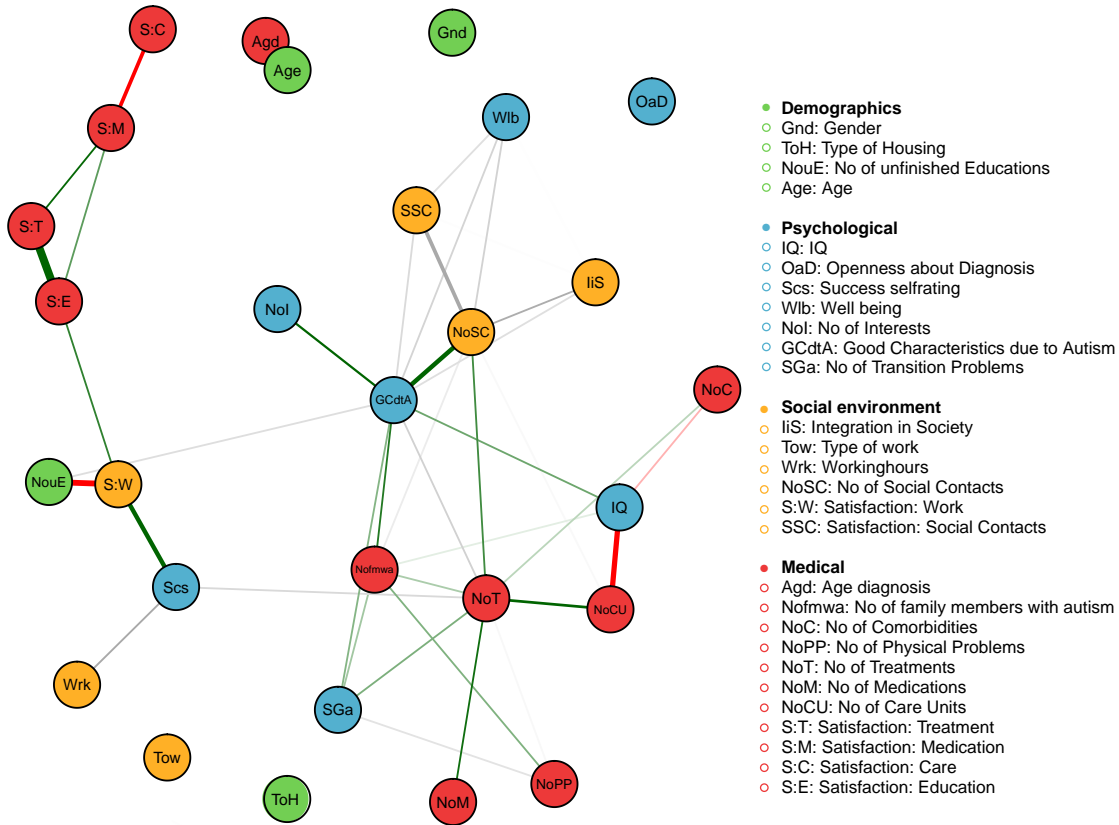


Figure 6: Visualization of the UGM estimated with PANDA for the ASD data. Green edges indicate positive relationships, red edges indicate negative relationships, and gray edges indicate relationships involving categorical variables for which no sign is defined. The width of an edge is proportional to its weight. The colors of the nodes map to the different domains of the attributes: Demographics, Psychological, Social Environment, and Medical.

7 Discussion

PANDA is a regularization technique through noise augmentation. We have shown that PANDA can effectively regularize the construction UGMs when the conditional distribution of the nodes given all other nodes in the graph comes from the Exponential family, and the nodes are not necessarily of the same type, in the regression-based framework. In the case of the GGMs, PANDA also offers counterparts to non regression based regularization such as the SPACE regularization, the SCIO estimator and the graphical ridge. The simulation studies showed PANDA offered

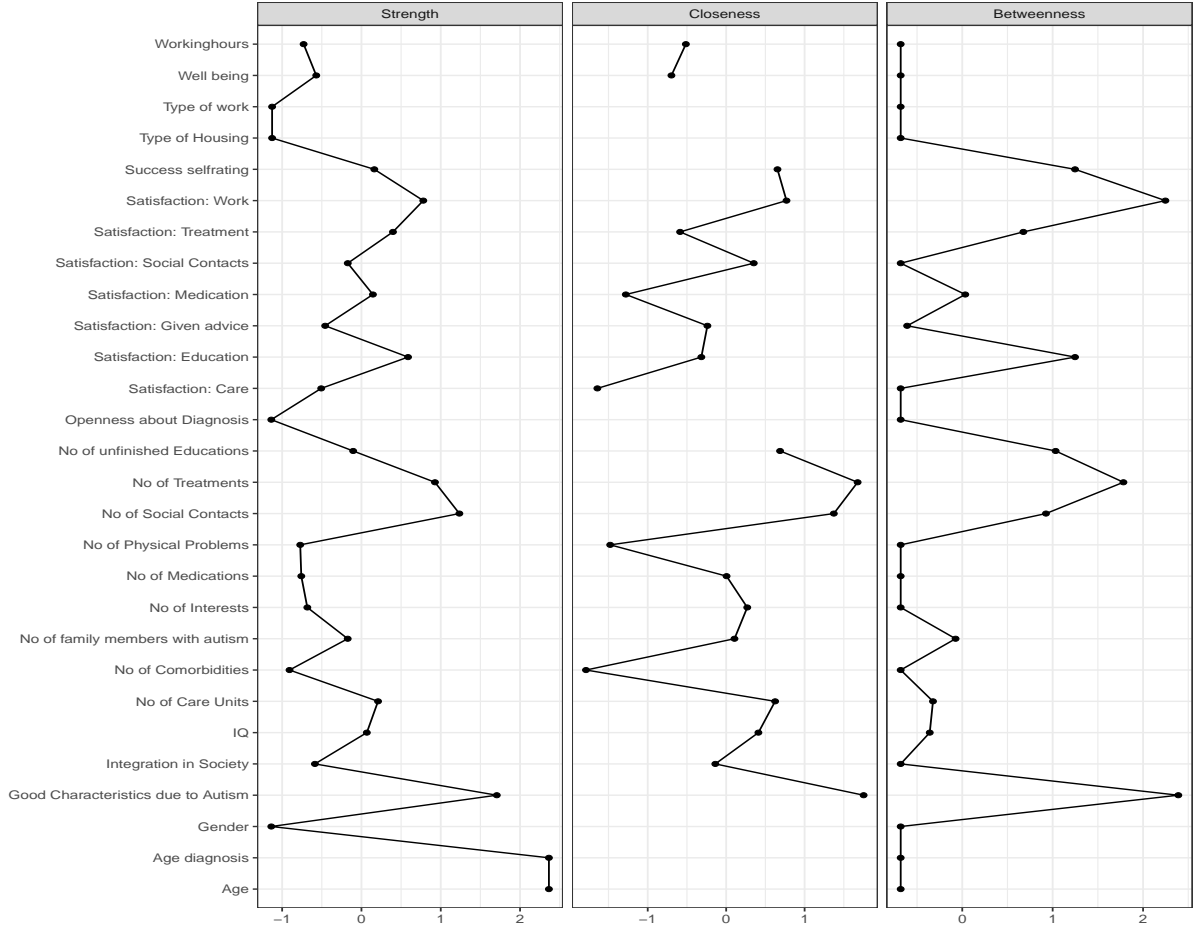


Figure 7: Centrality measures (strength, closeness and betweenness) for each node based on the UGM estimated with PANDA for the ASD data (the centrality measures are standardized; the larger the measure, the more important the corresponding node is; closeness is not defined for isolated nodes.)

non-inferior performance to some existing graph construction method. The case study also demonstrated the effectiveness of PANDA in constructing practically interpretable mixed graph models.

We also establish the almost sure convergence of the noise-augmented loss functions and its minimizer to the expected loss function with the designed regularization effects and the corresponding minimizer as n_e or m increases, providing the theoretical justification for the of PANDA to learn the graph structures empirically.

Computationally, PANDA is easy to implement in any standard software, leveraging existing functions for running GLM regression or matrix operations, with requiring users to employ sophisticated optimization techniques. However, a large n_e could slow down the computation, so n_e needs to chosen properly for practical implementation.

We are currently working on developing a PANDA technique for simultaneously constructing multiple graphs that promotes the sparsity in each graph and similarity between graphs. The results so far are promising.

Appendix

A Proof of Proposition 1

The expectation of $l_p(\Theta|\mathbf{x}, \mathbf{e}) = \sum_{i=1}^{n+n_e} \sum_{j=1}^p \left(\tilde{x}_{ij} - \sum_{k \neq j} \tilde{x}_{ik} \theta_{jk} \right)^2$ over the distribution of noise \mathbf{e} is

$$\mathbb{E}_{\mathbf{e}}(l_p(\Theta|\mathbf{x}, \mathbf{e})) = \sum_{i=1}^n \sum_{j=1}^p \left(x_{ij} - \sum_{k \neq j} x_{ik} \theta_{jk} \right)^2 + \mathbb{E}_{\mathbf{e}} \left(\sum_{i=1}^{n_e} \sum_{j=1}^p \left(e_{ijj} - \sum_{k \neq j} e_{ijk} \theta_{jk} \right)^2 \right) \quad (\text{A.1})$$

$$\begin{aligned} &= \sum_{i=1}^n \sum_{j=1}^p \left(x_{ij} - \sum_{k \neq j} x_{ik} \theta_{jk} \right)^2 + \sum_{i=1}^{n_e} \sum_{j=1}^p \mathbb{E}_{\mathbf{e}} \left(\sum_{k \neq j} e_{ijk} \theta_{jk} \right)^2 \\ &= l(\Theta|\mathbf{x}) + n_e \sum_{k \neq j} \theta_{jk}^2 \mathbb{V}(e_{ijk}). \end{aligned} \quad (\text{A.2})$$

The above equations suggest there are (at least) two ways to approximate the second term in Eqn (A.1) in a Monte Carlo manner. The first approach is straightforward, where the second term is approximated by $\sum_{j=1}^p \lim_{m \rightarrow \infty} m^{-1} \sum_{t=1}^m \sum_{i=1}^{n_e} \left(e_{ijj}^{(t)} - \sum_{k \neq j} e_{ijk}^{(t)} \theta_{jk} \right)^2$. The second approach is suggested by Eqn (A.2). Under the constraint $n_e \mathbb{V}(e_{ijk}) = O(1)$ and letting $n_e \rightarrow \infty$, the second term $n_e \sum_{k \neq j} \theta_{jk}^2 \mathbb{V}(e_{ijk})$ in Eqn (A.2) is $n_e \sum_{j=1}^p \sum_{k \neq j} \theta_{jk}^2 \left(\lim_{n_e \rightarrow \infty} n_e^{-1} \sum_{i=1}^{n_e} e_{ijk}^2 \right)$. The two ways of obtaining the expected penalty term in PANDA applied to GGM-NS (this proposition), UGM-NS (Proposition B), and GGM-CD (Proposition 3).

B Proof of Proposition 2

We first take the Taylor expansion of $l_p(\Theta|\mathbf{x}, \mathbf{e})$, which is the negative log-likelihood, at $e_{ijk} = 0$ for $i = 1, \dots, n_e$ and $k \neq j$, and then evaluate the expectation with regard to the distribution of e_{ijk} . e_{ijj} are pre-specified constants (see Table 1).

$$\begin{aligned} l_p(\Theta|\mathbf{x}, \mathbf{e}) &= l(\Theta|\mathbf{x}) + l_p(\Theta|\mathbf{e}) = l(\Theta|\mathbf{x}) + \sum_{j=1}^p \sum_{i=1}^{n_e} l_{ij}(\boldsymbol{\theta}_j | \mathbf{e}_{i,-j}) \\ &= l(\Theta|\mathbf{x}) - \sum_{j=1}^p \sum_{i=1}^{n_e} \left(h_j(e_{ijj}) + e_{ijj} \sum_{k \neq j} \theta_{jk} e_{ijk} + B_j \left(\sum_{k \neq j} \theta_{jk} e_{ijk} \right) \right) \\ &= l(\Theta|\mathbf{x}) + \sum_{i=1}^{n_e} \sum_{j=1}^p l_{ij}(\boldsymbol{\theta}_j | \mathbf{e}_{i,-j}) \Big|_{\mathbf{e}_{i,-j}=0} \\ &\quad + \sum_{i=1}^{n_e} \sum_{j=1}^p \left\{ e_{ijj} \sum_{k \neq j} (\theta_{jk} e_{ijk}) + \sum_{k \neq j} (\theta_{jk} e_{ijk}) B_j' \left(\sum_{k \neq j} \theta_{jk} e_{ijk} \Big|_{e_{ijk}=0} \right) \right. \\ &\quad \left. + \sum_{d=2}^{\infty} (d!)^{-1} \sum_{k \neq j} (\theta_{jk} e_{ijk})^d B_j^{(d)} \left(\sum_{k \neq j} \theta_{jk} e_{ijk} \Big|_{e_{ijk}=0} \right) \right\} \\ &= l(\Theta|\mathbf{x}) + C_1 + \sum_{i=1}^{n_e} \sum_{j=1}^p \left[(e_{ijj} + B_j'(0)) \sum_{k \neq j} (\theta_{jk} e_{ijk}) + \sum_{d=2}^{\infty} (d!)^{-1} B_j^{(d)}(0) \sum_{k \neq j} (\theta_{jk} e_{ijk})^d \right], \end{aligned}$$

where $C_1 = \sum_{j=1}^p \sum_{i=1}^{n_e} h_j(e_{ijj}) + B_j(0)$, a constant independent of Θ . The expectation of $l_p(\Theta|\mathbf{x}, \mathbf{e})$ with regard to the distribution of $e_{ijk} \sim N(0, \mathbb{V}(e_{jk}))$ is

$$\begin{aligned} \mathbb{E}_{\mathbf{e}}(l_p(\Theta|\mathbf{x}, \mathbf{e})) &= l(\Theta|\mathbf{x}) + C_1 + n_e \sum_{j=1}^p \left(\frac{1}{2} B_j''(0) \sum_{k \neq j} \theta_{jk}^2 \mathbb{V}(e_{jk}) \right) + O \left(n_e \sum_{j=1}^p \sum_{k \neq j} \left(\theta_{jk}^4 \mathbb{E}(e_{jk}^4) \right) \right) \\ &= l(\Theta|\mathbf{x}) + C_1 + n_e \sum_{j=1}^p \left(\frac{1}{2} B_j''(0) \sum_{k \neq j} \theta_{jk}^2 \mathbb{V}(e_{jk}) \right) + O \left(n_e \sum_{j=1}^p \sum_{k \neq j} \left(\theta_{jk}^4 \mathbb{V}^2(e_{jk}) \right) \right) \\ &= l(\Theta|\mathbf{x}) + n_e \sum_{j=1}^p \left(C_{j2} \sum_{k \neq j} \theta_{jk}^2 \mathbb{V}(e_{jk}) \right) + C_1 + O \left(n_e \sum_{j=1}^p \sum_{k \neq j} \left(\theta_{jk}^4 \mathbb{V}^2(e_{jk}) \right) \right), \end{aligned} \quad (\text{B.1})$$

where $C_{j2} = B_j''(0)$. Similar to the Proposition 1, there are at least 2 ways to realize the expectation in Eqn (B.1) empirically. The straightforward way is let $l_p(\Theta|\mathbf{e})$ to be approximated by $\lim_{m \rightarrow \infty} m^{-1} \sum_{t=1}^m \sum_{j=1}^p \sum_{i=1}^{n_e} l_{ij}(\boldsymbol{\theta}_j | \mathbf{e}_{i,-j}^{(t)})$. The second approach, suggested by Eqn (B.1),

under the constraint $n_e V(e_{jk}) = O(1)$, is by letting $n_e \rightarrow \infty$, and the second term in Eqn (B.1) $n_e \sum_{j=1}^p C_{j2} \sum_{k \neq j} \theta_{jk}^2 V(e_{ijk}) = n_e \sum_{j=1}^p C_{j2} \sum_{k \neq j} \left(\theta_{jk}^2 \lim_{n_e \rightarrow \infty} n_e^{-1} \sum_{i=1}^{n_e} e_{ijk}^2 n_e V(e_{jk}) \right)$. Between the two approaches, letting $n_e \rightarrow \infty \cap [n_e V(e_{jk}) = O(1)]$ offers that an additional benefit in that $O \left(\sum_{j=1}^p \sum_{k \neq j} \left(\theta_{jk}^4 n_e V^2(e_{jk}) \right) \right) \rightarrow 0$ in Eqn (B.1). In other words, the second order Taylor approximation of $E_{\mathbf{e}}(l_p(\Theta|\mathbf{x}, \mathbf{e}))$ is arbitrarily close to $E_{\mathbf{e}}(l_p(\Theta|\mathbf{x}, \mathbf{e}))$, which does not hold when $m \rightarrow \infty$. The residual term O , which is a function of Θ , might bring additional regularization effect Θ in addition to $\theta_{jk}^2 (n_e V(e_{jk}))$ when it is non-ignorable. If X_j is of the same type for $j = 1, \dots, p$, then $B_j''(0)$ is the same across j and $C_{j2} = B''(0) = C_j$, and Eqn (B.1) can be simplified as

$$l(\Theta|\mathbf{x}) + C_2 \sum_{j=1}^p \sum_{k \neq j} \theta_{jk}^2 (n_e V(e_{jk})) + C_1 + O \left(\sum_{j=1}^p \sum_{k \neq j} \left(\theta_{jk}^4 n_e V^2(e_{jk}) \right) \right). \quad (\text{B.2})$$

C Proof of Proposition 3

The expectation of $l_p(L, D|\mathbf{x}, \mathbf{e})$ over the distribution of \mathbf{e} for PANDA-CD is $E(l_p(L, D|\mathbf{x}, \mathbf{e}))$

$$\begin{aligned} &= E \left(\sum_{j=1}^p \hat{\sigma}_j^{-2} \sum_{i=1}^n \left(x_{ij} - \sum_{k=1}^{j-1} x_{ik} \theta_{jk} \right)^2 + \sum_{j=1}^p \hat{\sigma}_j^{-2} \sum_{i=1}^{n_e} \left(e_{ijj} - \sum_{k=1}^{j-1} e_{ijk} \theta_{jk} \right)^2 \right) \\ &= l(L, D|\mathbf{x}) + E \left(\sum_{i=1}^{n_e} \sum_{j=1}^p \hat{\sigma}_j^{-2} \left(\sum_{k=1}^{j-1} e_{ijk}^2 \theta_{jk}^2 \right) \right) = l(L, D|\mathbf{x}) + \sum_{i=1}^{n_e} \sum_{j=1}^p \hat{\sigma}_j^{-2} \left(\sum_{k=1}^{j-1} \frac{\lambda \sigma_j^2}{|\theta_{jk}|^\gamma} \theta_{jk}^2 \right) \\ &= l(L, D|\mathbf{x}) + \lambda n_e \sum_{j=1}^p \sum_{k=1}^{j-1} |\theta_{jk}|^{2-\gamma}. \end{aligned}$$

D Proof of Proposition 5

In NI, a noise term is added onto each observed data point x_{ij} , and the dimension ($n \times p$) of the noise-perturbed data $\tilde{\mathbf{x}}$ remains the same as the original data. We establish the equivalence between PANDA and NI in their expected regularization effects for each graph type separately.

D.1 NS for GGM

Denote the noise injected data by $\tilde{\mathbf{x}}_{ij} = \mathbf{x}_{ij} + \mathbf{e}_{ij}$ in regressing X_j on \mathbf{X}_{-j} , where e_{ijj} and e_{ijk} are defined in the same way as in PANDA.

$$\begin{aligned} E_{\mathbf{e}}(l_p(\Theta|\tilde{\mathbf{x}})) &= E_{\mathbf{e}} \left(\sum_{i=1}^n \sum_{j=1}^p \left(\tilde{x}_{ij} - \sum_{k \neq j} \tilde{x}_{ik} \theta_{jk} \right)^2 \right) \\ &= \sum_{i=1}^n \sum_{j=1}^p \left(x_{ij} - \sum_{k \neq j} x_{ik} \theta_{jk} \right)^2 + E_{\mathbf{e}} \left(\sum_{i=1}^n \sum_{j=1}^p \left(e_{ijj} - \sum_{k \neq j} e_{ijk} \theta_{jk} \right)^2 \right) \\ &= l(\Theta|\mathbf{x}) + \sum_{i=1}^n \sum_{j=1}^p \sum_{k \neq j} \theta_{jk}^2 V(e_{ijk}) \end{aligned}$$

D.2 CD for GGM

$\tilde{\mathbf{x}}_{ij} = \mathbf{x}_{ij} + \mathbf{e}_{ij}$, rescaled by σ_j^2 as in Algorithm 2.

$$E_{\mathbf{e}}(l_p(L, D|\tilde{\mathbf{x}})) = E_{\mathbf{e}} \left(n \sum_{j=1}^p \log \sigma_j^2 + \sum_{i=1}^n \sum_{j=1}^p \sigma_j^{-2} \left(\tilde{x}_{ijj} - \sum_{k=1}^{j-1} \tilde{x}_{ijk} \theta_{jk} \right)^2 \right)$$

$$\begin{aligned}
&= \mathbb{E}_{\mathbf{e}} \left(n \sum_{j=1}^p \log \sigma_j^2 + \sum_{i=1}^n \sum_{j=1}^p \sigma_j^{-2} \left(x_{ijj} - \sum_{k=1}^{j-1} x_{ijk} \theta_{jk} \right)^2 + \sum_{i=1}^n \sum_{j=1}^p \sigma_j^{-2} \left(e_{ijj} - \sum_{k=1}^{j-1} e_{ijk} \theta_{jk} \right)^2 \right) \\
&= l(L, D|\mathbf{x}) + \mathbb{E}_{\mathbf{e}} \left(\sum_{i=1}^n \sum_{j=1}^p \sigma_j^{-2} \left(e_{ijj} - \sum_{k=1}^{j-1} e_{ijk} \theta_{jk} \right)^2 \right) \\
&= l(L, D|\mathbf{x}) + \sum_{i=1}^n \sum_{j=1}^p \sum_{k \neq j} \theta_{jk}^2 \mathbb{V}(e_{ijk})
\end{aligned}$$

D.3 SCIO for GGM

\mathbf{x} is scaled by $\sqrt{2}$ and \mathbf{e} is scaled by 2.

$$\begin{aligned}
\mathbb{E}_{\mathbf{e}}(l_p(\boldsymbol{\theta}_j|\tilde{\mathbf{x}})) &= \mathbb{E}_{\mathbf{e}} \left(\frac{1}{2} \boldsymbol{\theta}_j^t \left(n^{-1} \sum_{i=1}^n \tilde{\mathbf{x}}_i \tilde{\mathbf{x}}_i^t \right) \boldsymbol{\theta}_j \right) - \mathbf{1}_j \boldsymbol{\theta}_j \\
&= \frac{1}{2} \boldsymbol{\theta}_j^t \left(n^{-1} \sum_{i=1}^n \mathbf{x}_i \mathbf{x}_i^t + 2n^{-1} \mathbb{E}_{\mathbf{e}} \left(\sum_{i=1}^n \mathbf{e}_{ij} \mathbf{e}_{ij}^t \right) \right) \boldsymbol{\theta}_j - \mathbf{1}_j \boldsymbol{\theta}_j \\
&= \frac{1}{2} \boldsymbol{\theta}_j^t \hat{\Sigma} \boldsymbol{\theta}_j - \mathbf{1}_j \boldsymbol{\theta}_j + \boldsymbol{\theta}_j^t \mathbb{V}(\mathbf{e}_{ij, -j}) \boldsymbol{\theta}_j
\end{aligned}$$

D.4 NS for UGM

We first take the Taylor expansion of $l_p(\boldsymbol{\theta}|\tilde{\mathbf{x}})$, which is the perturbed negative log-likelihood, around $\tilde{x}_{ik} = x_{ik}, k \neq j$, and then evaluate the expectation with regard to the distribution of e_{jk} for $j = 1, \dots, p$, and $k \neq j$. e_{ijj} , is set at 0, rather than 1 in PANDA

$$\begin{aligned}
\mathbb{E}_{\mathbf{e}}(l_p(\boldsymbol{\theta}|\tilde{\mathbf{x}})) &= -\mathbb{E}_{\mathbf{e}} \sum_{j=1}^p \sum_{i=1}^n \left(h_j(\tilde{x}_{ij}) + \tilde{x}_{ij} \sum_{k \neq j} \theta_{jk} \tilde{x}_{ik} - B_j \left(\sum_{k \neq j} \theta_{jk} \tilde{x}_{ik} \right) \right) \\
&= -\sum_{j=1}^p \sum_{i=1}^n \left(h_j(x_{ij}) + x_{ij} \sum_{k \neq j} \theta_{jk} x_{ik} - \mathbb{E}_{\mathbf{e}} B_j \left(\sum_{k \neq j} \theta_{jk} \tilde{x}_{ik} \right) \right) \\
&= l(\boldsymbol{\theta}|\mathbf{x}) + \sum_{j=1}^p \sum_{i=1}^n \sum_{d=2}^{\infty} (d!)^{-1} \mathbb{E}_{\mathbf{e}} B_j^{(d)} \left(\sum_{k \neq j} \theta_{jk} x_{ik} \right) \sum_{k \neq j} (\theta_{jk} e_{ijk})^d \\
&= l(\boldsymbol{\theta}|\mathbf{x}) + 2^{-1} \sum_{j=1}^p \sum_{i=1}^n B_j^{(d)} \left(\sum_{k \neq j} \theta_{jk} x_{ik} \right) \sum_{k \neq j} \theta_{jk}^2 \mathbb{V}(e_{ijk}) + nO \left(\sum_{j=1}^p \boldsymbol{\theta}_j^4 \cdot \mathbb{E}(\mathbf{e}_j^4) \right),
\end{aligned}$$

where $nO \left(\sum_{j=1}^p \boldsymbol{\theta}_j^4 \cdot \mathbb{E}(\mathbf{e}_j^4) \right)$ cannot be ignorable; in other words, the expected regularization effects with NI in UGMs with non-Gaussian nodes is approximate by the second order Taylor expansion.

D.5 Graphical ridge

$$\begin{aligned}
\mathbb{E}_{\mathbf{e}}(l_p(\Omega|\tilde{\mathbf{x}})) &= \mathbb{E}_{\mathbf{e}} \left(-\log(|\Omega|) + \frac{1}{2} \sum_{i=1}^n \tilde{\mathbf{x}}_i^T \Omega \tilde{\mathbf{x}}_i \right) \\
&= -\log(|\Omega|) + \mathbb{E}_{\mathbf{e}} \left(\frac{1}{2} \sum_{i=1}^n (\mathbf{x}_i + \mathbf{e}_i)^T \Omega (\mathbf{x}_i + \mathbf{e}_i) \right) \\
&= -\log(|\Omega|) + \frac{1}{2} \sum_{i=1}^n \mathbf{x}_i^T \Omega \mathbf{x}_i + \frac{1}{2} \mathbb{E}_{\mathbf{e}} \left(\sum_{i=1}^n \mathbf{e}_i^T \Omega \mathbf{e}_i \right) + 0 \\
&= -\log(|\Omega|) + \frac{1}{2} \sum_{i=1}^n \mathbf{x}_i^T \Omega \mathbf{x}_i + \frac{\lambda n}{2} \sum_{j,k=1}^p \omega_{jk}^2
\end{aligned}$$

E Proof of Theorem 1

We prove Theorem 1 for the cases of GGM, PGM, NBGM respectively. WLOG, we use the bridge-type noise $e_{ijk} \sim N(0, \lambda|\theta|^{-\gamma})$ to demonstrate the proofs, which can be easily extended to other types of noises. Prior to the proof of Theorem 1, we state a theoretical result in Claim 1, on which the subsequent proofs rely on.

Claim 1. *If $l_p(\Theta|\mathbf{x}, \mathbf{e})$ and $l_p(\Theta|\mathbf{x})$ are convex functions w.r.t. Θ and share the same parameter space Θ , then*

$$\left| \inf_{\Theta} l_p(\Theta|\mathbf{x}, \mathbf{e}) - \inf_{\Theta} l_p(\Theta|\mathbf{x}) \right| \leq \sup_{\Theta} |l_p(\Theta|\mathbf{x}, \mathbf{e}) - l_p(\Theta|\mathbf{x})|$$

Proof of Claim 1: Since both $\inf_{\Theta} l_p(\Theta|\mathbf{x}, \mathbf{e})$ and $\inf_{\Theta} l_p(\Theta|\mathbf{x})$ are convex optimization problems, each has a global optimum, denoted by $\hat{\Theta}$ and $\tilde{\Theta}$, respectively; and thus $\left| \inf_{\Theta} l_p(\Theta|\mathbf{x}, \mathbf{e}) - \inf_{\Theta} l_p(\Theta|\mathbf{x}) \right| = \left| l_p(\hat{\Theta}|\mathbf{x}, \mathbf{e}) - l_p(\tilde{\Theta}|\mathbf{x}) \right|$. Consider the following two scenarios,

i. if $l_p(\hat{\Theta}|\mathbf{x}, \mathbf{e}) \geq l_p(\tilde{\Theta}|\mathbf{x})$, then $l_p(\tilde{\Theta}|\mathbf{x}, \mathbf{e}) \geq l_p(\hat{\Theta}|\mathbf{x}, \mathbf{e}) \geq l_p(\tilde{\Theta}|\mathbf{x})$ and

$$\left| l_p(\hat{\Theta}|\mathbf{x}, \mathbf{e}) - l_p(\tilde{\Theta}|\mathbf{x}) \right| = l_p(\hat{\Theta}|\mathbf{x}, \mathbf{e}) - l_p(\tilde{\Theta}|\mathbf{x}) \leq l_p(\tilde{\Theta}|\mathbf{x}, \mathbf{e}) - l_p(\tilde{\Theta}|\mathbf{x}) = \left| l_p(\tilde{\Theta}|\mathbf{x}, \mathbf{e}) - l_p(\tilde{\Theta}|\mathbf{x}) \right|$$

ii. if $l_p(\hat{\Theta}|\mathbf{x}, \mathbf{e}) < l_p(\tilde{\Theta}|\mathbf{x})$, then $l_p(\hat{\Theta}|\mathbf{x}, \mathbf{e}) < l_p(\tilde{\Theta}|\mathbf{x}) < l_p(\hat{\Theta}|\mathbf{x})$ and

$$\left| l_p(\hat{\Theta}|\mathbf{x}, \mathbf{e}) - l_p(\tilde{\Theta}|\mathbf{x}) \right| = l_p(\tilde{\Theta}|\mathbf{x}) - l_p(\hat{\Theta}|\mathbf{x}, \mathbf{e}) \leq l_p(\hat{\Theta}|\mathbf{x}) - l_p(\hat{\Theta}|\mathbf{x}, \mathbf{e}) = \left| l_p(\hat{\Theta}|\mathbf{x}, \mathbf{e}) - l_p(\hat{\Theta}|\mathbf{x}) \right|.$$

All taken together, $\left| l_p(\hat{\Theta}|\mathbf{x}, \mathbf{e}) - l_p(\tilde{\Theta}|\mathbf{x}) \right| \leq \max\left(\left| l_p(\tilde{\Theta}|\mathbf{x}, \mathbf{e}) - l_p(\tilde{\Theta}|\mathbf{x}) \right|, \left| l_p(\hat{\Theta}|\mathbf{x}, \mathbf{e}) - l_p(\hat{\Theta}|\mathbf{x}) \right|\right) \leq \sup_{\Theta} |l_p(\Theta|\mathbf{x}, \mathbf{e}) - l_p(\Theta|\mathbf{x})|$. \blacksquare

E.1 GGM

For Gaussian nodes, the regularization effects of $n_e \rightarrow \infty$ and $m \rightarrow \infty$ are the same. The loss function in iteration $t + 1$ is

$$l_p(\Theta|\mathbf{x}, \mathbf{e}) = \sum_{i=1}^n \sum_{j=1}^p \left(x_{ij} - \sum_{k \neq j} x_{ik} \theta_{jk} \right)^2 + \frac{1}{m} \sum_{t=1}^m \sum_{i=1}^{n_e} \sum_{j=1}^p \left(e_{ijj} - \sum_{k \neq j} e_{ijk} \theta_{jk} \right)^2$$

Note that $e_{ijk} = \sqrt{\lambda|\theta|^{-\gamma}} z_{ijk}$, where $z_{ijk} \sim N(0, 1)$. Therefore, $l_p(\Theta|\mathbf{x}, \mathbf{e})$

$$\begin{aligned} &= l(\Theta|\mathbf{x}) + \frac{1}{m} \sum_{t=1}^m \sum_{i=1}^{n_e} \sum_{j=1}^p \left(\sum_{k \neq j} \frac{\lambda \theta_{jk}^2}{|\theta_{jk}^{(t)}|^\gamma} z_{ijk}^2 + 2 \sum_{l < v \neq j} \frac{\lambda \theta_{jl} \theta_{jv}}{|\theta_{jv}^{(t)} \theta_{jl}^{(t)}|^{\frac{\gamma}{2}}} z_{ijl} z_{ijv} \right) \\ &= l(\Theta|\mathbf{x}) + \frac{1}{m} \sum_{t=1}^m \sum_{j=1}^p \sum_{k \neq j} \left(\frac{\lambda \theta_{jk}^2}{|\theta_{jk}^{(t)}|^\gamma} \sum_{i=1}^{n_e} z_{ijk}^2 \right) + \frac{2}{m} \sum_{t=1}^m \sum_{j=1}^p \sum_{l < v \neq j} \left(\frac{\lambda \theta_{jl} \theta_{jv}}{|\theta_{jv}^{(t)} \theta_{jl}^{(t)}|^{\frac{\gamma}{2}}} \sum_{i=1}^{n_e} z_{ijl} z_{ijv} \right) \\ &\sim l(\Theta|\mathbf{x}) + \sum_{j=1}^p \sum_{k \neq j} \left(\frac{\lambda n_e \theta_{jk}^2}{|\theta_{jk}^{(t)}|^\gamma} \Gamma\left(\frac{mn_e}{2}, \frac{2}{mn_e}\right) \right) \end{aligned}$$

$$\begin{aligned}
& + \sum_{j=1}^p \sum_{l < v \neq j} \left(\frac{\lambda n_e \theta_{jl} \theta_{jv}}{|\theta_{jv}^{(t)} \theta_{jl}^{(t)}|^{\frac{\gamma}{2}}} \left(\Gamma \left(\frac{mn_e}{2}, \frac{2}{mn_e} \right) - \Gamma \left(\frac{mn_e}{2}, \frac{2}{mn_e} \right) \right) \right) \\
& \sim l_p(\Theta | \mathbf{x}) + \sum_{j=1}^p \sum_{k \neq j} \left(\frac{\lambda n_e \theta_{jk}^2}{|\theta_{jk}^{(t)}|^{\gamma}} \left(\Gamma \left(\frac{mn_e}{2}, \frac{2}{mn_e} \right) - 1 \right) \right) \\
& + \sum_{j=1}^p \sum_{l < v \neq j} \left(\frac{\lambda n_e \theta_{jl} \theta_{jv}}{|\theta_{jv}^{(t)} \theta_{jl}^{(t)}|^{\frac{\gamma}{2}}} \left(\Gamma \left(\frac{mn_e}{2}, \frac{2}{mn_e} \right) - \Gamma \left(\frac{mn_e}{2}, \frac{2}{mn_e} \right) \right) \right).
\end{aligned}$$

As $m \rightarrow \infty$, or $n_e \rightarrow \infty$ while keeping λn_e at constant, we have

$$\rightarrow l_p(\Theta | \mathbf{x}) + \sum_{j=1}^p \sum_{k \neq j} \left(\frac{\lambda n_e \theta_{jk}^2}{|\theta_{jk}^{(t)}|^{\gamma}} N \left(0, \frac{2}{mn_e} \right) \right) + \sum_{j=1}^p \sum_{l < v \neq j} \left(\frac{\lambda n_e \theta_{jl} \theta_{jv}}{|\theta_{jv}^{(t)} \theta_{jl}^{(t)}|^{\frac{\gamma}{2}}} N \left(0, \frac{4}{mn_e} \right) \right) \quad (\text{E.1})$$

$$\rightarrow l_p(\Theta | \mathbf{x}) + (mn_e)^{-1/2} C_1 N(0, 1) \text{ where } C_1 = \lambda n_e \left(2 \sum_{j=1}^p \left\| \left(\frac{\boldsymbol{\theta}_{j,-j}}{|\boldsymbol{\theta}_{j,-j}^{(t)}|^{\frac{\gamma}{2}}} \right) \left(\frac{\boldsymbol{\theta}_{j,-j}}{|\boldsymbol{\theta}_{j,-j}^{(t)}|^{\frac{\gamma}{2}}} \right)^T \right\|_2^2 \right)^{1/2}. \quad (\text{E.2})$$

Assume $|\theta_{jk}|$ belongs to a compact parameter space and is bounded by B and (λn_e) is held at a constant, Given Proposition 1, per the strong LLN, the average over n_e noise terms or over m loss functions converges almost surely to its mean for all $\Theta \in \Theta$. Therefore, $\sup_{\Theta} |l_p(\Theta | \mathbf{x}, \mathbf{e}) - l_p(\Theta | \mathbf{x})| \xrightarrow{\text{a.s.}} 0$ as $m \rightarrow \infty$ or $n_e \rightarrow \infty$. Per Claim 1, $\inf_{\Theta} l_p(\Theta | \mathbf{x}, \mathbf{e}) \xrightarrow{\text{a.s.}} \inf_{\Theta} l_p(\Theta | \mathbf{x})$, and $\arg \inf_{\Theta} l_p(\Theta | \mathbf{x}, \mathbf{e}) \xrightarrow{\text{a.s.}} \arg \inf_{\Theta} l_p(\Theta | \mathbf{x})$ due to the convexity of the loss function.

E.2 PGM

The averaged perturbed loss function over m iterations upon convergence is

$$l_p(\Theta | \mathbf{x}, \mathbf{e}) = l(\Theta | \mathbf{x}) - \frac{1}{m} \sum_{t=1}^m \sum_{i=1}^{n_e} \sum_{j=1}^p \left(e_{ijj} \sum_{k \neq j} e_{ijk}^{(t)} \theta_{jk} - \log(e_{ijj}!) - \exp \left(\sum_{k \neq j} e_{ijk}^{(t)} \theta_{jk} \right) \right) \quad (\text{E.3})$$

$$= l(\Theta | \mathbf{x}) - \frac{1}{m} \sum_{t=1}^m \sum_{j=1}^p e_{ijj} \sum_{k \neq j} \sum_{i=1}^{n_e} \theta_{jk} e_{ijk}^{(t)} + \frac{1}{m} \sum_{t=1}^m \sum_{j=1}^p \sum_{i=1}^{n_e} \exp \left(\sum_{k \neq j} \theta_{jk} e_{ijk}^{(t)} \right) + C$$

$$= l(\Theta | \mathbf{x}) - \frac{1}{m} \sum_{t=1}^m \sum_{j=1}^p e_{ijj} \sum_{k \neq j} \left(\frac{\sqrt{\lambda} \theta_{jk}}{|\theta_{jk}|^{\frac{\gamma}{2}}} \sum_{i=1}^{n_e} z_{ijk} \right) + \frac{1}{m} \sum_{t=1}^m \sum_{j=1}^p \sum_{i=1}^{n_e} \exp \left(\sum_{k \neq j} \frac{\sqrt{\lambda} \theta_{jk}}{|\theta_{jk}|^{\frac{\gamma}{2}}} z_{ijk} \right) + C, \quad (\text{E.4})$$

where $e_{ijj} = 1$ and C is a constant not related to Θ . As illustrated in Figure 2, the regularization effect are different for different values n_e and m . In general for non-Gaussian nodes, the regularization effects of $n_e \rightarrow \infty$ given a fixed m and $n_e \lambda = O(1)$ and $m \rightarrow \infty$ given a fixed n_e are different. We thus consider each case separately in the proof.

Case 1: $n_e \rightarrow \infty$, $n_e \lambda = O(1)$ and fixed m

Assume $m = 1$ WLOG. Since $n_e \rightarrow \infty$ and $\lambda n_e = O(1)$, therefore, $\exp(\sum_{k \neq j} \frac{\sqrt{\lambda} \theta_{jk}}{|\theta_{jk}|^{\frac{\gamma}{2}}} z_{ijk})$ in Eqn (E.4) approaches 1, and Eqn (E.4) is approximated arbitrarily well by the second order Taylor expansion around $\sum_{k \neq j} \theta_{jk} e_{ijk} = 0$. Thus

$$l_p(\Theta | \mathbf{x}, \mathbf{e}) \rightarrow l(\Theta | \mathbf{x}) - \sum_{j=1}^p \sum_{k \neq j} \left(\frac{\sqrt{\lambda} \theta_{jk}}{|\theta_{jk}|^{\frac{\gamma}{2}}} \sum_{i=1}^{n_e} z_{ijk} \right) + \sum_{j=1}^p \sum_{i=1}^{n_e} \sum_{k \neq j} \frac{\sqrt{\lambda} \theta_{jk}}{|\theta_{jk}|^{\frac{\gamma}{2}}} z_{ijk} \quad (\text{E.5})$$

$$\begin{aligned}
& + \frac{1}{2} \sum_{j=1}^p \sum_{i=1}^{n_e} \left(\sum_{k \neq j} \frac{\sqrt{\lambda} \theta_{jk}}{|\theta_{jk}|^{\frac{\gamma}{2}}} z_{ijk} \right)^2 + O(n_e^{-1}) N(1, C_2) + \text{const.} \\
\rightarrow l(\Theta|\mathbf{x}) & + \frac{1}{2} \sum_{j=1}^p \sum_{k \neq j} \left(\frac{\lambda \theta_{jk}^2}{|\theta_{jk}|^\gamma} \sum_{i=1}^{n_e} z_{ijk}^2 \right) + \sum_{j=1}^p \sum_{k < l \neq j} \left(\frac{\lambda \theta_{jk} \theta_{jl}}{|\theta_{jk} \theta_{jl}|^{\frac{\gamma}{2}}} \sum_{i=1}^{n_e} z_{ijk} z_{ijl} \right) \\
& + O(n_e^{-1}) N(1, C_2) + \text{const.} \\
\rightarrow l(\Theta|\mathbf{x}) & + \frac{1}{2} \sum_{j=1}^p \sum_{k \neq j} \left(\frac{\lambda n_e \theta_{jk}^2}{|\theta_{jk}|^\gamma} \right) + O(n_e^{-1}) N(1, C_2) + O(n_e^{-0.5}) C_1 N(0, 1) + \text{const.} \\
\rightarrow l(\Theta|\mathbf{x}) & + \frac{\lambda n_e}{2} \sum_{j=1}^p \sum_{j \neq k} |\theta_{jk}|^{2-\gamma} + \text{const.}, \text{ as } t, n_e \rightarrow \infty \text{ and } \lambda n_e = O(1).
\end{aligned} \tag{E.6}$$

C_1 and C_2 are functions of Θ , the corresponding asymptotic normal distributions are resulted from summation over n_e noises. Specifically,

$$C_1 = \frac{\lambda n_e}{2} \left(2 \sum_{j=1}^p \left\| \left(|\boldsymbol{\theta}_{j,-j}|^{1-\frac{\gamma}{2}} \right) \left(|\boldsymbol{\theta}_{j,-j}|^{1-\frac{\gamma}{2}} \right)^T \right\|_2^2 \right)^{1/2} \tag{E.7}$$

The third and fourth term in Eqn (E.5) corresponds to the second and first order of the fourth term in Eqn (E.3), which cancel out when $n_e \rightarrow \infty$ since $e_{ijj} = 1$. The a.s. convergence of sums of random variables in Eqn (E.6) to their mean is essentially due to the LLN under $\lambda n_e = O(1)$. Therefore due to convexity,

$$\arg \inf_{\Theta} l_p(\Theta|\mathbf{x}, \mathbf{e}) \xrightarrow{a.s.} \arg \inf_{\Theta} l_p(\Theta|\mathbf{x})$$

Case 2: $m \rightarrow \infty$ and fixed n_e

When n_e is fixed, Eqn (E.4) can no longer be approximated arbitrarily well by second order Taylor expansion, preventing the two noise terms from canceling out. Therefore, we need $m \rightarrow \infty$ to realize the expected likelihood-driven regularization effect, and it is different from those outlined in Proposition 1.

$$\begin{aligned}
l(\Theta|\mathbf{x}, \mathbf{e}) & \sim l(\Theta|\mathbf{x}) - \sum_{j=1}^p \sum_{k \neq j} \frac{\sqrt{\lambda} n_e \theta_{jk}}{\sqrt{m} |\theta_{jk}|^{\frac{\gamma}{2}}} N(0, 1) + \frac{1}{m} \sum_{t=1}^m \sum_{j=1}^p \sum_{i=1}^{n_e} \text{LogN} \left(0, \sum_{k \neq j} \frac{\lambda \theta_{jk}^2}{|\theta_{jk}|^\gamma} \right) + \text{const.} \\
\rightarrow l(\Theta|\mathbf{x}) & + n_e \sum_{j=1}^p \exp \left(\left(\sum_{j \neq k} \frac{\sqrt{\lambda} \theta_{jk}}{|\theta_{jk}|^{\frac{\gamma}{2}}} \right)^2 \right) + \text{const. as } m \rightarrow \infty, \text{ by LLN} \\
\rightarrow l(\Theta|\mathbf{x}) & + n_e \sum_{j=1}^p \exp \left(\left(\lambda \sum_{j \neq k} |\theta_{jk}|^{1-\frac{\gamma}{2}} \right)^2 \right) + \text{const. as } t, m \rightarrow \infty
\end{aligned} \tag{E.8}$$

The likelihood driven regularization effects are super-linearly compared with lasso, when using lasso NDG, but with finite n_e , intuitively illustrated in Figure 2. Though the convergence of regularization effects are almost surely, we further show that by CLT, the convergence is in normal distribution, in cases of both $n_e \rightarrow \infty$ and $m \rightarrow \infty$. Convergence in normal explains the evenly distributed blue and green crosses around red and orange lines in Figure 2.

$$l(\Theta|\mathbf{x}, \mathbf{e}) \rightarrow l_p(\Theta|\mathbf{x}) - \sum_{j=1}^p \sum_{k \neq j} \frac{\sqrt{\lambda} n_e \theta_{jk}}{\sqrt{m} |\theta_{jk}|^{\frac{\gamma}{2}}} N(0, 1) + \text{const.}$$

$$+ \left(\frac{n_e}{m} \sum_{j=1}^p \left(\exp \left(\left(\sum_{k \neq j} \frac{\sqrt{\lambda} \theta_{jk}}{|\theta_{jk}|^{\frac{\gamma}{2}}} \right)^2 \right) - 1 \right) \exp \left(\left(\sum_{k \neq j} \frac{\sqrt{\lambda} \theta_{jk}}{|\theta_{jk}|^{\frac{\gamma}{2}}} \right)^2 \right) \right)^{\frac{1}{2}} N(0, 1) \quad (\text{E.9})$$

as $m \rightarrow \infty$ or $n_e \rightarrow \infty$ while keeping λn_e at constant. Since the average of $m \rightarrow \infty$ perturbed loss functions is taken, per the strong LLN and assuming Θ to be compact, the average converges almost surely to its mean, for all $\Theta \in \Theta$. Therefore

$$\begin{aligned} & \sup_{\Theta} |l_p(\Theta|\mathbf{x}, \mathbf{e}) - l_p(\Theta|\mathbf{x})| \xrightarrow{\text{a.s.}} 0, \text{ as } m \rightarrow \infty \\ & \Rightarrow \inf_{\Theta} l_p(\Theta|\mathbf{x}, \mathbf{e}) \xrightarrow{\text{a.s.}} \inf_{\Theta} l_p(\Theta|\mathbf{x}), \text{ as } m \rightarrow \infty \\ & \Rightarrow \arg \inf_{\Theta} l_p(\Theta|\mathbf{x}, \mathbf{e}) \xrightarrow{\text{a.s.}} \arg \inf_{\Theta} l_p(\Theta|\mathbf{x}), \text{ as } m \rightarrow \infty, \text{ due to convexity.} \end{aligned}$$

E.3 EGM

The averaged perturbed loss function over m iterations upon convergence is

$$l_p(\Theta|\mathbf{x}, \mathbf{e}) = l(\Theta|\mathbf{x}) - \frac{1}{m} \sum_{t=1}^m \sum_{i=1}^{n_e} \sum_{j=1}^p \left(\sum_{k \neq j} e_{ijk}^{(t)} \theta_{jk} - e_{ijj} \exp \left(\sum_{k \neq j} e_{ijk}^{(t)} \theta_{jk} \right) \right),$$

where $e_{ijj} = 1$. Comparing the above loss function with the loss function in Eqn (E.3), we could see you are equivalence. Therefore, the proof for PGM also applies in the case of EGM.

E.4 NBGM

The averaged perturbed loss function over m iterations upon convergence is

$$\begin{aligned} l_p(\Theta|\mathbf{x}, \mathbf{e}) &= l(\Theta|\mathbf{x}) \\ &- \frac{1}{m} \sum_{t=1}^m \sum_{i=1}^{n_e} \sum_{j=1}^p \left(\log \left(\frac{\Gamma(e_{ijj} + r_j) r_j^{r_j}}{\Gamma(e_{ijj} + 1) \Gamma(r_j)} \right) + e_{ijj} \sum_{k \neq j} e_{ijk}^{(t)} \theta_{jk} - (r_j + e_{ijj}) \log \left(r_j + \exp \left(\sum_{k \neq j} e_{ijk}^{(t)} \theta_{jk} \right) \right) \right) \end{aligned} \quad (\text{E.10})$$

$$\begin{aligned} &= l(\Theta|\mathbf{x}) - \frac{1}{m} \sum_{t=1}^m \sum_{i=1}^{n_e} \sum_{j=1}^p e_{ijj} \sum_{k \neq j} e_{ijk}^{(t)} \theta_{jk} + \frac{1}{m} \sum_{t=1}^m \sum_{i=1}^{n_e} \sum_{j=1}^p (r_j + e_{ijj}) \log \left(r_j + \exp \left(\sum_{k \neq j} e_{ijk}^{(t)} \theta_{jk} \right) \right) + \text{const.} \\ &= l(\Theta|\mathbf{x}) - \frac{1}{m} \sum_{t=1}^m \sum_{j=1}^p e_{ijj} \sum_{k \neq j} \left(\frac{\sqrt{\lambda} \theta_{jk}}{|\theta_{jk}|^{\frac{\gamma}{2}}} \sum_{i=1}^{n_e} z_{ijk} \right) \\ &+ \frac{1}{m} \sum_{t=1}^m \sum_{j=1}^p \sum_{i=1}^{n_e} (r_j + 1) \log \left(r_j + \exp \left(\sum_{k \neq j} \frac{\sqrt{\lambda} \theta_{jk}}{|\theta_{jk}|^{\frac{\gamma}{2}}} z_{ijk} \right) \right) + \text{const.} \end{aligned} \quad (\text{E.11})$$

Case 1: $n_e \rightarrow \infty$ and $n_e \lambda = O(1)$ and fixed m

Let $m = 1$ WLOG. Since $n_e \rightarrow \infty$ and $\lambda n_e = O(1)$, $\exp \left(\sum_{k \neq j} \frac{\sqrt{\lambda} \theta_{jk}}{|\theta_{jk}|^{\frac{\gamma}{2}}} z_{ijk} \right)$ approaches 1 and Eqn (E.4) is approximated arbitrarily well by the second order Taylor expansion. Letting $e_{ij} = 1$ as

specified in Table 1, we have

$$l_p(\Theta|\mathbf{x}, \mathbf{e}) = l(\Theta|\mathbf{x}) - \sum_{j=1}^p \sum_{k \neq j} \left(\frac{\sqrt{\lambda} \theta_{jk}}{|\theta_{jk}|^{\frac{\gamma}{2}}} \sum_{i=1}^{n_e} z_{ijk} \right) + \sum_{j=1}^p \sum_{i=1}^{n_e} \sum_{k \neq j} \frac{\sqrt{\lambda} \theta_{jk}}{|\theta_{jk}|^{\frac{\gamma}{2}}} z_{ijk} \quad (\text{E.12})$$

$$\begin{aligned} & + \frac{1}{2} \sum_{j=1}^p \sum_{i=1}^{n_e} \frac{r_j}{r_j + 1} \left(\sum_{k \neq j} \frac{\sqrt{\lambda} \theta_{jk}}{|\theta_{jk}|^{\frac{\gamma}{2}}} z_{ijk} \right)^2 + O(n_e^{-1}) N(1, C_2) + \text{const.} \\ \rightarrow l(\Theta|\mathbf{x}) & + \frac{1}{2} \sum_{j=1}^p \sum_{k \neq j} \frac{r_j}{r_j + 1} \left(\frac{\lambda \theta_{jk}^2}{|\theta_{jk}|^\gamma} \sum_{i=1}^{n_e} z_{ijk}^2 \right) + \sum_{j=1}^p \sum_{k < l \neq j} \frac{r_j}{r_j + 1} \left(\frac{\lambda \theta_{jk} \theta_{jl}}{|\theta_{jk} \theta_{jl}|^{\frac{\gamma}{2}}} \sum_{i=1}^{n_e} z_{ijk} e_{0ijl} \right) \\ & + O(n_e^{-1}) N(1, C_2) + \text{const.} \end{aligned} \quad (\text{E.13})$$

$$\rightarrow l(\Theta|\mathbf{x}) + \frac{1}{2} \sum_{j=1}^p \sum_{k \neq j} \frac{r_j}{r_j + 1} \left(\frac{\lambda \theta_{jk}^2}{|\theta_{jk}|^\gamma} \sum_{i=1}^{n_e} z_{ijk}^2 \right) + O(n_e^{-1}) N(1, C_2) + O(n_e^{-0.5}) C_1 N(0, 1) + \text{const.}$$

$$\rightarrow l(\Theta|\mathbf{x}) + \frac{\lambda n_e}{2} \sum_{j=1}^p \sum_{j \neq k} \frac{r_j}{r_j + 1} |\theta_{jk}|^{2-\gamma} + \text{const.}, \text{ as } t, n_e \rightarrow \infty \text{ and } \lambda n_e = O(1)$$

C_1 and C_2 are functions of Θ , the corresponding asymptotic normal distributions are resulted from summation over n_e noises. Specifically,

$$C_1 = \frac{\lambda n_e}{2} \left(2 \sum_{j=1}^p \left(\frac{r_j}{r_j + 1} \right)^2 \left\| \left(|\boldsymbol{\theta}_{j,-j}|^{1-\frac{\gamma}{2}} \right) \left(|\boldsymbol{\theta}_{j,-j}|^{1-\frac{\gamma}{2}} \right)^T \right\|_2^2 \right)^{1/2} \quad (\text{E.14})$$

The third and forth term in Eqn (E.12) corresponds to the third and first order of the forth term in Eqn (E.10), with augmented response variable $e_{ij} = 1$, these two terms cancel out each other when $n_e \rightarrow \infty$. The a.s. convergence of sums of random variables in Eqn (E.13) to their mean is essentially due to LLN under $\lambda n_e = O(1)$. Therefore due to convexity,

$$\arg \inf_{\Theta} l_p(\Theta|\mathbf{x}, \mathbf{e}) \xrightarrow{\text{a.s.}} \arg \inf_{\Theta} l_p(\Theta|\mathbf{x})$$

Case 2: $m \rightarrow \infty$ and fixed n_e

When n_e is fixed, Eqn (E.11) can no longer be approximated arbitrarily well by second order Taylor expansion, preventing the two noise terms from canceling out. Therefore, we need $m \rightarrow \infty$ to realize the expected likelihood-driven regularization effect, and it is different from those outlined in Proposition 1.

$$\begin{aligned} l(\Theta|\mathbf{x}, \mathbf{e}) & \sim l(\Theta|\mathbf{x}) - \sum_{j=1}^p \sum_{k \neq j} \frac{\sqrt{\lambda} n_e \theta_{jk}}{\sqrt{m} |\theta_{jk}^{(t-1)}|^{\frac{\gamma}{2}}} N(0, 1) + \frac{1}{m} \sum_{t=1}^m \sum_{i=1}^{n_e} Z + \text{const.} \\ & \rightarrow l(\Theta|\mathbf{x}) + n_e \text{E}(Z) + \text{const. as } m \rightarrow \infty, \text{ by LLN} \end{aligned} \quad (\text{E.15})$$

where r.v. $Z = \sum_{j=1}^p (r_j + 1) \log \left(r_j + \exp \left(\sum_{k \neq j} e_{ijk}^{(t)} \theta_{jk} \right) \right) \triangleq \sum_{j=1}^p Z_j$. Since $\log(r_j + \exp(x)) \rightarrow \max(\log(r_j), x)$, as $x \rightarrow \pm\infty$, hence r.v. Z has finite variance. The likelihood driven regularization effects are sub-linearly compared with lasso, when using lasso NDG, but with finite n_e , intuitively illustrated in Figure 2. Though the convergence of regularization effects are almost surely, we further show that by CLT, the convergence is in normal distribution, in cases of both $n_e \rightarrow \infty$ and $m \rightarrow \infty$. Convergence in normal explains the evenly distributed blue and green crosses around red and orange lines in Figure 2.

$$l_p(\Theta|\mathbf{x}) = l(\Theta|\mathbf{x}) + \text{E}(Z) + \frac{n_e}{\sqrt{m}} \text{sd}(Z) N(0, 1) \quad (\text{E.16})$$

as $m \rightarrow \infty$ or $n_e \rightarrow \infty$ and $\lambda n_e = O(1)$. Since the average of $m \rightarrow \infty$ perturbed loss functions is taken, by the strong LLN and assuming Θ to be compact, the average converges almost surely to its mean for all $\Theta \in \Theta$. Therefore,

$$\begin{aligned} & \sup_{\Theta} |l_p(\Theta|\mathbf{x}, \mathbf{e}) - l_p(\Theta|\mathbf{x})| \xrightarrow{\text{a.s.}} 0, \text{ as } m \rightarrow \infty \\ \Rightarrow & \inf_{\Theta} l_p(\Theta|\mathbf{x}, \mathbf{e}) \xrightarrow{\text{a.s.}} \inf_{\Theta} l_p(\Theta|\mathbf{x}), \text{ as } m \rightarrow \infty \\ \Rightarrow & \arg \inf_{\Theta} l_p(\Theta|\mathbf{x}, \mathbf{e}) \xrightarrow{\text{a.s.}} \arg \inf_{\Theta} l_p(\Theta|\mathbf{x}), \text{ as } m \rightarrow \infty \text{ due to convexity} \end{aligned}$$

E.5 BGM

The averaged perturbed loss function over m iterations upon convergence is

$$l_p(\Theta|\mathbf{x}, \mathbf{e}) = l(\Theta|\mathbf{x}) - \frac{1}{m} \sum_{t=1}^m \sum_{i=1}^{n_e} \sum_{j=1}^p \left(\frac{e_{ijj} + 1}{2} \sum_{k \neq j} e_{ijk}^{(t)} \theta_{jk} - \log \left(1 + \exp \left(\sum_{k \neq j} e_{ijk}^{(t)} \theta_{jk} \right) \right) \right),$$

which is a special case of Eqn (E.10) by setting $r_j = 1$. As such, the proof for NBGM also applies to BGM.

F proof of Proposition 6

In the case such as multicollinearity, PANDA with certain sparsity regularization might experience difficulty in learning minimizer $\hat{\Theta}_p^{(n_e)}$ (or $\hat{\Theta}_p^{(m)}$) when n_e (or m) $\rightarrow \infty$. In such a case, we prove that there exists $\epsilon > 0$ and a sub-sequence $[n_e]_i$ (or $[m]_i$), such that letting $\nu_i \triangleq \hat{\Theta}_p^{[n_e]_i}$ (or $\hat{\Theta}_p^{[m]_i}$), then $d(\nu_i, \hat{\Theta}^0) > \epsilon$. Denote $\mu_i = l_p(\nu_i|\mathbf{x}, \mathbf{e})$, then by Eqn (31), there exist sub-sequence $[i]_k$, such that,

$$\Pr \left(\sup_{\Theta} |\bar{l}_p(\Theta|\mathbf{x}, \mathbf{e}) - \bar{l}_p(\Theta|\mathbf{x})| > \delta \right) < \frac{1}{k}, k \in N \quad (\text{F.1})$$

Since Θ is compact, the subsequence $[i]_k$ converges to a point $\hat{\Theta}^* \in \Theta$ and $d(\hat{\Theta}^*, \hat{\Theta}^0) \geq \epsilon$, so $\hat{\Theta}^* \notin \hat{\Theta}^0$. On the other hand, for any $\Theta \in \Theta$, we have

$$\begin{aligned} \bar{l}_p(\hat{\Theta}^*|\mathbf{x}, \mathbf{e}) - \bar{l}_p(\Theta|\mathbf{x}) &= (\bar{l}_p(\hat{\Theta}^*|\mathbf{x}, \mathbf{e}) - \bar{l}_p(\nu_{[i]_k}|\mathbf{x}, \mathbf{e})) + (\bar{l}_p(\nu_{[i]_k}|\mathbf{x}, \mathbf{e}) - \mu_{[i]_k}(\nu_{[i]_k})) \\ &\quad + (\mu_{[i]_k}(\nu_{[i]_k}) - \mu_{[i]_k}(\Theta)) + (\mu_{[i]_k}(\Theta) - \bar{l}_p(\Theta|\mathbf{x})) \end{aligned}$$

By the continuity of loss function and $\lim_{i_k \rightarrow \infty} \nu_{[i]_k} = \hat{\Theta}^*$, the first term is arbitrarily small with $i_k \rightarrow \infty$ and by equation (F.1), the second and forth terms are arbitrarily small with $i_k \rightarrow \infty$, and the third term is non-positive. By the arbitrariness of $\Theta \in \Theta$, we must have $\hat{\Theta}^* \in \hat{\Theta}^0$, which is a contradiction and the Proposition is proved.

By Claim 1, after applying bias correction scalers we only need to prove $\frac{1}{n+n_e} |l_p(\Omega|\tilde{\mathbf{x}}, \tilde{\mathbf{e}}) - l_p(\Omega|\tilde{\mathbf{x}})| \rightarrow 0, \forall \Omega \in \Omega$ almost surely and obtain its probability bound. With bias correction scaler, the perturbed empirical loss function is

$$l_p(\Omega|\tilde{\mathbf{x}}, \tilde{\mathbf{e}})$$

$$\begin{aligned}
&= -(n+n_e)\log(\Omega) + \frac{n+n_e}{n} \sum_{i=1}^n \mathbf{x}_i^T \Omega \mathbf{x}_i + \frac{n+n_e}{n_e} \frac{1}{m} \sum_{t=1}^m \sum_{i=1}^{n_e} \mathbf{e}_i^T \Omega \mathbf{e}_i \\
&= \frac{n+n_e}{n} l(\Omega|\mathbf{x}) + \frac{n+n_e}{mn_e} \sum_{t=1}^m \sum_{i=1}^{n_e} \sum_{j,k=1}^p (e_{ij}e_{ik}) \omega_{jk} \\
&= \frac{n+n_e}{n} l(\Omega|\mathbf{x}) + \frac{\lambda(n+n_e)}{m} \sum_{t=1}^m \left(\sum_{j,k=1}^p \omega_{jk} \frac{1}{n_e} \sum_{i=1}^{n_e} (e_{ij}e_{ik}) \right) \\
&= \frac{n+n_e}{n} l(\Omega|\mathbf{x}) + \frac{\lambda(n+n_e)}{m} \sum_{t=1}^m \left(\sum_{j,k=1}^p \omega_{jk} \frac{1}{n_e} \sum_{i=1}^{n_e} \left(e_{ij} \left(\frac{\omega_{jk}^{(t-1)}}{\omega_{jj}^{(t-1)}} e_{ij} + \sqrt{\frac{\omega_{jj}^{(t-1)} \omega_{kk}^{(t-1)} - \omega_{jk}^{(t-1)}}{\omega_{jj}^{(t-1)}}} e_{0i} \right) \right) \right)
\end{aligned}$$

where e_{ij} and e_{0i} are zero-mean independent Gaussian variables, hence e_{ij}^2 and $e_{ij} * e_{0i}$ are uncorrelated.

$$\begin{aligned}
l_p(\Omega|\tilde{\mathbf{x}}, \tilde{\mathbf{e}}) &\sim l_p(\Omega|\tilde{\mathbf{x}}) + \frac{\lambda(n+n_e)}{m} \sum_{t=1}^m \left(\sum_{j,k=1}^p \omega_{jk} \omega_{jk}^{(t-1)} \frac{1}{n_e} \sum_{i=1}^{n_e} \left(\chi_1^2 - 1 + \sqrt{\frac{\omega_{jj}^{(t-1)} \omega_{kk}^{(t-1)} - \omega_{jk}^{(t-1)}}{\omega_{jk}^{2(t-1)}}} \frac{\chi_1^2 - \chi_1^2}{2} \right) \right) \\
&\rightarrow l_p(\Omega|\tilde{\mathbf{x}}) + \frac{\lambda(n+n_e)}{\sqrt{mn_e}} \left(\sum_{j,k=1}^p \omega_{jk} \omega_{jk}^{(t-1)} \sqrt{2} N(0, 1) + \sum_{j,k=1}^p \omega_{jk} \sqrt{\omega_{jj}^{(t-1)} \omega_{kk}^{(t-1)} - \omega_{jk}^{(t-1)}} N(0, 1) \right) \\
l_p(\Omega|\tilde{\mathbf{x}}) &= \frac{n+n_e}{n} l(\Omega|\mathbf{x}) + \lambda(n+n_e) \sum_{j,k=1}^p \omega_{jk}^2, \text{ as } t, n_e \rightarrow \infty \text{ or } t, m \rightarrow \infty
\end{aligned}$$

Assume that $\omega_{jk} \subset \Omega \in \boldsymbol{\Omega}$ is bounded by B , then after convergence,

$$\begin{aligned}
&\frac{1}{n+n_e} \sup_{\Omega} |l_p(\Omega|\tilde{\mathbf{x}}, \tilde{\mathbf{e}}) - l_p(\Omega|\tilde{\mathbf{x}})| \rightarrow \frac{\lambda p^2}{\sqrt{mn_e}} (\sqrt{2} B^2 + B \sqrt{B^2 + B}) N(0, 1) \rightarrow 0 \\
&\Rightarrow \inf_{\Omega} l_p(\Omega|\mathbf{x}, \mathbf{e}) \xrightarrow{a.s.} \inf_{\Omega} l_p(\Omega|\mathbf{x}) \text{ as } m \rightarrow \infty \text{ or } n_e \rightarrow \infty \\
&\Rightarrow \arg \inf_{\Omega} l_p(\Omega|\mathbf{x}, \mathbf{e}) \xrightarrow{a.s.} \arg \inf_{\Omega} l_p(\Omega|\mathbf{x}) \text{ as } m \rightarrow \infty \text{ or } n_e \rightarrow \infty.
\end{aligned}$$

G Proof of Corollary 8

Upon convergence of the PANDA algorithm, the MLE given noise augmented data in each iteration of the regression with outcome node X_j is the minimizer $\hat{\boldsymbol{\theta}}_{\mathbf{e},j}$ of the noised negative log-likelihood. By the mean-value theorem, there exists $\tilde{\boldsymbol{\theta}}_j \in (\boldsymbol{\theta}_j, \hat{\boldsymbol{\theta}}_{j,\mathbf{e}})$,

$$\begin{aligned}
0 &= \frac{\partial}{\partial \boldsymbol{\theta}} l_p(\hat{\boldsymbol{\theta}}_{j,\mathbf{e}}|\mathbf{x}, \mathbf{e}) = \frac{\partial}{\partial \boldsymbol{\theta}} l_p(\boldsymbol{\theta}_j|\mathbf{x}, \mathbf{e}) + (\hat{\boldsymbol{\theta}}_{j,\mathbf{e}} - \boldsymbol{\theta}_j) \frac{\partial^2}{\partial \boldsymbol{\theta}^2} l_p(\tilde{\boldsymbol{\theta}}_j|\mathbf{x}, \mathbf{e}) \\
&\Rightarrow (\hat{\boldsymbol{\theta}}_{j,\mathbf{e}} - \boldsymbol{\theta}_j) = \frac{\partial}{\partial \boldsymbol{\theta}} n^{-1} l_p(\boldsymbol{\theta}_j|\mathbf{x}, \mathbf{e}) \left(\frac{\partial^2}{\partial \boldsymbol{\theta}^2} n^{-1} l_p(\tilde{\boldsymbol{\theta}}_j|\mathbf{x}, \mathbf{e}) \right)^{-1} \quad (\text{G.1})
\end{aligned}$$

For the first term on the r.h.s of Eqn (G.1), since the expectation of the score function is 0

$$\begin{aligned}
\mathbb{E}_{\mathbf{x}} \left(\frac{\partial}{\partial \boldsymbol{\theta}} n^{-1} l_p(\boldsymbol{\theta}_j|\mathbf{x}, \mathbf{e}) \right) &= \mathbb{E}_{\mathbf{x}} \left(\frac{\partial}{\partial \boldsymbol{\theta}} n^{-1} l(\boldsymbol{\theta}_j|\mathbf{x}) \right) + n^{-1} \sum_{i=1}^{n_e} \frac{\partial}{\partial \boldsymbol{\theta}} l(\boldsymbol{\theta}_j|\mathbf{e}_i) = n^{-1} \sum_{i=1}^{n_e} \frac{\partial}{\partial \boldsymbol{\theta}} l(\boldsymbol{\theta}_j|\mathbf{e}_i) \\
&\Rightarrow \frac{\partial}{\partial \boldsymbol{\theta}} n^{-1} l_p(\boldsymbol{\theta}_j|\mathbf{x}, \mathbf{e}) = \frac{\partial}{\partial \boldsymbol{\theta}} n^{-1} \sum_{i=1}^n l(\boldsymbol{\theta}_j|\mathbf{x}_i) - 0 + n^{-1} \frac{\partial}{\partial \boldsymbol{\theta}} \sum_{i=1}^{n_e} l(\boldsymbol{\theta}_j|\mathbf{e}_i)
\end{aligned}$$

Then by CLT, as $n \rightarrow \infty$,

$$\frac{\partial}{\partial \boldsymbol{\theta}} n^{-1} l_p(\boldsymbol{\theta}_j | \mathbf{x}, \mathbf{e}) \rightarrow N \left(n^{-1} \sum_{i=1}^{n_e} \frac{\partial}{\partial \boldsymbol{\theta}} l(\boldsymbol{\theta}_j | \mathbf{e}_i), \text{V} \left(\frac{\partial}{\partial \boldsymbol{\theta}} n^{-1} l(\mathbf{x} | \boldsymbol{\theta}_j) \right) \right) \stackrel{\Delta}{\approx} N(\boldsymbol{\phi}_j, I(\boldsymbol{\theta}_j))$$

Assume $\text{V}(e_{jk} n_e) = o(\sqrt{n})$ for a given $\boldsymbol{\theta}_{jk}$ such as $\lambda n_e = o(\sqrt{n})$ for the lasso-type noise, then

$$\frac{\partial}{\partial \boldsymbol{\theta}} n^{-1} l_p(\boldsymbol{\theta}_j | \mathbf{x}, \mathbf{e}) \rightarrow N(\mathbf{0}, I(\boldsymbol{\theta}_j))$$

when assuming NGD Eqn (2) with $\gamma = 1$ for \mathbf{e} , we have $\text{E}(\boldsymbol{\phi}_j) = \frac{\lambda n_e}{n} \sigma^2 \text{sign}(\boldsymbol{\theta}_0)$ for Gaussian nodes, $\text{E}(\boldsymbol{\phi}_j) = \frac{\lambda n_e}{8n} \text{sign}(\boldsymbol{\theta}_0) + \frac{\lambda^2 n_e}{n} O(|\boldsymbol{\theta}_0|)$ for Bernoulli nodes, $\text{E}(\boldsymbol{\phi}_j) = \frac{\lambda n_e}{2n} \text{sign}(\boldsymbol{\theta}_0) + \frac{\lambda^2 n_e}{n} O(|\boldsymbol{\theta}_0|)$ for Exponential and Poisson nodes and $\text{E}(\boldsymbol{\phi}_j) = \frac{\lambda n_e r}{2(r+1)n} \text{sign}(\boldsymbol{\theta}_0) + \frac{\lambda^2 n_e}{n} O(|\boldsymbol{\theta}_0|)$ for NB nodes. For the second term on the right-hand side of Eqn (G.1), per LLN $\frac{\partial^2}{\partial \boldsymbol{\theta}^2} n^{-1} l(\boldsymbol{\theta}_j | \mathbf{x}) \rightarrow \text{E}_{\mathbf{x}} \left(\frac{\partial^2}{\partial \boldsymbol{\theta}^2} n^{-1} l(\boldsymbol{\theta}_j | \mathbf{x}) \right)$ as $n \rightarrow \infty$, and $\hat{\boldsymbol{\theta}}_{j,e} \rightarrow \tilde{\boldsymbol{\theta}}_j \rightarrow \boldsymbol{\theta}_j$ when assuming the $\lambda n_e = o(\sqrt{n})$ then

$$\frac{\partial^2}{\partial \boldsymbol{\theta}^2} n^{-1} l_p(\tilde{\boldsymbol{\theta}}_j | \mathbf{x}, \mathbf{e}) \rightarrow \text{E}_{\mathbf{x}} \left(\frac{\partial^2}{\partial \boldsymbol{\theta}^2} n^{-1} l_p(\boldsymbol{\theta}_j | \mathbf{x}, \mathbf{e}) \right) \rightarrow -I_p(\boldsymbol{\theta}_j | \mathbf{e}) \text{ as } n \rightarrow \infty$$

Therefore conditional on \mathbf{e} , as $n \rightarrow \infty$ and $\lambda n_e = o(\sqrt{n})$,

$$\sqrt{n}(\hat{\boldsymbol{\theta}}_{j,e} - \boldsymbol{\theta}_j) | \mathbf{e} \rightarrow N(\mathbf{0}, I_p(\boldsymbol{\theta}_j | \mathbf{e})^{-1} I(\boldsymbol{\theta}_j) I_p(\boldsymbol{\theta}_j | \mathbf{e})^{-1}) \stackrel{\Delta}{\approx} N(\mathbf{0}, \hat{\Sigma}_{j,e}) \quad (\text{G.2})$$

The asymptotic normality in Eqn (G.2) is estimated by plugging $\hat{\boldsymbol{\theta}}_{j,e}$ into pelf. When $\lambda n_e = O(\sqrt{n})$, instead of $\mathbf{0}$, we suggest setting its mean at $-\sqrt{n} \boldsymbol{\phi}_j I_p(\hat{\boldsymbol{\theta}}_{j,e} | \mathbf{e})$, which corrects the bias caused by regularization effect. With finite sample size, the asymptotic normality in Eqn (G.2) is a conditional distribution given a set of augmented noise. To take into consideration the variability introduced by the augmented noise so as to precisely estimate $\boldsymbol{\theta}_j$ and its variance. We could either reduce the variability of noise by increasing n_e , or stabilize it by taking the mean of m consecutive estimations. In the Bayesian framework,

$$\begin{aligned} \text{E}(\boldsymbol{\theta}_j | \mathbf{x}) &= \text{E}_{\mathbf{e}}(\text{E}(\boldsymbol{\theta}_j | \mathbf{x}, \mathbf{e})) = \text{E}_{\mathbf{e}}(\hat{\boldsymbol{\theta}}_{j,e}) = m^{-1} \sum_{t=1}^m \hat{\boldsymbol{\theta}}_{j,e}^{(t)} \triangleq \bar{\boldsymbol{\theta}}_j \text{ as } m \rightarrow \infty \\ \text{V}(\boldsymbol{\theta}_j | \mathbf{x}) &= \text{E}_{\mathbf{e}}(\text{V}(\boldsymbol{\theta}_j | \mathbf{x}, \mathbf{e})) + \text{V}_{\mathbf{e}}(\text{E}(\boldsymbol{\theta}_j | \mathbf{x}, \mathbf{e})) = \text{E}_{\mathbf{e}}(\hat{\Sigma}_{j,e}) + \text{V}_{\mathbf{e}}(\hat{\boldsymbol{\theta}}_{j,e}) \\ &= m^{-1} \sum_{t=1}^m \hat{\Sigma}_{j,e}^{(t)} + (m-1)^{-1} \sum_{t=1}^m \left(\hat{\boldsymbol{\theta}}_{j,e}^{(t)} - \bar{\boldsymbol{\theta}}_j \right) \left(\hat{\boldsymbol{\theta}}_{j,e}^{(t)} - \bar{\boldsymbol{\theta}}_j \right)^T \text{ as } m \rightarrow \infty \\ &\triangleq \bar{\Sigma}_j + \Lambda_j \end{aligned}$$

Per the large-sample Bayesian theory, the posterior mean and variance of $\boldsymbol{\theta}_j$ given \mathbf{x} are asymptotically equivalent ($n \rightarrow \infty$) to the MLE for $\boldsymbol{\theta}$ and the inverse information matrix of $\boldsymbol{\theta}_j$ contained in \mathbf{x} . In other words,

$$\sqrt{n}(\bar{\boldsymbol{\theta}}_j - \boldsymbol{\theta}_j) \rightarrow N(\mathbf{0}, \bar{\Sigma}_j + \Lambda_j).$$

In the case of a finite m (as in practical application), $\text{V}(\boldsymbol{\theta}_j | \mathbf{x})$ is estimated by $\bar{\Sigma}_j + (1 + m^{-1})\Lambda_j$ with the correction for the finite m .

Applying Proposition 8 to GGMs with lasso-type noise, we have

$$\sqrt{n}(\hat{\boldsymbol{\theta}}_j - \boldsymbol{\theta}_j) \rightarrow N \left(n^{-1/2} \lambda n_e \text{sign}(\boldsymbol{\theta}) M_j^{-1}, \sigma_j^2 M^{-1}(\mathbf{x}'_{-j} \mathbf{x}_{-j}) M_j^{-1} \right),$$

where $M_j = (\mathbf{x}'_{-j} \mathbf{x}_{-j} + \text{diag}(\lambda n_e |\boldsymbol{\theta}|^{-1}))$ and σ_j^2 is the variance of the error term in the linear regression, and is estimated by

$$\hat{\sigma}_j^2 = \text{SSE}_j (n - \nu_j)^{-1} = (n - \nu_j)^{-1} (\mathbf{x}_{-j} \boldsymbol{\theta} + \boldsymbol{\epsilon}_j)' (I - H_j) (\mathbf{x}_{-j} \boldsymbol{\theta} + \boldsymbol{\epsilon}_j)$$

$$=(n - \nu_j)^{-1} \epsilon_j'(I - H_j)\epsilon_j + (n - \nu_j)^{-1} (\boldsymbol{\theta}' \mathbf{x}'_{-j}(I - H_j)\mathbf{x}_{-j}\boldsymbol{\theta} + 2\boldsymbol{\theta}' \mathbf{x}'_{-j}(I - H_j)\epsilon_j)$$

where $H_j = \mathbf{x}_{-j}(\mathbf{x}'_{-j}\mathbf{x}_{-j} + \mathbf{diag}(\lambda n_e |\boldsymbol{\theta}|^{-1}))^{-1} \mathbf{x}'_{-j}$ and $\nu_j = \text{trace}(H_j)$.

H Proof of Proposition 7

WLOG, we derive the Fisher information the case of the bridge-type noise, which can be easily generalized to other types of noise. In the GLM framework, the Fisher information matrix $I_p(\boldsymbol{\theta}_j)$ on the augmented data is obtained by taking the expectation of the negative second derivative of the perturbed loss function in Eqn (10) with respect to $\boldsymbol{\theta}_j$ over the distribution of data \mathbf{x} and augmented noise \mathbf{e} .

$$\begin{aligned} I_p(\boldsymbol{\theta}_j) &= \mathbb{E}_{\mathbf{x}} (\mathbf{x}'_{-j} \mathbf{B}_j''(\mathbf{x}_{-j}) \mathbf{x}_{-j}) + \mathbb{E}_{\mathbf{e}} (\mathbf{e}_{j,-j}^T \mathbf{B}_j''(\mathbf{e}_{j,-j}) \mathbf{e}_{j,-j}) \\ &= I_{\mathbf{x}}(\boldsymbol{\theta}_j) + \mathbb{E}_{\mathbf{e}} \left(\sum_{i=1}^{n_e} \mathbf{e}_{ij,-j}^T \mathbf{B}_j''(\mathbf{e}_{ij,-j} \boldsymbol{\theta}_j) \mathbf{e}_{ij,-j} \right) \end{aligned}$$

Take the second-order Taylor Expansion around $\mathbf{e}_{ij,-j} \boldsymbol{\theta}_j = 0$, we have

$$\begin{aligned} I_p(\boldsymbol{\theta}_j) &= I_{\mathbf{x}}(\boldsymbol{\theta}_j) + n_e \mathbf{B}_j''(0) \mathbf{V}(\mathbf{e}_{ij,-j}) + O(\lambda^2 n_e) \\ &= I_{\mathbf{x}}(\boldsymbol{\theta}_j) + (\lambda n_e) \mathbf{B}_j''(0) \mathbf{diag}\{|\theta_{j1}|^{-\gamma}, \dots, |\theta_{jp}|^{-\gamma}\} + O(\lambda(\lambda n_e)), \end{aligned}$$

where $\mathbf{B}_j''(\mathbf{x}_{-j}) = \mathbf{diag}\{B_j''(\mathbf{x}_{1,-j} \boldsymbol{\theta}_j), \dots, B_j''(\mathbf{x}_{n,-j} \boldsymbol{\theta}_j)\}$, $\mathbf{B}_j(\mathbf{e}_{j,-j}) = \mathbf{diag}\{B_j''(\mathbf{e}_{1,-j} \boldsymbol{\theta}_j), \dots, B_j''(\mathbf{e}_{n_e,-j} \boldsymbol{\theta}_j)\}$, and $\mathbf{V}(\mathbf{e}_{ij,-j})$ is the covariance matrix of $\mathbf{e}_{ij,-j}$.

I Proof of Corollary 3

WLOG, we derive the Fisher information in the case of the bridge-type noise, which can be easily generalized to other types of noise. In the PANDA-NS algorithm for constructing GGM, during the regression with outcome node X_j , the average of the minimizer of the l loss functions is

$$\bar{\boldsymbol{\theta}}_j = m^{-1} \sum_{t=1}^m \left(\mathbf{x}'_{-j} \mathbf{x}_{-j} + \sum_{i=1}^{n_e} \mathbf{e}_{i,j,-j}^{(t)'} \mathbf{e}_{i,j,-j}^{(t)} \right)^{-1} \mathbf{x}'_{-j} \mathbf{x}_j,$$

where $e_{ijk} \sim N(0, \lambda |\theta_{jk}|^{-1})$. Let $\sum_{i=1}^{n_e} \mathbf{e}_{i,j,-j}^{(t)'} \mathbf{e}_{i,j,-j}^{(t)} = \mathbb{E}(\sum_{i=1}^{n_e} \mathbf{e}_{i,j,-j}^{(t)'} \mathbf{e}_{i,j,-j}^{(t)}) + \bar{A} = \mathbf{diag}(\lambda n_e |\boldsymbol{\theta}_j|^{-\gamma}) + \bar{A}$. Let $S_j = (\mathbf{x}'_{-j} \mathbf{x}_{-j} + \mathbf{diag}(\lambda n_e |\boldsymbol{\theta}_j|^{-1}))^{-1}$. The Taylor expansion of the inverse of sum of two matrices, assuming A to be a small increment, is $(S_j^{-1} + \bar{A})^{-1} = S_j - S_j \bar{A} S_j + S_j \bar{A} S_j \bar{A} S_j + \dots$. Therefore,

$$\bar{\boldsymbol{\theta}}_j = S_j \mathbf{x}'_{-j} \mathbf{x}_j - S_j (m^{-1} \sum_{t=1}^m \bar{A} + O(\lambda^2 n_e)) S_j \mathbf{x}'_{-j} \mathbf{x}_j$$

and the minimizer of the average of m loss functions is

$$\hat{\boldsymbol{\theta}}_j = \left(\mathbf{x}'_{-j} \mathbf{x}_{-j} + \sum_{i=1}^{n_e m} \hat{\mathbf{e}}_{ij}' \hat{\mathbf{e}}_{ij} \right)^{-1} \mathbf{x}'_{-j} \mathbf{x}_j = \left(\mathbf{x}'_{-j} \mathbf{x}_{-j} + \mathbf{diag}(\lambda n_e |\boldsymbol{\theta}_j|^{-1}) + \hat{A} \right)^{-1} \mathbf{x}'_{-j} \mathbf{x}_j$$

$e_{ijk} \sim N(0, \lambda |m \theta_{jk}|^{-1})$ for the same regularization effect .

$$\begin{aligned} (m^{-1} \sum_{t=1}^m \bar{A})_{kk} &= m^{-1} \sum_{t=1}^m \sum_{i=1}^{n_e} \bar{e}_{ijk}^2 - \lambda n_e |\theta_{jk}|^{-1} \sim \lambda |m \theta_{jk}|^{-1} (\chi_{n_e m}^2 - n_e m) \\ \hat{A}_{kk} &= \sum_{i=1}^{n_e m} \hat{e}_{ijk}^2 - \lambda n_e |\theta_{jk}|^{-1} \sim \lambda |m \theta_{jk}|^{-1} (\chi_{n_e m}^2 - n_e m) \\ (m^{-1} \sum_{t=1}^m \bar{A})_{kl} &= m^{-1} \sum_{t=1}^m \sum_{i=1}^{n_e} \bar{e}_{ijk} \bar{e}_{ijl} \sim \lambda |\theta_{jk} \theta_{jl}|^{-\frac{1}{2}} m^{-1} \sum_{t=1}^m \sum_{i=1}^{n_e} N(0, 1) N(0, 1) \end{aligned}$$

$$\begin{aligned}\hat{A}_{kl} &= \sum_{i=1}^{n_e m} \hat{e}_{ijk} \hat{e}_{ijl} \sim \frac{\lambda}{m} |\theta_{jk} \theta_{jl}|^{-\frac{1}{2}} \sum_{i=1}^{n_e m} N(0, 1) N(0, 1) \\ &\Rightarrow (m^{-1} \sum_{t=1}^m \bar{A})_{kk} \sim \hat{A}_{kk}, (m^{-1} \sum_{t=1}^m \bar{A})_{kl} \sim \hat{A}_{kl}\end{aligned}$$

Therefore, given \mathbf{x}_j and n_e , $\bar{\theta}_j$ and $\hat{\theta}_j$ first-order approximately follow the same distribution, whose variability is because of finite n_e . When letting $n_e \rightarrow \infty$ and $\lambda n_e = O(1)$, we have exactly $\bar{\theta}_j \sim \hat{\theta}_j$.

References

- Allen, D. M. (1974). The relationship between variable selection and data augmentation and a method for prediction. *Technometrics*, 16(1):125–127.
- Allen, G. I. and Liu, Z. (2012). A log-linear graphical model for inferring genetic networks from high-throughput sequencing data. *IEEE International Conference on Bioinformatics and Biomedicine*, pages 1–6.
- Begeer, S., Wierda, M., and Venderbosch, S. (2013). Allemaal autisme, allemaal anders. rapport nva enquete 2013 [all autism, all different. dutch autism society survey 2013]. bilthoven: Nva, 83 pp. *Bilthoven: NVA*.
- Belloni, A., Chernozhukov, V., and Wang, L. (2012). Square-root lasso: Pivotal recovery of sparse signals via conic programming. *Biometrika*, 98:791–806.
- Bickel, P. J. and Levina, E. (2008). Regularized estimation of large covariance matrices. *Annals of Statistics*, 36:199–227.
- Brown, W. M., Gedeon, T. D., and Groves, D. I. (2003). Use of noise to augment training data: A neural network method of mineral potential mapping in regions of limited known deposit examples. *Natural Resources Research*, 12(2):141–152.
- Cai, T., Liu, W., and Luo, X. (2011). A constrained l1 minimization approach to sparse precision matrix estimation. *Journal of the American Statistical Association*, 106:594–607.
- Chen, J. and Chen, Z. (2008). Extended bayesian information criteria for model selection with large model spaces. *Biometrika*, 95(3):759–771.
- Chiu, T., Leonard, T., and Tsui, K. (1996). The matrix-logarithm covariance model. *Journal of the American Statistical Association*, 91:198–210.
- Fellinghauer, B., Bühlmann, P., Ryffel, M., von Rhein, M., and Reinhardt, J. D. (2013). Stable graphical model estimation with random forests for discrete, continuous, and mixed variables. *Computational Statistics and Data Analysis*, 64:132–142.
- Foygel, R. and Drton, M. (2010). Extended bayesian information criteria for gaussian graphical models. In *Advances in neural information processing systems*, pages 604–612.
- Fruchterman, T. M. and Reingold, E. M. (1991). Graph drawing by force-directed placement. *Software: Practice and experience*, 21(11):1129–1164.
- Gal, Y. and Ghahramani, Z. (2016). Dropout as a bayesian approximation: Representing model uncertainty in deep learning. *Proceedings of the 33rd International Conference on Machine Learning*, JMLR: W&CP volume 48.
- Grandvalet, Y., Canu, S., and Boucheron, S. (1997). Noise injection: Theoretical prospects. *Neural Computation*, 9:1093–1108.

- Grandvalet, Y. (1998). Least absolute shrinkage is equivalent to quadratic penalization. *ICANN 98. Springer London*, 0000:201–206.
- Haslbeck, J. and Waldorp, L. J. (2015). Structure estimation for mixed graphical models in high-dimensional data. *arXiv preprint arXiv:1510.05677*.
- Haslbeck, J. M. and Waldorp, L. J. (2016). mgm: Structure estimation for time-varying mixed graphical models in high-dimensional data. *J Stat Softw*.
- Hastie, T., Tibshirani, R., and Friedman, J. (2009a). *The Elements of Statistical Learning*. Springer, New York, 2 edition.
- Hastie, T., Tibshirani, R., and Friedman, J. (2009b). *The Elements of Statistical Learning*. Springer, New York, 2 edition.
- Hoffing, H. and Tibshirani, R. J. (2009). Estimation of sparse binary pairwise markov networks using pseudo-likelihoods. *The Journal of Machine Learning Research*, 10:883–906.
- Holmstrom, L. and Koistinen, P. (1992). Using additive noise in back-propagation training. *IEEE transactions on neural networks*, 3(1):24–38.
- Huang, J., Liu, N., Pourahmadi, M., and Liu, L. (2006). Covariance matrix selection and estimation via penalised normal likelihood. *Biometrika*, 93:85–98.
- J. Friedman, T. H. and Tibshirani, T. (2008). Sparse inverse covariance estimation with the graphical lasso. *Biometrics*, 9:432–441.
- Jalali, A., Ravikumar, P. K., Vasuki, V., and Sanghavi, S. (2011). On learning discrete graphical models using group-sparse regularization. *International Conference on Artificial Intelligence and Statistics*, page 378–387.
- Kang, G., Li, J., and Tao, D. (2018). Shakeout: A new approach to regularized deep neural network training. *IEEE Transactions on Pattern Analysis and Machine Intelligence*, 40(5):1245–1258.
- Kuang, Z., Geng, S., and Page, D. (2017). A screening rule for l_1 -regularized ising model estimation. *Neural Information Processing Systems*.
- Kuismin, M. O., Kemppainen, J. T., and Sillanpää, M. J. (2017). Precision matrix estimation with rope. *Journal of Computational and Graphical Statistics*, 26(3):682–694.
- Lam, C. and Fan, J. (2009). Sparsistency and rates of convergence in large covariance matrices estimation. *Annals of Statistics*, 37:4254–4278.
- Leclerc, R. D. (2008). Survival of the sparest: robust gene networks are parsimonious. *Molecular Systems Biology*, 4(1):213.
- Lee, J., Sun, D., Sun, Y., and Taylor, J. (2016). Exact post-selection inference, with application to the lasso. *The Annals of Statistics*, 44(3):907–927.
- Levina, E., Rothman, A., and Zhu, J. (2008). Sparse estimation of large covariance matrices via a nested lasso penalty. *Annals of Applied Statistics*, 2:245–263.
- Li, Q. and Lin, N. (2010). The bayesian elastic net. *Bayesian Analysis*, 5(1):151–170.
- Li, Y. and Liu, F. (2017). Whiteout: Gaussian adaptive noise regularization in feedforward neural networks. *arXiv:1612.01490v3*.
- Liu, H. and Wang, L. (2012). Tiger: a tuning-insensitive approach for optimally estimating gaussian graphical models. *Electron. J. Statist.*, 11:241–294.

- Liu, W. and Xi, L. (2015). Fast and adaptive sparse precision matrix estimation in high dimensions. *Journal of Multivariate Analysis*, 135:153 – 162.
- Matsuoka, K. (1992). Noise injection into inputs in back- propagation learning. *IEEE Transactions on Systems, Man, and Cybernetics*, 22(3):436–440.
- Meinshausen, N. and Bühlmann, P. (2006). High-dimensional graphs and variable selection with the lasso. *The Annals of Statistics*, 34(3):1436–1462.
- Noh, H., You, T., Mun, J., and Han, B. (2017). Regularizing deep neural networks by noise: Its interpretation and optimization. *arxiv*, arXiv:1710.05179v2.
- O. Banerjee, L. E. G. and d’Aspremont, A. (2008). Model selection through sparse maximum likelihood estimation for multivariate gaussian or binary data. *Journal of Machine Learning Research*, 9:485–516.
- Opsahl, T., Agneessens, F., and Skvoretz, J. (2010). Node centrality in weighted networks: Generalizing degree and shortest paths. *Social networks*, 32(3):245–251.
- Park, T. and Casella, G. (2008). The bayesian lasso. *Journal of the American Statistical Association*, 103(482):681–686.
- Peng, J., Wang, P., Zhou, N., and Zhu, J. (2009). Partial correlation estimation by joint sparse regression models. *Journal of the American Statistical Association*, 104:735–746.
- Polson, N. G., Scott, J. G., and Windle, J. (2012). The bayesian bridge. *arXiv:1109.2279*.
- Pourahmadi, M. (1999). Joint mean-covariance models with applications to longitudinal data: Unconstrained parameterisation. *Biometrika*, 86:677–690.
- Pourahmadi, M. (2000). Maximum likelihood estimation of generalized linear models for multivariate normal covariance matrix. *Biometrika*, 87:425–435.
- R Core Team (2017). *R: A Language and Environment for Statistical Computing*. R Foundation for Statistical Computing, Vienna, Austria.
- Ravikumar, P., Raskutti, G., Wainwright, M., and Yu, B. (2008). Model selection in gaussian graphical models: high-dimensional consistency of l1-regularized mle. *In Neural Information Processing Systems*, 21.
- Ravikumar, P., Wainwright, M. J., and Lafferty, J. D. (2010). High-dimensional ising model selection using ℓ_1 -regularized logistic regression. *Ann. Statist.*, 38(3):1287–1319.
- Rothman, A., P. Bickel, E. L., and Zhu, J. (2008). Sparse permutation invariant covariance estimation. *Electronic Journal of Statistics*, 2:494–515.
- Skurichina, M. and Duin, R. P. W. (1999). Regularization of linear classifiers by adding redundant features. *Pattern Analysis and Applications*, 2(1):44 – 52.
- Srivastava, N., Hinton, G., Krizhevsky, A., Sutskever, I., and Salakhutdinov, R. (2014). Dropout: A simple way to prevent neural networks from overfitting. *Journal of Machine Learning Research*, 15:1929–1958.
- Sun, T. and Zhang, C.-H. (2012). Scaled sparse linear regression. *Biometrika*, 99:879–898.
- Taylor, J. and Tibshirani, R. (2017). Postselection inference for l_1 -penalized likelihood models. *The Canadian Journal of Statistics*, 46(1):41–61.

- Wager, S., Wang, S., and Liang, P. (2013). Dropout training as adaptive regularization. *NIPS'13 Proceedings of the 26th International Conference on Neural Information Processing Systems*, 1:351–359.
- Wan, Y.-W., Allen, G. I., Baker, Y., Yang, E., Ravikumar, P., and Liu, Z. (2015). *XMRF: Markov Random Fields for High-Throughput Genetics Data*. R package version 1.0.
- Wang, H. (2012). Bayesian graphical lasso models and efficient posterior computation. *Bayesian Anal.*, 7(4):867–886.
- Xu, X. and Ghosh, M. (2015). Bayesian variable selection and estimation for group lasso. *Bayesian Analysis*, 10(4):909–936.
- Yang, E., Allen, G. I., Liu, Z., and Ravikumar, P. K. (2012a). Graphical models via generalized linear models. *Advances in Neural Information Processing Systems*, 25:1367–1375.
- Yang, E., Allen, G. I., Liu, Z., and Ravikumar, P. K. (2014). Mixed graphical models via exponential families. *Proceedings of the Seventeenth International Conference on Artificial Intelligence and Statistics*, page 1042–1050.
- Yang, E., Ravikumar, P., Allen, G. I., and Liu, Z. (2012b). Graphical models via generalized linear models. *Advances in Neural Information Processing Systems*, 25:1367–1375.
- Yang, E., Ravikumar, P., Allen, G. I., and Liu, Z. (2015). Graphical models via univariate exponential family distributions. *Journal of Machine Learning Research*, 16:3813–3847.
- Yuan, M. (2010). High dimensional inverse covariance matrix estimation via linear programming. *Journal of Machine Learning Research*, 11:2261–2286.
- Yuan, M. and Lin, Y. (2007). Model selection and estimation in the gaussian graphical model. *Biometrika*, 94:19–35.

Supplementary Materials to

Panda: AdaPtive Noisy Data Augmentation for Regularization of

Undirected Graphical Models

Yinan Li¹, Xiao Liu², and Fang Liu¹

¹ Department of Applied and Computational Mathematics and Statistics

² Department of Psychology

University of Notre Dame, Notre Dame, IN 46556, U.S.A.

S.1 PANDA for NS in a single UGM

Algorithm 1 PANDA for NS in a single UGM

1: **Input**

1. random initial parameter estimates $\bar{\boldsymbol{\theta}}_j^{(0)}$ for $j = 1, \dots, p$.
2. A NGD in Eqns (2) to (5) and the associated tuning parameters, maximum iteration T , noisy data size n_e , width of moving average (MA) window m , threshold τ_0 , banked parameter estimates after convergence r .

2: $t \leftarrow 0$; convergence $\leftarrow 0$

3: **WHILE** $t < T$ **AND** convergence = 0

4: $t \leftarrow t + 1$

5: **FOR** $j = 1$ to p

a) Generate \mathbf{e}_j from the NGD with $\bar{\boldsymbol{\theta}}_j^{(t-1)}$ plugged in the variance term of the NGD.

b) Obtain augmented data $\tilde{\mathbf{x}}_j$ by row-combining $(\mathbf{x}_j, \mathbf{x}_{-j})$ with $(\mathbf{e}_{jj}, \mathbf{e}_{.j})$.

c) Obtain MLE $\hat{\boldsymbol{\theta}}_j^{(t)}$ by regressing $\tilde{\mathbf{x}}_j$ on all other columns $\tilde{\mathbf{x}}_{-j}$ with a proper GLM

d) If $t > m$, calculate the MA $\bar{\boldsymbol{\theta}}_j^{(t)} = m^{-1} \sum_{l=t-m+1}^t \hat{\boldsymbol{\theta}}_j^{(l)}$; otherwise $\bar{\boldsymbol{\theta}}_j^{(t)} = \hat{\boldsymbol{\theta}}_j^{(t)}$. Calculate $l_j^{(t)}$ with $\bar{\boldsymbol{\theta}}^{(l)}$ plugged in, where l is the negative log-likelihood in Eqn (10)..

End FOR

6: Calculate the loss function $\bar{l}^{(t)} = m^{-1} \sum_{l=t-m+1}^t \sum_{j=1}^p l_j^{(l)}$ and apply one of the convergence criteria listed in Remark 2 to $\bar{l}^{(t)}$. Let convergence $\leftarrow 1$ if the convergence is reached.

7: **End WHILE**

8: Continue to execute the command lines 4 and 5 for another r iterations, and record $\bar{\boldsymbol{\theta}}_j^{(l)}$ for $l = t + 1, \dots, t + r$. Let $\bar{\boldsymbol{\theta}}_{jk} = (\bar{\boldsymbol{\theta}}_{jk}^{(t+1)}, \dots, \bar{\boldsymbol{\theta}}_{jk}^{(t+r)})$.

9: Set $\hat{\boldsymbol{\theta}}_{jk} = \hat{\boldsymbol{\theta}}_{kj} = 0$ if $(|\max\{\bar{\boldsymbol{\theta}}_{jk}\} \cdot \min\{\bar{\boldsymbol{\theta}}_{jk}\}| < \tau_0) \cap (\max\{\bar{\boldsymbol{\theta}}_{jk}\} \cdot \min\{\bar{\boldsymbol{\theta}}_{jk}\} < 0)$ or $(|\max\{\bar{\boldsymbol{\theta}}_{kj}\} \cdot \min\{\bar{\boldsymbol{\theta}}_{kj}\}| < \tau_0) \cap (\max\{\bar{\boldsymbol{\theta}}_{kj}\} \cdot \min\{\bar{\boldsymbol{\theta}}_{kj}\} < 0)$; $\hat{\boldsymbol{\theta}}_{jk} = \hat{\boldsymbol{\theta}}_{kj} = \min\{\bar{\boldsymbol{\theta}}_{jk}^{(t+r)}, \boldsymbol{\theta}_{kj}^{(t+r)}\}$ otherwise.

S.2 PANDA-CD Algorithm

Algorithm 2 PANDA-CD in a single GGM

- 1: **Pre-processing**: standardize observed data \mathbf{x} .
 - 2: **Input**
 - random initial parameter estimates $\bar{\boldsymbol{\theta}}_j^{(0)}$ and $\hat{\sigma}_j^2$ for $j = 2, \dots, p$; let $\hat{\sigma}_1^{-2} = s^{-2}$ where s^2 is the sample variance of \mathbf{x}_1 .
 - A NGD in Eqns (2) to (5) and the associated tuning parameters, maximum iteration T , noisy data size n_e , MA window width m , threshold τ_0 , banked parameter estimates after convergence r , inner loop K in alternatively estimating $\boldsymbol{\theta}_j$ and σ_j^2
 - 3: $t \leftarrow 0$; convergence $\leftarrow 0$
 - 4: **WHILE** $t < T$ **AND** convergence = 0
 - 5: $t \leftarrow t + 1$
 - 6: **FOR** $j = 2$ to p
 - 7: **FOR** $k = 1 : K$
 - a) Generate n_e rows of noisy data $\mathbf{e}_{1:(j-1)}$, from the NGD with $\bar{\boldsymbol{\theta}}_j^{(t-1)}$ plugged in the variance term of the NGD to obtain augmented data as depicted in Figure 3.
 - b) Obtain the OLS estimate $\hat{\boldsymbol{\theta}}_j^{(t)}$ by regressing $\tilde{\mathbf{x}}_j$ on $\tilde{\mathbf{x}}_{1:j-1}$, according to Eqn (18).
 - c) If $t > m$, calculate the MA $\bar{\boldsymbol{\theta}}_j^{(t)} = m^{-1} \sum_{l=t-m+1}^t \hat{\boldsymbol{\theta}}_j^{(l)}$; otherwise $\bar{\boldsymbol{\theta}}_j^{(t)} = \hat{\boldsymbol{\theta}}_j^{(t)}$. Calculate the sum of squared error $\text{SSE}_j^{(t)}$ given $\bar{\boldsymbol{\theta}}_j^{(t)}$ and $\hat{\sigma}_j^{2(t)} = \text{SSE}_j^{(t)}/n$ (Eqn 17).
 - 8: **End FOR**
 - 9: **End FOR**
 - 10: Continue to execute the command lines 5 and 6 for another r iterations, and record $\bar{\boldsymbol{\theta}}_j^{(l)}$ for $l = t + 1, \dots, t + r$, calculate the degrees of freedom $\nu_j^{(t)} = \text{trace}(\mathbf{x}_j(\tilde{\mathbf{x}}_j' \tilde{\mathbf{x}}_j)^{-1} \mathbf{x}_j')$ and $\hat{\sigma}_j^{2(l)} = \text{SSE}_j^{(t)}/(n - \nu_j^{(l)})$. Let $\bar{\boldsymbol{\theta}}_{jk} = (\bar{\theta}_{jk}^{(t+1)}, \dots, \bar{\theta}_{jk}^{(t+r)})$.
 - 11: Set $\hat{\theta}_{jk} = 0$ if $(|\max\{\bar{\boldsymbol{\theta}}_{jk}\} \cdot \min\{\bar{\boldsymbol{\theta}}_{jk}\}| < \tau_0) \cap (\max\{\bar{\boldsymbol{\theta}}_{jk}\} \cdot \min\{\bar{\boldsymbol{\theta}}_{jk}\}) < 0$ for $k > j$; otherwise, set $\hat{\theta}_{jk} = \bar{\theta}_{jk}^{(t)}$. Set $\hat{D} = \mathbf{diag}(\hat{\sigma}_1^{2(t)}, \dots, \hat{\sigma}_p^{2(t)})$. Calculate $\hat{\Omega} = \hat{L}' \hat{D} \hat{L}$
-

S.3 PANDA-SCIO Algorithm

Algorithm 3 PANDA-SCIO in a single GGM

- 1: **Pre-processing:** Standardize observed data \mathbf{x} .
 - 2: **Input**
 - initial parameter estimates $\hat{\boldsymbol{\theta}}_j^{(0)} = \hat{\Omega}^{(0)} = (n^{-1}\mathbf{x}^T\mathbf{x} + 0.1I)^{-1}$
 - tuning parameters, maximum iteration T , noisy data size n_e , thresholds τ_0, τ_1 , MA window width m , banked parameter estimates after convergence r
 - 3: $t \leftarrow 0$ and $d \leftarrow C$ (C is a large positive number)
 - 4: **WHILE** $t < T$ **AND** $d < \tau$
 - 5: $t \leftarrow t + 1$
 - 6: **FOR** $j = 1$ to p
 - a) Set $\bar{\Omega}_j^{(t-1)} = \bar{\Omega}_j^{(t-1)} \mathbf{1} \left(|\bar{\Omega}_j^{(t-1)}| > \tau_1 \right) + \tau_1 \mathbf{1} \left(0 < \bar{\Omega}_j^{(t-1)} < \tau_1 \right) - \tau_1 \mathbf{1} \left(0 > \bar{\Omega}_j^{(t-1)} > -\tau_1 \right)$
 - b) Generate Gaussian noisy data \mathbf{e}_j from a NGD in Eqns (2) to (5) with $\bar{\Omega}_j^{(t-1)}$ plugged in the variance term of the NGD.
 - c) Obtain augmented data $\tilde{\mathbf{x}}_j$ by row-combining $\mathbf{z} = \sqrt{\frac{n+n_e}{n}}\mathbf{x}$ and $\mathbf{d}_j = \sqrt{\frac{2(n+n_e)}{n_e}}\mathbf{e}_j$
 - d) Calculate $\hat{\boldsymbol{\theta}}_j^{(t)} = (n + n_e)(\tilde{\mathbf{x}}_j^T \tilde{\mathbf{x}}_j)^{-1} \mathbf{1}_j$
 - e) If $t > m$, calculate MA $\bar{\boldsymbol{\theta}}_j^{(t)} = m^{-1} \sum_{l=t-m+1}^t \hat{\boldsymbol{\theta}}_j^{(l)}$; otherwise $\bar{\boldsymbol{\theta}}_j^{(t)} = \hat{\boldsymbol{\theta}}_j^{(t)}$
 - f) If $t > m$, calculate $d = m^{-1} \left(\sum_{l=t-m+1}^t l_j^{(l)} - \sum_{l=t-m}^{t-1} l_j^{(l)} \right)$, where $l_j^{(l)}$ is the loss functions in Eqn (21) with $\bar{\boldsymbol{\theta}}_j^{(l)}$ plugged in.
 - End FOR**
 - 7: Calculate the loss function $\bar{l}^{(t)} = m^{-1} \sum_{l=t-m+1}^t \sum_{j=1}^p l_j^{(l)}$ and apply one of the convergence criteria listed in Remark 2 to $\bar{l}^{(t)}$. Let convergence $\leftarrow 1$ if the convergence is reached.
 - 8: **End WHILE**
 - 9: Continue to execute the command lines 5 to 7 for another r iterations, and record $\bar{\boldsymbol{\theta}}_j^{(l)}$ for $l = t + 1, \dots, t + r$. Let $\bar{\boldsymbol{\theta}}_{jk} = (\bar{\theta}_{jk}^{(t+1)}, \dots, \bar{\theta}_{jk}^{(t+r)})$.
 - 10: Set $\hat{\omega}_{jk} = \hat{\omega}_{kj} = 0$ if $(|\max\{\bar{\boldsymbol{\theta}}_{jk}\} \cdot \min\{\bar{\boldsymbol{\theta}}_{jk}\}| < \tau_0) \cap (\max\{\bar{\boldsymbol{\theta}}_{jk}\} \cdot \min\{\bar{\boldsymbol{\theta}}_{jk}\} < 0)$ or $(|\max\{\bar{\boldsymbol{\theta}}_{kj}\} \cdot \min\{\bar{\boldsymbol{\theta}}_{kj}\}| < \tau_0) \cap (\max\{\bar{\boldsymbol{\theta}}_{kj}\} \cdot \min\{\bar{\boldsymbol{\theta}}_{kj}\} < 0)$ for $k \neq j = 1, \dots, p$; otherwise, set $\hat{\omega}_{jk} = \min \left\{ \bar{\theta}_{jk}^{(t+r)}, \boldsymbol{\theta}_{kj}^{(t+r)} \right\}$
-